IDENTIFICATION OF SURVIVAL MARKER CXXC5 AND METASTATIC MODELING
OF ENDOMETRIAL CANCER.

By

Alyssa Michelle Fedorko

A DISSERTATION

Submitted to
Michigan State University
in partial fulfillment of the requirements
for the degree of

Genetics – Doctor of Philosophy

2019

PUBLIC ABSTRACT

IDENTIFICATION OF SURVIVAL MARKER CXXC5 AND METASTATIC MODELING
OF ENDOMETRIAL CANCER.

By

Alyssa Michelle Fedorko

Endometrial cancer originates from the innermost lining of the uterus. Despite being the fourth most common cancer in women and the most prevalent gynecologic malignancy in the United States, there has been no improvement in treatment strategies for endometrial cancer over the past two decades due to lack of relevant models and inadequate prognostic markers. Problems in dealing with this disease will become more imminent in the future as the incidence and prevalence of this disease is increasing overall. Determination of therapeutic modality still relies heavily on two subjective measures: surgical staging and pathological classification. We have used three independent human endometrial cancer datasets to identify a gene, *CXXC5*, that when upregulated on an RNA or protein level correlates with poor outcomes for patients. This study identified an objective genetic fingerprint of endometrial tumors to pinpoint patients who are more likely to experience a poor outcome due to their disease and also resulted in the development of an immune-competent mouse model that develops distant metastatic disease in the lungs. Presently, there are no markers available that reliably predict either disease recurrence or poor survival. Thus, it is crucial that we identify targets for prevention of disease, markers that predict disease outcome, and targets for new therapies.

ABSTRACT

IDENTIFICATION OF SURVIVAL MARKER CXXC5 AND METASTATIC MODELING
OF ENDOMETRIAL CANCER.

By

Alyssa Michelle Fedorko

Endometrial cancer is the most common gynecologic malignancy in the U.S. with metastatic disease remaining the major cause of patient death. Therapeutic strategies have remained essentially unchanged for decades. A significant barrier to progression in treatment modalities stems from a lack of clinically applicable *in vivo* models to accurately mimic endometrial cancer; specifically, ones that form distant metastases and maintain an intact immune system. To address this problem, we have established the first immune competent orthotopic tumor model for metastatic endometrial cancer by creating a green fluorescent protein (GFP) labeled cell line from an endometrial cancer that developed in a $Pgr^{cre/+}Pten^{f/f-}Kras^{G12D}$ genetically engineered mouse. These cancer cells (Mouse Endometrial Cancer PTEN deleted K-ras activated; MECPK) were grafted into the mechanically abraded uterine lumen of ovariectomized recipient mice treated with estrogen and subsequently developed local and metastatic endometrial tumors. We noted primary tumor formation in 59% and 86% of mixed background and C57BL/6 animals respectively at 4 weeks and distant lung metastases in 78% of mixed background mice after 2 months. Importantly this model is driven by PTEN and KRAS mutations, which are commonly found in human endometrial cancer. Immunohistochemical analysis indicates that tumors from this model are similar to human endometrial cancers with activated AKT and ERK pathways. This orthotopic tumor model is the first immunocompetent animal model that closely resembles human

metastatic endometrial cancer, modeling both local metastasis and hematogenous spread to lung and has significant potential to advance the study of endometrial cancer and its metastasis.

Additionally, there is a need to identify and classify new potential diagnostic and therapeutic targets in the genesis of endometrial cancer in order to more accurately tailor an individualized treatment regime. Thus, it is necessary to identify markers that predict more aggressive cancers. We have conducted a transcriptome analysis of 136 endometrial cancers from women who either experienced an event, meaning they died from their disease or had a recurrence of disease, or from women with cancer that did not experience such an event from their disease. In these samples, we found a clustering of upregulated genes in the women who experienced an event. Next, we used The Cancer Genome Atlas (TCGA) to validate the genes that appeared as significant in our dataset with their dataset. From comparison of the two datasets, we narrowed in on a particular gene, CXXC5 which, when overexpressed in an endometrial tumor, is highly predictive of negative outcome (recurrence or death of the patient). Using a third independent human dataset, we confirmed yet again that high transcript levels of CXXC5 correlates with detrimental outcomes. Current literature contains little information on how the protein coded by this gene functions in the endometrium and what possible role CXXC5 could have in contributing to a more aggressive cancer phenotype.

To everyone who kept me sane throughout the journey.

TABLE OF CONTENTS

LIST OF TABLES

LIST OF FIGURES

KEY TO ABBREVIATIONS

ACS American Cancer Society

BER base-excision repair

CA cancer antigen

CBC complete blood count

CEA carcinoembryonic antigen

DES diethylstilbestrol

DFS disease free survival

dMMR mismatch repair-deficient

Dox doxycycline

EKG electrocardiogram

FDA The US Food and Drug Administration

GO Gene Ontology

HNPCC hereditary nonpolyposis colorectal cancer

HR homologous recombination

LVSI lymphovascular space invasion

MS mass spectrometry

MSI microsatellite-instable

NTC non-targeting control

OS overall survival

OVX ovariectomy

PARP poly adenosine diphosphate ribose polymerase

PAS periodic acid Schiff stain

PD-L1 programmed death-ligand 1

PFS progression-free survival

POLE polymerase epsilon

SEER Surveillance, Epidemiology, and End Results

TCGA The Cancer Genome Atlas

TET tetracycline

Chapter 1: INTRODUCTION

Background and Problem

The endometrium is the innermost layer of the uterus which thickens during the menstrual cycle to prepare for potential implantation of an embryo. Endometrial cancer originates from this layer and is the most common gynecologic malignancy in the United States accounting for approximately half of all that are diagnosed (1-3). It is the fourth most common cancer in women, and it is projected to be the sixth most common cause of cancer deaths in 2018 (4). The American Cancer Society (ACS) predicts that there will be about 63,230 new cases of cancer of the uterine corpus diagnosed in 2018 with about 11,350 deaths (5). Based on 2010-2014 cases and deaths, the age-adjusted number of deaths was 4.6 per 100,000 women per year and the number of new cases of uterine cancer was 25.7 per 100,000 women per year (6). A woman's risk of developing uterine cancer at some point during her lifetime is approximately 2.8% based on 2012-2014 data (6). As of 2014, in the United States, there were an estimated 710,228 women living with diagnosed uterine cancer (6). Based on the National Cancer Institute's Surveillance, Epidemiology, and End Results (SEER) Program data from 2007-2013, 81.3% of women survive 5 years. This is less than the 98.6% of men and 89.7% of women who survive 5 years after diagnosis of prostate or breast cancer respectively (7, 8). When compared to other cancer types, uterine cancer is fairly common representing 3.6% of all new cancer cases in the United States (6). Endometrial cancer affects mainly postmenopausal women. The vast majority of endometrial cancer cases are diagnosed in women between the ages of 45-74, the median age of diagnosis being 62 years. Black women are more likely to die from this

1

cancer type but overall endometrial cancer is slightly more common in white women (4). Further, the 5-year-survival for stage IV cases (advanced stage cases) is roughly 15% (9). None of these associations, however, is an accurate predictor of disease outcome for recurrence or survival and is especially lacking in prognostic value for stage I patients.

Most women who will experience a relapse event do so within the first three years after initial diagnosis (10, 11). Women who receive a diagnosis of recurrent or metastatic disease have a poor overall prognosis, regardless of treatment modality (12). In contrast to initial diagnosis, current data suggests that histology has no predictive value for treatment response in patients with recurrent disease (13). Presently, there are no markers available that reliably predict either disease recurrence or poor survival. Thus, it is crucial that we identify targets for prevention of disease, markers that predict disease outcome, and targets for new therapies. This type of cancer in particular lends itself to research in this avenue. Immune response in a subset of these cancers, specifically those tumors with DNA mismatch repair defects with microsatellite instability (MSI) and those with Polymerase Epsilon (POLE) mutation that are prone to increased mutation rate, may be the key to survival (14).

Anatomy

Grossly, the body or corpus of the uterus is shaped like an inverted triangle (**Figure 1**). The most inferior portion is continuous with the cervix and is termed the lower uterine segment or isthmus while the remaining superior portion is called the fundus. There are no specific anatomic landmarks to distinguish these two divisions.

2

The uterus itself is composed of three main layers: endometrium, myometrium, and serosa. The serosa constitutes the thin outermost layer of the uterus while the myometrium is the thickest layer composed of smooth muscle fibers. The endometrium is the innermost lining of the uterus. It is comprised of a superficial layer of glandular epithelium and stroma. Endometrial cancer arises from this innermost layer and may manifest in many ways based on anatomical relationships to other structures. Tumor growth may be confined to the endometrial layer. It is possible for tumor to invade to the underlying myometrium and even deeper into and past the serosal surface of the uterus and into the pelvis extending to the rectum, bladder, and into the cervical canal. It is even possible for peritoneal disease to occur via transmigration from the fallopian tubes. Further, given the rich blood supply available, it is not uncommon for distant spread of disease to occur via hematogenous mechanisms. This layer is hormone sensitive causing the thickness to change throughout the menstrual cycle or as a result of stimulation with other hormones (15).

Figure 1. Gross Appearance of a Normal Uterus. Specimen from a young woman includes fundus, lower uterine segment, cervix with vaginal cuff, right and left fallopian tubes as well as right and left ovaries. Image from Anatomy of the Female Genital Tract: https://www.slideshare.net/dreyngerous/anatomy-of-female-genital-tract

Normal Menstrual Cycle Physiology Impacts on the Endometrium

The normal menstrual cycle consists of stimulatory and inhibitory signals that are managed in a tightly coordinated fashion and culminate with the release of a single mature oocyte from one of the ovaries (**Figure 2**). The average menstrual cycle lasts approximately 28-35 days (16, 17). Of these days, 14 to 21 are spent in the follicular phase and about 14 days are spent in the luteal phase. During the early follicular phase, serum estradiol and progesterone concentrations are low due to relatively low hormonal action from the ovaries. In this phase, the endometrium is relatively indistinct due to menses and transitions to a thin line visible by ultrasonography once menses has completed.

The mid-follicular phase begins as follicle-stimulating hormone secretion increases modestly (18). This increases estradiol production resulting in proliferation of the endometrium, which increases in size becoming thicker and also increases the number of glands present in the tissue resulting in a "triple stripe" pattern on ultrasound (19). As the late follicular phase begins, serum concentrations of estradiol and inhibin A increase daily while follicle-stimulating hormone and luteinizing hormone concentrations fall from the negative feedback effects of estradiol. The endometrium gradually thickens during this time due to stimulatory effects of estradiol. Mucus production also increases in this period (20).

Luteal phase occurs when serum estradiol concentrations continue to rise then reach a peak about one day prior to ovulation. During this time, the mid-cycle surge causes a switch from the negative feedback control of luteinizing hormone to a positive feedback effect resulting in a large increase in luteinizing hormone serum concentrations and a modest increase in follicle-stimulating hormone (21). Gradually increasing serum progesterone concentrations during this phase causes cessation of mitoses in the endometrium (22). The glands become more organized. The "triple stripe" is lost on ultrasonography and the endometrium becomes brighter (19).

In middle to late luteal phase, progesterone serum concentrations gradually rise leading to slowing of luteinizing hormone pulses. This decrease in pulsing results in a gradual fall in serum progesterone and estradiol. Decline in both of these hormones leads to loss of blood supply to the endometrium further leading to endometrial sloughing and the beginning of menses (18). After this period, the hypothalamic-pituitary

axis counteracts negative feedback, follicle-stimulating hormone levels begin to rise and

the cycle repeats.
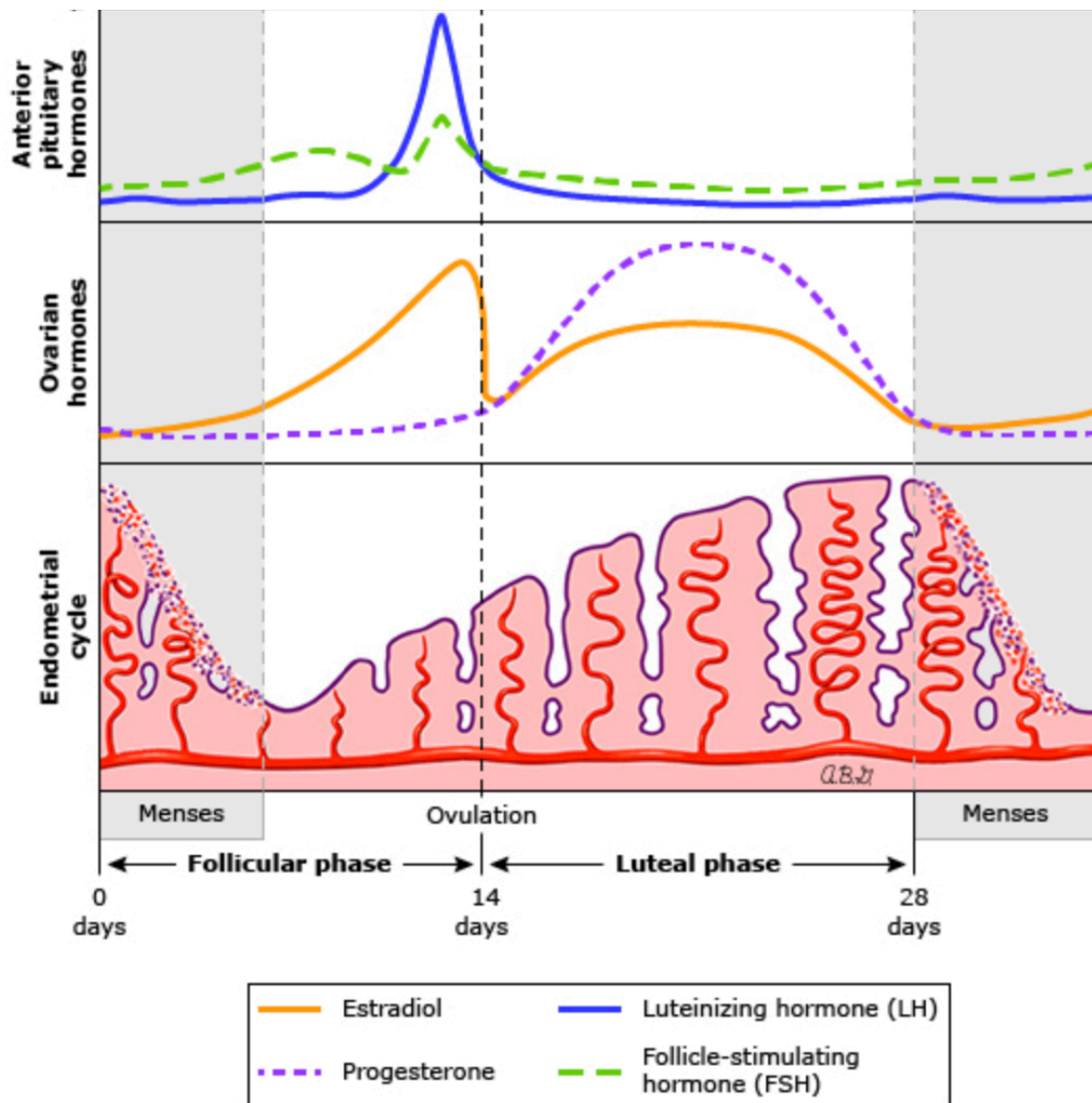
Figure 2. The Normal Menstrual Cycle and Hormonal Changes. Adapted from:

https://www.uptodate.com/contents/image?imageKey=ENDO%2F62189&topicKey=EN

DO%2F7418&source=see_link

Risk Factors

Given the hormone-sensitive nature of the endometrium and the impact estrogen has on endometrial proliferation, it should come as no surprise that one of the risk factors for endometrial cancer development is unopposed estrogen stimulation of the tissue (23, 24). Estrogenic stimulation that is in absence of the appropriate opposition of progestins leads to increased mitotic activity in endometrial cells thereby leading to more frequent errors in DNA replication each division and subsequent potential increase in mutation burden (25). Clinically, these changes can result in endometrial hyperplasia or development of endometrial cancer. The concept of excess estrogens being responsible for increased risk of endometrial cancer development is supported by epidemiological data from patients with nulliparity, early age of menarche, late menopause, and chronic anovulation (26). As these patients have increased estrogenic exposure they too have a greater incidence of developing endometrial cancer. In the past, estrogens were used as part of hormone replacement strategies. This was later defined as a risk factor for endometrial cancer in 1975 when age-adjusted rates for endometrial cancer peaked at 33.8 per 100,000 (27, 28).

Estrone is aromatized from androstenedione in adipose cells and studies have shown that serum concentrations of these steroids are correlated with overall body weight in postmenopausal women (29). In this way, excess adipose tissue is thought to be the mechanism accounting for increased estrogen production and about 17% to 46% of the endometrial cancer incidence in postmenopausal women (29).

As with most cancer types, age is one of the most important risk factors for developing endometrial cancer. Endometrial cancer primarily occurs in post-

menopausal women with the median age of diagnosis being 62 years (6). More than half of all cases are diagnosed in women who are over the age of 50 with only 5% of cases being diagnosed in women younger than 40 (9, 30). The total number of endometrial cancer cases in the United States continues to increase yearly due to an aging population yet the age-adjusted incidence rate has remained stable over the past decade (4).

Further, race seems to dictate a role in endometrial cancer development. The highest endometrial cancer rates occur in northern Europe and North America while being the lowest in Asia and Africa (31). These differences are likely attributable to factors like regional obesity levels, hormone replacement therapy usage, and other reproductive factors. In the United States, non-Hispanic white women have the highest age-adjusted incidence of endometrial cancer compared to Asian, Hispanic, and African-American women (32). However, African-American women have a much higher mortality rate and a lower overall 5-year survival when compared to non-Hispanic white women. At each stage of diagnosis, there is a disparity in better relative survival of about 7% favoring non-Hispanic white women over African-Americans (4). Incidence rates for white women have stabilized over the years while rates for African-American women have continued to rise by about 2% per year since the early 2000s (4). Factors proposed to explain this disparity in racial groups includes differences in the frequency of high-risk tumor types, socioeconomic disparities in access to healthcare, and differences in common comorbidities within the patient populations. African-American women are more commonly diagnosed with higher stage, grade, and poor outcome histologies (33). However, there is not any difference in the recommended therapeutic

strategy to treat the disease in this population (33). African-American race was identified as an independent factor associated with decreased overall survival (OS) and lower likelihood of responsiveness to chemotherapy as compared to white women (13, 34). These results suggest that race influences outcome despite being treated in a similar fashion clinically. This disparity is more likely explained by environmental or social aspects as global gene expression profiles show no clear distinguishing differences between racial groups (35).

While most cases of endometrial cancer are attributed as being sporadic in nature, there are some cases that result from hereditary factors. Hereditary nonpolyposis colorectal cancer (HNPCC), otherwise known as Lynch syndrome, is inherited as an autosomal-dominant trait predisposing an individual to early-onset colon, ovary, rectal, ureter/renal pelvis, small bowel, and endometrial cancers. 2-5% of all endometrial cancers can be attributed to Lynch syndrome (36). Additionally, 10% of women under the age of 50 who are diagnosed with endometrial cancer have the syndrome (36). Lynch syndrome women face a lifetime risk of 50% for endometrial cancer diagnosis which is similar to that of developing colon cancer (37). About half of all Lynch patients have a gynecologic malignancy and a colonic cancer with the gynecologic cancer preceding the colon cancer (38). Women with Lynch syndrome and endometrial carcinoma include lower uterine segment involvement of disease, high-grade disease component in the tumor, and prominent numbers of tumor-infiltrating lymphocytes (39). Lynch syndrome arises most commonly due to germline mutations in the mismatch repair pathway genes *MLH1, MSH2, PMS2* and *MSH6*. An effective

strategy in preventing development of endometrial cancer in these patients is prophylactic hysterectomy (40, 41).

Some patients have an autosomal-dominant germline mutation in the phosphatase and tensin homolog (*PTEN*) gene termed Cowden syndrome. Mutation in this gene confers a lifetime risk of endometrial cancer of between 5-10% (37). Patients with this syndrome develop multiple noncancerous, tumor-like growths termed hamartomas. Hamartomas are most commonly found on the skin and other mucous membranes including the intestines. These growths usually become apparent by the patient's late twenties (42). In addition to being at an increased risk of developing endometrial cancer, patients also face increased lifetime risk of developing breast cancer, thyroid cancer, colorectal cancer, kidney cancer, and melanoma (42). Individuals with Cowden syndrome tend to develop these particular cancers at a younger age (beginning in their thirties or forties) as compared to the rest of the population (43).

Protective Factors

Any factor or treatment that reduces circulating estrogen levels will be protective against development of endometrial cancer for the reasons discussed above. Some examples of estrogen reducing factors include exercise, weight loss, and cigarette smoking (44). Progestins are able to antagonize estrogenic effects to prevent endometrial hyperplasia and in this way, are able to prevent precursor lesion progression to endometrial cancer (45).

Pathologic Evaluation

Classification of uterine tumors was last revised in 2007 (46). The system used is relatively simple and encompasses the vast majority of all endometrial carcinomas. It also allows for the ability to distinguish between neoplasms that have different prognostic outcomes. Two distinctive cell types being present within a single tumor is common and these are referred to as "mixed carcinomas" (46). In these cases, the second component must be minimally 10% of the neoplasm (46).

Grade defines the extent of differentiation of a particular carcinoma. By definition, a grade 1 lesion is well differentiated, and these lesions are usually associated with a favorable prognosis. Grade 2 lesions are intermediately differentiated (moderately well) and have a variable prognosis. Finally, grade 3 lesions are poorly differentiated and likewise typically carry a poor overall prognosis for the patient. By definition, serous, clear-cell and undifferentiated carcinomas are considered to be high grade and do not carry a numerical designation. Endometrioid cell types, including variants and mucinous carcinomas, are classified by architectural criteria as well as nuclear grade (47). Architectural grade is designated as: grade 1 – an adenocarcinoma in which <5% of the tumor growth is in solid sheets; grade 2 – an adenocarcinoma in which 6-50% of the neoplasm is arranged in solid sheets of neoplastic cells; grade 3 – an adenocarcinoma in which >50% of the neoplastic cells are in solid masses.

Precursor Lesions

Endometrial hyperplasia is classified and divided based on architectural features as either "simple" or "complex" and by cytological features as either "typical" or

"atypical" (48). Four subgroups are possible based on this classification scheme: simple hyperplasia (simple + typical), complex hyperplasia (complex + typical), simple atypical hyperplasia (simple + atypical), and complex atypical hyperplasia (complex + atypical).

Simple hyperplasia is defined by an increase in the number of glands contained within the endometrium. These glands may be dilated and slightly crowded as compared to normal or may have an irregular border with crowding. The endometrium itself is thicker than usual, and the stroma is more densely cellular. Foam cells may be present within the stroma. This type infrequently progresses to endometrial cancer.

Complex hyperplasia contains back-to-back glands with most of these glands having irregular outlines, and the endometrium has an increased thickness. The ratio of glands to stroma is much higher than what is observed in simple hyperplasia and there may be very scant amounts of stroma between glands. Mitotic figures are highly variable but epithelial stratification is common with apparent layers of 2 to 4 cells.

Atypical hyperplasia is defined by glandular proliferation with cytological atypia displayed as nuclear enlargement, presence of observable nucleoli, or a change in nuclear morphology from elongated to ovoid or round along with changes in chromatin status. Overall architecture may be classified as simple or complex however in most cases it is complex in nature. **Table 1** summarizes the rate of progression to cancer for each hyperplasia subtype.

Endometrial hyperplasias are commonly resultant from prolonged unopposed estrogen stimulation, and as such, may regress if the estrogenic stimulus is removed or if a source of progesterone or antiestrogen is added to counteract the excess estrogenic effects. In some cases, hyperplasias may coexist with invasive adenocarcinoma or may

themselves progress to carcinomas. Architectural and cytological atypia are indicative of the probability of progression to adenocarcinoma (46, 48, 49).

Table 1. Endometrial Hyperplasia Subtypes and Progression to Endometrial Cancer. Based on the classification scheme devised by Kurman and Norris (48)

Hyperplasia Subtype	% Progression to Cancer
Simple Hyperplasia without Atypia	1
Complex Hyperplasia without Atypia	3
Simple Atypical Hyperplasia	8
Complex Atypical Hyperplasia	29

Endometrial intraepithelial carcinoma is a distinctive precursor lesion of serous carcinoma (50-54). Serous carcinomas most often arise in post-menopausal women in the background of an atrophic uterus or a uterus containing polyps as opposed to the more typical hyperplastic endometrium with unopposed estrogenic stimulation. Occasionally, this lesion will occur in the absence of any detectable invasive carcinoma. In these particular cases, it might be associated with a synchronous serous carcinoma of the peritoneum.

Histologic Classification

Classification of endometrial carcinomas can be made based on the cell types present within the tumor and consists of four major subtypes: villoglandular, secretory, ciliated cell, and adenocarcinoma with squamous differentiation (**Figure 3**). Each of

these classifications is significant in that several hold prognostic values. A breakdown of the occurrence of each type is summarized in **Table 2**.

Endometrial adenocarcinoma constitutes the most common form of endometrial carcinoma comprising approximately 75-80% of all cases (55). This type can vary from undifferentiated to differentiated. In differentiated cases, glands are present and are formed from tall columnar cells that share the same apical side. This results in a round or oval gland formation. As differentiation decreases, solid growth increases and fewer glands are present.

The subtypes of endometrioid adenocarcinoma are as follows:

- Villoglandular carcinomas are a relatively common subtype of endometrial adenocarcinoma (56). This subtype is characterized by fibrovascular cores covered by neoplastic columnar cells. The nuclei of these cells are usually low grade and the cytoplasmic borders are straight on the apical edge. Cells in this type typically resemble cells of other endometrioid adenocarcinomas and maintain a similar average age of diagnosis, depth of invasion, and nodal spread however, they tend to be better differentiated.

- Secretory carcinomas are a rare subtype of endometrial adenocarcinoma representing no more than 2% of cases (57). It is composed of columnar epithelial cells with intracytoplasmic vacuoles similar to those of secretory endometrium. Secretions are not the typical mucin, but glycogen differentiating it from the mucinous type. It is typically well-differentiated,

low grade, and in a glandular pattern. This subtype in particular is significant to identify in that it confers a less aggressive clinical course.

- Ciliated carcimona is very rare. This type of cell growth is identified more commonly in cases of endometrial hyperplasia and benign metaplasia. Prior exogenous estrogen use seems to be an associated factor for development of this subtype and is reported to have a good overall prognosis (58).

- Adenocarcinoma with squamous differentiation constitutes about 10-25% of endometrial adenocarcinomas and contain foci of squamous differentiation. In the past, these tumors were sometimes divided into adenoacanthoma or adenosquamous carcinoma based on whether the squamous component appeared benign or malignant (59, 60). However, a grey area exists for about 30% of these cases as they are not clearly able to be defined as either benign or malignant. This subtype behaves similarly to other endometrioid carcinomas lacking squamous components (61).

Serous carcinoma closely resembles carcinomas of the same type arising from the ovary and fallopian tube. It displays a papillary growth pattern and is usually discovered at an advanced stage in older-aged women. The papillary extensions are typically lined by a layer of epithelial cells which contain almost no cytoplasm. The epithelial cells are strangely shaped, stratified, and display atypism, pleomorphism, increased number of mitotic figures, as well as other unusual forms. The papillary extensions may shed or slough ending in terminal papillary excrescences and single

cells. Irregular gaping glands lined by cuboidal cells with scallop-appearing apical borders may also be present in the deeper tissue layers of the tumor. Lymphatic invasion is common for this type as it invades into the myometrium. Serous carcinomas may be difficult to distinguish from clear-cell carcinomas but often have a greater extent of papillary processes, greater atypia of the nuclei, and less cytoplasm in the cells. Psammoma bodies are common while solid growth is less common.

Serous carcinomas are representative of about 10% of all endometrial cancers. They are particularly aggressive and as such are often deeply invasive and unlike other subtypes tend to spread to the peritoneum. Advanced-stage and recurrence are common even in cases where the initial tumor appears to be only minimally invasive (62-64). Metastatic disease is often identified as microscopic foci. Given this, more than half of patients are typically up-staged after surgical staging is complete. If a serous carcinoma is found to be truly uterine-confined, then it carries a favorable overall prognosis. In contrast, if any extrauterine disease is present, even microscopically, then overall prognosis becomes poor and risk of recurrence is much greater.

Mucinous carcinoma is relatively common in the endocervix but is relatively rare in the endometrium. It has been reported to represent anywhere between 1-9% of all endometrial adenocarcinomas (65). This particular tumor resembles mucinous carcinoma of the ovary or endocervix if the mucinous cell type is the major component of the tumor. Mucinous carcinomas occur in two patterns: in the first, cells are columnar in shape with nuclei oriented towards the basal layer; in the second, cells appear more pseudostratified much like adenocarcinoma of the colon or mucinous carcinoma of the ovary. At least 50% of the tumor must be composed of a given type to be considered as

having that characteristic patterning. These tumors often contain papillary processes or cystically dilated glands lined by columnar epithelium of pseudostratified columnar epithelium. Tumors of this type are characteristically positive for carcinoembryonic antigen (CEA), periodic acid Schiff stain (PAS), and mucicarmine, but are diastase resistant. Distinguishing features from secretory endometrium and clear-cell carcinoma are containing more mucin and less glycogen. Tissue is well-differentiated and maintains glandular architecture (65). Endometrial origin must be validated as these tumors can often appear in the endocervix (66). Histologically, endocervical and endometrial origins cannot be distinguished based on morphology or staining characteristics (67). Endometrial mucinous carcinoma carries the same prognostic values as common endometrial carcinoma.

Clear-cell carcinoma is commonly recognized by the characteristic clearing of the cytoplasm of the neoplastic cells. This lesion may occur as solid, glandular, tubulocystic, or papillary forms and accounts for approximately 4% of all endometrial adenocarcinomas (68, 69). Clear-cell carcinomas of the vagina and cervix commonly result from exposure to diethylstilbestrol (DES). However, in the case of the endometrium, this type is almost exclusively found in post-menopausal women with a mean age of diagnosis of 68 years; similar to the age of diagnosis for serous carcinomas, and about half a decade later than the typical age of diagnosis for the usual endometrial adenocarcinoma. This type has an unfavorable prognosis as it is usually aggressive with a 5-year survival ranging from 20-65%. The hallmark indicator of clear-cell type is indicated by neoplastic cells with cytoplasmic clearing composed of cellular

glycogen. Patterning appears most commonly as a mixture of the four previously mentioned patterns.

Squamous carcinoma is extremely rare and represents less than 1% of endometrial carcinomas and only about 60 reported cases (70, 71). The average age of diagnosis is 65 years of age and occurs mostly in postmenopausal women. Cervical origin needs to be ruled out before this type can be considered a uterine primary. It is commonly associated with cervical stenosis, pyometra, and chronic inflammation. More than half of the reported cases have been confined to the uterus which confers a relatively favorable prognosis. However, in advanced-stage cases, less than 15% of women survive 2 years after initial diagnosis. Unlike other types, histologic grade does not appear to correlate with survival probability.

Mixed cell type carcinoma is the designation given to tumors that manifest two or more different cell types where each type comprises 10% or more of the tumor.

Undifferentiated carcinoma of the endometrium constitutes a distinct tumor type. Histologically, these tumors appear as medium-sized proliferative round or polygonal cells growing in sheets without any specific pattern. No specific differentiation markers of glandular, squamous, or sarcomatous origin are present. In less than one-fifth of cases, epithelial membrane antigen and keratins are detectable. Neurosecretory granules may be present in a small minority of cases and are detectable by immunohistochemical methods. These products are not released into the patient's global circulation and thus no aberrant symptoms have been reported. Behavior of these carcinomas is usually aggressive, and patients present at advanced stages when diagnosed.

Dedifferentiated carcinoma of the endometrium is composed of FIGO grade 1 or 2 endometrioid adenocarcinomas which are adjacent to areas of undifferentiated carcinoma. These tumors appear as malignant cells in sheets with no specific architectural patterning. Dedifferentiated carcinomas are often associated with Lynch syndrome.

Metastatic carcinoma to the endometrium occurs when malignancies from other organs metastasize to the endometrium. The ovaries are the most common site of genital origin. The most common sites of extragenital origin are the breast, stomach, colon, pancreas, and kidneys. Metastatic disease often presents clinically as abnormal vaginal bleeding. Biopsy or curettage is the typical initial specimen presented for evaluation. The disease may appear as a single large focus or many individual or small groupings of cells within normal endometrium and myometrium. In these cases, lymphatics are usually involved. Specific stains for melanin, mucin, or CEA would suggest that the tumor cells are not of endometrial origin. In certain cases, unusual signature cell types, such as signet-ring cells, may be present upon histological evaluation indicating gastrointestinal tract origin. On occasion detection of metastatic disease in the uterus is the first indication of an occult primary lesion elsewhere (72).

Precursors

- Hyperplasia without atypia
- Atypical hyperplasia/endometrioid intraepithelial neoplasia

Endometrial carcinomas

- Endometrioid carcinoma
  - Squamous differentiation
  - Villoglandular
  - Secretory
- Mucinous carcinoma
- Serous endometrial intraepithelial carcinoma
- Serous carcinoma
- Clear cell carcinoma
- Neuroendocrine tumors
  - Low-grade neuroendocrine tumor
    - Carcinoid tumor
  - High-grade neuroendocrine tumor
    - Small cell neuroendocrine carcinoma
    - Large cell neuroendocrine carcinoma
- Mixed cell adenocarcinoma
- Undifferentiated carcinoma
- Dedifferentiated carcinoma

Figure 3. Endometrial Carcinoma Subtypes and Precursors. Adapted from: https://www.uptodate.com/contents/image?imageKey=ONC%2F95023&topicKey=ONC%2F3192&source=see_link

Table 2. Summary of Endometrial Carcinoma Proportions Based on Histology.

Adapted from https://www.uptodate.com/contents/image?imageKey=ONC%2F109367&topicKey=ONC%2F3192&search=villoglandular%20carcinoma&source=outline_link&selectedTitle=2~2.

Histology	Approximate portion of endometrial carcinomas (%)
Endometrioid	77
Mucinous	1
Serous	7
Clear cell	2
Mixed cell type	8
Carcinosarcoma	3
Miscellaneous	1

Natural Course of Disease and Prognostic Factors

Specific characteristics of uterine tumors dictate important aspects of how the disease spreads. Patients can be categorized into high- or low-risk groups based on FIGO stage, grade, extent of myometrial invasion, and lymphovascular space invasion. Categorization based on risk guides the use of adjuvant therapies in treatment plan. Not surprisingly, the patients at highest risk for mortality or recurrence have high FIGO stage disease; disease that has spread outside of the uterus at the time of diagnosis. Surgicopathologic stage has been used due to its validated prognostic utility and clear

superiority over clinical staging. FIGO staging has often been viewed as the strongest predictive factor of outcome for women with endometrial cancer.

Patients with Stage IV disease have intraperitoneal or distant metastatic disease by definition. They also have the poorest prognosis in terms of 5-year survival ranging from 20 to 25% (73). Patients with Stage IIIC disease have nodal metastases and have poorer prognosis over patients without nodal disease. Stage IIIC patients have a 57% 5-year survival rate as compared with 74-91% in the node negative population (Stage I-II)(73). Location of positive nodes is also indicative of outcome. For example, patients with positive pelvic nodes (Stage IIIC1) have a better prognosis over patients with positive paraaortic nodes (Stage IIIC2). In 2009, FIGO staging issued a revision to the stage III criteria to reflect these outcome measures by adding the C1 and C2 designation respectively (74).

Stage IIIA patients have negative lymph node involvement but have involvement of other areas such as the adnexa, serosa, or peritoneal fluids. In 2009, peritoneal fluid cytology was dropped as a stage-defining factor (74). Of the patients with positive cytology (about 12%). 25% will have positive pelvic nodes, and approximately 20% will have metastases to the paraaortic lymph nodes (55).

Of the clinical Stage I-II patients, 6% have disease that has spread to the adnexa. Within this subpopulation 32% will have pelvic node metastases and 20% will have paraaortic node involvement as compared to the less than 10% positive pelvic nodes and about 5% positive paraaortic nodes if adnexal disease was not present (55). About 4-6% of patients with uterine-confined disease will have positive cytological findings. The significance of positive cytology in these patients is under debate, but it is

generally accepted that positive cytological findings carry about the same prognostic significance as adnexal involvement.

Histologic differentiation is used as a surrogate for indicating the degree of tumor spread. Several studies have shown that as grade becomes less differentiated the tendency towards myometrial invasion becomes greater leading to higher rates of nodal involvement in the pelvic and paraaortic regions. Overall survival has also been shown as related to histologic grade.

Depth of myometrial invasion has been correlated with increased probability of extrauterine tumor spread as well as recurrence, treatment failure, and decreased survival probability (75). Prognostic value of myometrial invasion is maintained even in the case of a node negative patient.

Several studies indicate lymphatic space invasion as a reliable indicator of potential recurrence and death. This factor is independent of both histological differentiation and depth of myometrial invasion (76). Findings indicate that lymphovascular space invasion is an indicator of death from early clinical but not early surgical stage disease suggesting that this factor is useful in identifying patients who have spread of disease to lymph nodes or other distant sites. However, the status of this factor becomes less important in patients who have had thorough sampling of lymph nodes with negative results. Lymphovascular space invasion is identified in about 15% of cases of endometrial adenocarcinoma (55, 77). In about a third of these cases pelvic lymph nodes are positive which is about four times more often than if lymphovascular space invasion is negative. Similarly, risk of paraaortic lymph node involvement is 19% representing a six-fold increase over negative involvement. Invasion

is identified in 35-95% of endometrial cancers of serous histologies consistent with increased risk of recurrence or death (78).

Historical Classification System for Endometrial Carcinomas

In 1983, Bokhman suggested a relatively simple classification system for endometrial cancers (79). This system divided cancers into two major etiological pathways: estrogen dependent or estrogen independent. Based on histologic and clinical features, endometrial cancers have typically been divided into type I or type II tumors whose characteristics are summarized in **Table 3**. Between these two groups, type I tumors are more common accounting for about 85% of all cases (79). Additionally, type I tumors tend to be found in younger women and are usually thought to arise via a precursor lesion through atypical endometrial hyperplasia (79). As previously discussed, unopposed estrogens are a risk factor for endometrial cancer development and type I tumors are associated with a history of hyperestrogenism. Type I tumors have a favorable prognosis in that they tend to be well-differentiated as well as having minimal invasion into the myometrium (79). Conversely, type II tumors account for a smaller portion of endometrial cancers (79). Tumors in this group tend to occur in older women and as such most commonly develop in the setting of an atrophic endometrium (79). Of the relapsed cases reported, about half are from tumors falling in this group. Tumors of serous and clear-cell histologies as well as grade 3 tumors fit into the type II category (79).

Table 3. Summary of Comparative Clinical and Molecular Features of Type I and Type II Endometrial Cancers. Endometrial cancers have been historically classified into two groups: Type I and Type II based on estrogen dependency status. Summary characteristics based on (79-81).

	Type I	Type II
Stage and Histology	Include stage 1 or 2 tumors of endometrioid histology	Include stage 3 endometrioid tumors in addition to tumors of non-endometrioid histology
Proportion	~80% of endometrial carcinomas	~10-20% of endometrial carcinomas
Prognosis and Hormone Response	Favorable prognosis: estrogen-responsive.	Tumors are often high grade with a poor prognosis. Not associated with estrogen stimulation.
Precursor lesions	Often associated with endometrial hyperplasia.	Preceded by an intraepithelial neoplasm.
Clinical	Usually younger, heavier white women.	Older, thinner or black women.
Ploidy	Diploid	Aneuploid
PTEN mutation status	Mutant	Non-mutant
P53 overexpression	No	Yes
Microsatellite instability	Present	No
K-ras overexpression	Yes	Yes

Genomic Classification of Endometrial Carcinomas

While the historical classification system provides a simple clinical picture of this disease, molecular features of an individual's tumor, such as DNA mutation frequency

and copy number changes have been proposed to more accurately predict future tumor behavior. Studies from 373 endometrial cancers in The Cancer Genome Atlas (TCGA) of the United States National Cancer Institute defined four major genomic subtypes (82-84).

These groups are:

1) Copy number low, typically low-grade endometrioid histotypes that are microsatellite stable (**MSS**), with near diploid genomes. This group has 16 different genes with frequent alterations in the PI3K pathway (92% of tumors), alterations in the RTK/RAS/β-catenin pathway (83% of tumors), and somatic *CTNNB1* mutations (52% of tumors). This group is comprised of low-grade endometrioid, high-grade endometrioid, serous, and mixed-histology tumors at a rate of 60%, 8.7%, 2.3%, and 25% respectively.

2) Copy number high **(CNH)** high-grade (serous-like) cancers have frequent genomic gain and loss typified by serous histology and *TP53* mutation in 90% of samples as well as amplifications of *MYC* and *ERBB2* oncogenes. This group contained 97.7% of serous carcinomas, 75% of the mixed histology carcinomas, 5% of the low-grade endometrioid endometrial cancers, and 19.6% of grade 3 endometrioid endometrial cancers within the entire cohort of samples.

3) The hyper-mutated microsatellite instability-high (**MSI-H**) group of endometrioid type histology have a defect in DNA mismatch repair and low levels of somatic copy number alterations. However, this group typically has mutations in 21 genes including genes in the RTK/RAS/β-catenin pathway (69.5% of tumors) and the

PIK3CA/PIK3R1 PTEN pathway (95% of tumors). Frequent MLH1 promoter methylation is present leading to decreased *MLH1* gene expression. 28.6% of low-grade endometrioid and 54.3% of high-grade endometrioid endometrial cancers from the cohort fell into this group. *KRAS* mutations were present in 35% of tumors within this group. MSI status itself has not been shown to correlate as a prognostic factor in clinical outcome (85).

4) The ultra-mutated group is characterized by high-grade endometrioid cancers with defects in the polymerase epsilon (POLE) gene exonuclease domain (ultra-mutant **POLE**). Mutation in this gene promotes increased rates of spontaneous mutation leading to tumorigenesis (14). 6.4% of low-grade and 17.4% of high-grade tumors within the cohort fell into this category. POLE tumors are associated with younger age (<60 years of age).

General Clinical Management and Treatment of Endometrial Cancer Patients

Currently, surgical staging is used to define the extent of the disease as well as the risk of recurrence. Additionally, pathologic classification is used in combination with surgical staging to dictate the course of treatment (86-92). Cases are stratified following surgical staging based on the risk of potential relapse and persistent disease. These characteristics are defined by the stage at diagnosis and presence of any prognostic factors.

Preoperatively, the patient is evaluated for surgical risks, possible metastatic spread, and then the most appropriate form of surgical intervention is determined. Patients with endometrial cancer are frequently elderly and suffer from several other

comorbidities such as diabetes, obesity, hypertension, and cardiac disease. In a study conducted with 426 endometrial cancer patients, it was found that approximately 87% had operable qualifications (93). Preoperative assessment occasionally discovers the need to involve consultation from other specialties. Minimally, cardiopulmonary function needs to be assessed to determine potential surgical approaches. A complete blood count (CBC), chest radiograph, electrolyte assessment to check renal function, and electrocardiogram (EKG) are typical initial evaluations in this patient population. As with any surgery, preoperative counseling should also be conducted to inform the patient and obtain permission to remove the uterus, ovaries, and fallopian tubes. Counseling should also include verification of permission to explore, biopsy, and remove disease from the abdominal cavity where it appears present. Possible lymph node removal should also be discussed.

For newly diagnosed cases, treatment course is dictated by stratification of endometrial cancers into risk groups based on risk of disease recurrence characterized by stage of the disease, tumor histology, and other pathological factors, if present. Based on these factors, tumors fall into the low, intermediate, or high-risk group. Endometrial cancers falling into the low-risk group include tumors of grade 1 or 2 endometrial cancer with endometrioid histology. Disease is uterine-confined. Some patients do not undergo nodal evaluation and are considered unstaged. Risk of nodal involvement for these patients is generally <5%, and it is suggested that surgical staging not be performed for this population. Probability of recurrence in this group is very low following surgical treatment and removal of disease. The standard initial approach for this population is surgical staging with total hysterectomy, bilateral salpingo-

oophorectomy (BSO), lymph node evaluation, and evaluation for the presence of extrauterine disease. Local recurrence remains the most likely risk however, this is <5%. Thus, surveillance is recommended following surgery without adjuvant therapy. Women wishing to preserve fertility may be candidates for medically-based therapy such as progestins. Women with low-risk disease have an excellent overall prognosis with expected survival >90% and low recurrence rates (94, 95).

Uterine-contained cancer invading the myometrium or cancer invading the cervical stroma is indicative of intermediate-risk criteria. Patients in this group have a risk of recurrence that is higher than patients with endometrium-confined disease. This group can be further subdivided into low and high-intermediate-risk based on depth of myometrial invasion, whether the tumor is grade 2 or 3, and the presence or absence of lymphovascular invasion. Patients with involvement of the lower uterine segment may be at risk for nodal involvement however, it remains unclear whether this represents an independent determinant of survival outcome. Observation (low-intermediate-risk) or radiation therapy (high-intermediate-risk) are the adjuvant treatment options for intermediate-risk disease. The role of adjuvant chemotherapy in women with high intermediate-risk disease is inconclusive. Some clinicians prefer to offer chemotherapy in a subset of high intermediate risk patients with evidence of lymphovascular space invasion (LVSI). This form of combined treatment is currently being evaluated in clinical trials. Patients with low intermediate-risk disease have an excellent prognosis. Recurrence rates are about 5% without any additional therapy. High intermediate-risk patients have a recurrence rate ranging from 5% with adjuvant radiation to 30% if no

additional treatment is given after surgery (86, 96). Regardless whether radiation therapy is given or not, survival can be expected at a rate above 80%.

Stage III or higher disease defines high-risk cases irrespective of grade or histology. However, serous or clear cell histology are considered high-risk regardless of stage. Women in this group are at high risk for recurrence and death from their disease. This group is clinically heterogeneous and as such there is no universal approach to treatment of these patients. Stage of disease as well as other high-risk features is taken into account when developing a treatment plan. Women with high-risk, stage I or II disease are treated based on presence or absence of myometrial invasion. Observation of myometrial invasion may indicate use of chemotherapy with vaginal brachytherapy, or pelvic radiation alone. Observation may be used in the absence of invasion into the myometrium. Patients with stage III or IV disease are provided adjuvant chemotherapy after surgical resection. In many cases, pelvic radiotherapy is added when high-risk features for local recurrence are present. Patients with stage III or IV disease that is unresectable during surgery are treated with chemotherapy. The use of pelvic radiotherapy in these patients is based on disease burden.

Of the women who have a relapse of their disease, most will occur in the first three years after initial diagnosis. Recurrent disease presents in many forms and may be localized to the vagina, confined to the pelvis, or may be present as metastatic disease with abdominal cavity involvement or involvement of other organs. Clinical evaluation of women with suspected recurrent or metastatic endometrial cancer should include pelvic examination with biopsies of suspect areas, physical examination with

particular attention paid to nodal regions, whole-body imaging to evaluate for potential metastatic disease, and measurement of cancer antigen (CA) 125.

For patients with metastatic endometrial cancer at the time of diagnosis, surgical cytoreduction may be one venue of treatment especially in the case of patients who are newly diagnosed, and complete resection of their disease appears feasible. The preferred treatment regimen is six cycles of carboplatin and paclitaxel. Medical therapy is offered to patients who are not surgical candidates. Women with metastatic disease who are not candidates for surgery have a poor clinical prognosis with a five-year survival of less than 20% (6). Given this, treatment is usually done with the intent of palliation rather than curing the disease.

Thorough physical examination may lead to the discovery of suspicious lymph nodes in the supraclavicular, inguinal, and/or pelvic areas. Pleural effusions, ascites, and omental caking may also be present and detectable. Cervical, vaginal, or adnexal spread may be visualized during the pelvic examination. Chest radiographs are conducted to determine whether spread to the lungs has occurred as well as to assess cardiopulmonary status. Additional studies such as CT scans and MRIs may be conducted. Women who develop metastatic disease are usually administered a combination-based platinum regimen the most common of which are carboplatin plus paclitaxel. Alternatively, the triple drug combination of paclitaxel, doxorubicin, and cisplatin may be used though this particular combination often has greater toxicity than carboplatin and paclitaxel (97, 98). The use of these more intensive treatment regimens has been shown to improve progression-free survival as well as overall survival (99). However, this also increased the occurrence of serious nausea as well as vomiting and

diarrhea. Dual treatment with carboplatin plus paclitaxel resulted in significantly reduced incidence of grade 2 or greater toxicity with sensory neuropathy, thrombocytopenia, emesis, diarrhea, and metabolic dysfunctions when compared to paclitaxel, doxorubicin, and cisplatin triple therapy (97). Patients receiving triple therapy with prophylactic filgrastim however, had a significant improvement in response rates, progression-free survival, overall survival, but an increased risk of serious neuropathy when compared to dual therapy (100).

Endocrine therapy remains a potential therapeutic route for initial treatment of patients who are not candidates for cytoreduction or chemotherapy. This route may also be appropriate as a second-line option for certain patient populations. Patients with grade 1 or 2 endometrioid endometrial cancer, positive estrogen and progesterone receptors, or who are asymptomatic or have minimally symptomatic disease are expected to have a more favorable response to endocrine therapy (101-104). Endocrine therapies harbor a relatively favorable side effect profile and thus are usually well-tolerated by patients as compared to chemotherapy. Response to endocrine therapy is most common in low grade tumors and between 15% and 30% of patients are responsive (104). The vast majority of these responses are either partial or brief in length although some patients may remain in a progression-free state for two years or longer (105). Progestins, tamoxifen, and aromatase inhibitors are some medical options with the aromatase inhibitors having the poorest response rates with less than 10% of the treated patient population responding (106, 107). Limited study sets indicate that hormone receptor expression does not dictate treatment outcomes with these particular agents (106).

After platinum-based chemotherapy, second-line therapies exist based on mismatch repair status and microsatellite stability status as these particular cancers may be especially susceptible to immune checkpoint inhibitors. With this in mind, evaluation of mismatch repair protein status is done for all metastatic endometrial cancers if it has not been evaluated at the time of original diagnosis. Mismatch repair status assists in management of second-line treatment. However, irrespective of the result, all patients with metastatic disease have a poor prognosis and as such should be offered the option of a referral to palliative care. Patients harboring mismatch repair-deficient (dMMR) or microsatellite-instable (MSI) endometrial cancers who have progressed during platinum-based chemotherapy are typically offered endocrine therapy or pembrolizumab, an immune checkpoint inhibitor. Decision for the course of treatment is a joint decision between the patient and doctor. Endocrine therapy may be favored if the tumor is a grade 1 or 2 endometrioid endometrial cancer, if it has positive estrogen or progesterone receptor status, or if the disease is asymptomatic or minimally symptomatic to the patient. A lack of any of these mentioned features would suggest that the patient is a better candidate for immunotherapy. Side effect profile is another consideration when choosing between these two therapeutic strategies. Immunotherapy may cause dermatologic, gastrointestinal, hepatic, endocrine, and other inflammatory events however, these are generally tolerated. Endocrine therapies alternating with tamoxifen are often associated with hot flashes and potential thromboembolic events.

For many advanced solid tumors, immune checkpoint inhibitors have proven effective treatments, this is especially the case for dMMR and MSI tumors (108, 109). The US Food and Drug Administration (FDA) has approved pembrolizumab for the

treatment of dMMR and MSI tumors if the tumors have progressed following first-line treatment and for which a satisfactory treatment alternative does not exist (110). A phase II study was conducting using pembrolizumab which included 9 patients harboring metastatic dMMR disease not of colorectal origin. 71% of these particular patients experienced an immune-related response rate and immune-related progression-free survival (PFS) of 67% (111). Programmed death-ligand 1 (PD-L1) may serve as a biomarker for identifying patients likely to experience favorable outcomes with this treatment course. The KEYNOTE-O28 study was conducted looking at 24 patients with pretreated locally advanced or metastatic endometrial cancers. In these tumors, >1% of the tumor cells had detectable PD-L1. 13% of patients in this study experienced a partial response to treatment and 13% had stable disease over a median timespan of 25 weeks (112). 17% of patients experienced grade 3 toxicities related to the treatment.

For patients with intact mismatch repair proteins who have progressed on platinum-based chemotherapy, second-line treatment modality is dependent on the length of time between the end of first-line treatment and the diagnosis of disease relapse (113, 114).

Common Genetic Alterations and Targeted Therapeutics for Endometrial Cancer

Endometrial cancers harbor common mutations that allow for molecular classification and targeted therapeutics particularly in patients with advanced or recurrent disease. There are several clinical trials aimed at targeting molecular components of this disease in an effort to improve outcomes for patients. Traditionally,

focus is centered around histotype-specific treatment regimens mentioned previously but may also be driven by biomarkers. Evidence suggests that in addition to type I and type II tumors being distinct in histological, genotypic, and phenotypic profiles, patients may also harbor distinct molecular profiles. With this in mind, increasing interest has been placed on personalized therapeutic strategies exploiting biomarkers from the patients' dominant molecular profile.

PI3K/AKT/mTOR pathway is the major signaling pathway which lies downstream of several growth factor receptor kinases such as epidermal growth factor receptor, fibroblast growth factor receptor, platelet-derived growth factor receptor, and insulin growth factor receptor. This particular pathway has been well characterized and is known to modulate cell survival and growth and is most commonly altered in the case of type I endometrial cancers (115). This pathway is summarized in **Figure 4**.
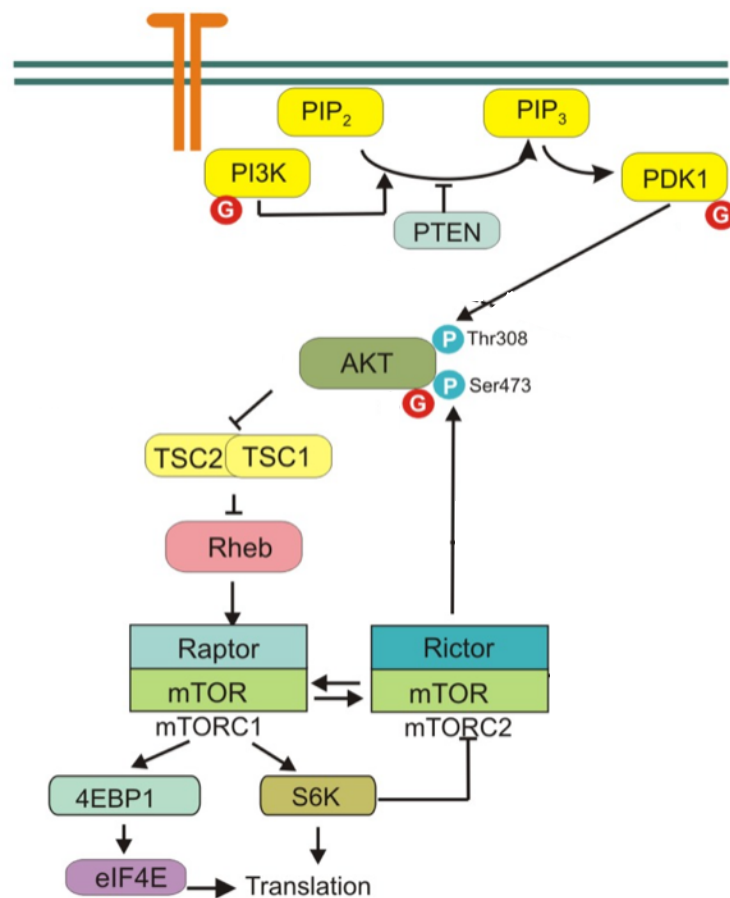
Figure 4. The PI3K/AKT/mTOR pathway. PI3K activation leads to phosphorylation of PIP2 (phosphatidylinositol 4,5-bisphosphate) to the secondary messenger PIP3 (phosphatidylinositol 3,4,5-triphosphate). PTEN regulates the reverse process dephosphorylating PIP3 to PIP2. PI3K activation leads to increases in PIP3 which in turn activates AKT. AKT itself leads to cellular growth, proliferation of cells, increases angiogenesis, and decreases apoptosis. Mammalian target of rapamycin complexes mTORC1 and mTORC2 are two important regulators of this pathway. Adapted from Jozwiak, 2014 (116).

The most common alterations in this pathway are due to loss of PTEN which normally functions as a tumor suppressor through inactivation of PIP3 to PIP2 and PI3K activating mutations of the catalytic domain in the PIK3CA gene. *PTEN* functions include inhibition of cellular migration, inhibition of the ability of cells to spread, and adhesion capabilities. PTEN deficiency leads to activation of the PI3K pathway. About 40% of all endometrial cancers display loss of heterozygosity of chromosome 10q23 leading to possible *PTEN* involvement as this is where the gene is located. *PTEN* mutation is the most frequent genetic alteration in endometrial cancers accounting for 30-50% of tumors. PI3KCA, the catalytic subunit of PI3K, is frequently amplified or mutated in endometrial cancers leading to constitutive pathway activation in 2-14% of type I amplified cases, 46% of type II amplified cases, and mutated in 30% of all cases (117).

mTOR lies downstream of phosphatidylinostinol 3 kinase/PTEN/AKT pathway and contains two subunits named mTORC1 and mTORC2. mTOR is a seronine/threonine kinase family member and is highly conserved. Activated AKT acts to directly phosphorylate mTOR but may also indirectly phosphorylate mTOR by phosphorylating tuberous sclerosis complex 2 (TSC2) which can in turn activate mTORC1. mTORC1 is then able to phosphorylate and activate transcription factors such as ribosomal S6 kinase-1 (S6K-1) and eukaryote translation initiation factor 4E binding protein-1 (4E-BP1). This cascade leads to the synthesis of proteins necessary for proliferation and survival. The actions of mTORC2 are much less well-defined but are thought to activate AKT in response to mTORC1 inhibitors. Temsirolimus, the antineoplastic agent that acts as a mTOR kinase inhibitor, has been tested in

chemotherapy naïve recurrent and metastatic endometrial cancers as part of a phase II trial. It was demonstrated that about a quarter of patients responded to treatment with this drug. Response was seen in all groups regardless of histologic subgroup, grade, or PTEN status. Ridaforolimus is a small-molecule inhibitor of mTOR that has shown some utility in chemotherapy-treated patients.

The *RAS/RAF/MEK pathway* is a key pathway for the regulation of cell cycle progression, proliferation, survival, and angiogenesis (**Figure 5**). Point mutations and gene amplifications of the *RAS* proto-oncogenes has been identified across various malignant tumor types. Endometrioid endometrial cancer and endometrial hyperplasia have been reported as having activating mutations in the *K-ras* gene. Endometrial hyperplasia harboring mutations in this gene suggests its mutation as an early precursor event in cancer development. For the most part *K-ras* mutations have not been linked to tumor grade, depth of myometrial invasion, stage of disease, or overall survival. Activating mutations in this gene may lead to increased PI3K pathway activity independent of traditional signaling. Growth receptors commonly affected in endometrial cancer are directly responsible for control and regulation of this pathway. MEK inhibitors and small molecule inhibitors of RAF kinase are under investigation as possible disease targets. Selumetinib is one such orally deliverable MEK inhibitor. However, due to severe side effects, trials using this drug have been halted. Other trials currently focus on blockade of Ras/Raf/MEK and PI3K/AKT/mTOR pathways simultaneously. Interestingly, metformin may also act as a novel inhibitor of the mTOR pathway.
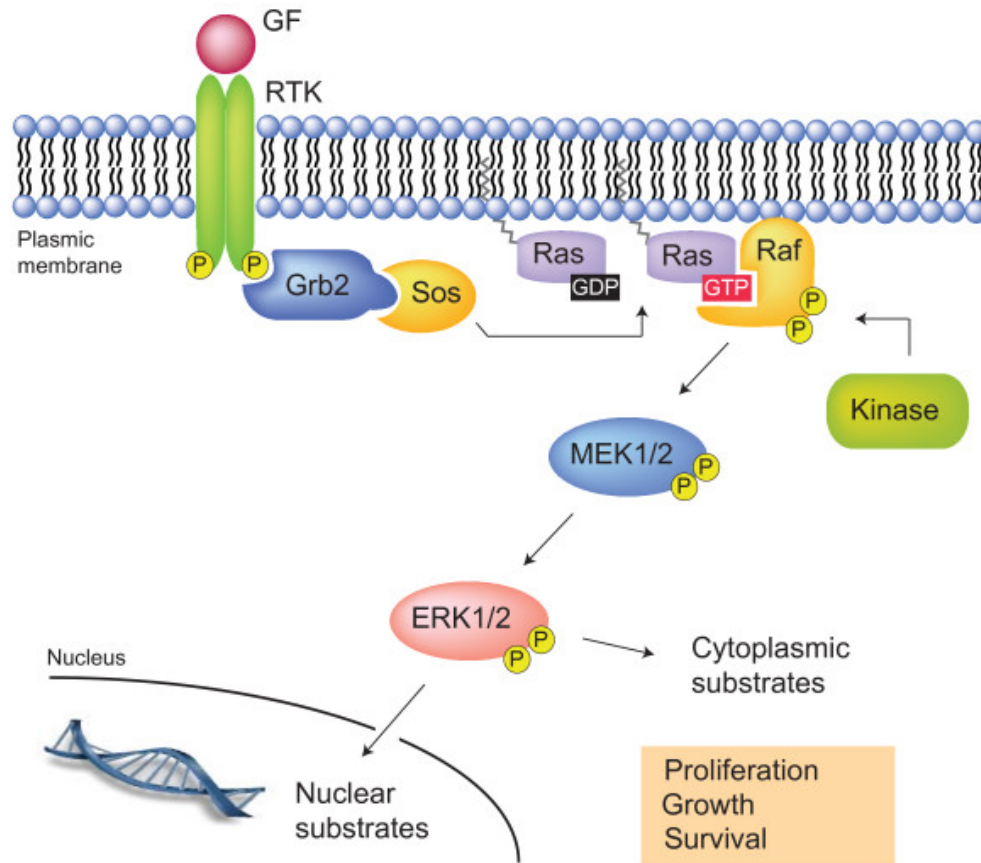
Figure 5. The RAS/RAF/MEK pathway. Adapted from Frémin, 2010 (118).

VEGF overexpression is a negative prognostic factor for endometrial cancer patients as it carries an association with lymph node metastasis and deep invasion into the myometrium. Expression of this protein remains highly variable and depends on histological subtype and stage of disease. The highest levels of expression are observed in early-stage, well-differentiated tumors. Bevacizumab and other such antiangiogenic agents have had mixed results when treating recurrent endometrial cancer. Tyrosine kinase receptor inhibitors such as sunitinib malate are also under investigation.

EFGR/Her/ErbB are a family of genes composed of four tyrosine kinase receptors that are structurally similar. These are epidermal growth factor receptor (EGFR), ErbB2 (aka HER2/neu), ErbB3 (aka HER3), and ErbB4 (aka HER4). Activation of these receptors results in a cascade ultimately leading to cell proliferation and survival. These receptors also have the ability to activate other key pathways such as VEGF, PI3K/AKT, and the Ras/Raf/MEK pathway. Therapies directed at this family include small molecule tyrosine kinase inhibitors such as erlotinib, gefitinib, and lapatinib as well as monoclonal antibodies directed against EGFR such as cetuximab and trastuzumab.

HER2/neu is a proto-oncogene normally expressed at low levels in the normal cycling endometrium. It shares some homology with the epidermal growth factor receptor and is often over expressed or amplified in about a third of type I endometrial cancer cases and up to 80% of type II cases. It is associated with advanced stage of disease, dedifferentiated state, more aggressive cell types, and deep invasion into the myometrium. Despite these correlations, HER2/neu overexpression and/or amplification has not been clearly correlated with disease outcome as some studies show significance while others do not. Thus far, trastuzumab therapy has failed to achieve significant response rates. The small molecule tyrosine kinase inhibitors erlotinib, gefitinib, and lapatinib have also had poor overall response rates in patients.

Microsatellite instability (MSI) is found in approximately 20-45% of type I tumors and 0-5% of type II tumors. It is caused by inactivating alterations in the DNA repair genes *MLH1*, *MSH2*, *MSH6*, and *PMS2*. MSI causes instability in areas of nucleotide repeats by inserting or deleting nucleotides in these areas. This may result in

40

frameshifts and subsequent inactivation of genes such as PTEN. As previously discussed, MSI was originally described in the context of HNPCC and endometrial cancer remains one of the most common extracolonic tumors associated with this disease. MSI has been reported in both hereditary and sporadic cases. MSI has been reported to occur in anywhere between 9% and 43% of all endometrial cancers. Hypermethylation of the *hMLH1* promoter has been found in between 71% and 92% of sporadic endometrial carcinoma cases and is less common in the *hMSH2* promoter region. Promoter methylation is likely an important mechanism of gene inactivation and development of MSI within tumors. The importance of MSI remains debated but defects in mismatch repair potentially alter tumor responsiveness to radiation and chemotherapy. *PTEN* mutation and MSI resultant from hypermethylation appear to be very common and early alterations in cancer progression for type I cases.

TP53 acts as a tumor-suppressor gene. The protein product of this gene is involved in maintenance of the G1 cell cycle checkpoint. Thus, mutations permit replication of cells that have acquired mutations. *p53* gene mutations produce a protein product with a longer half-life leading to protein accumulation inside the cell. This protein may also be overexpressed in its wild-type form due to DNA damage and is detectable by immunohistochemical methods. Alterations of this gene appear to be an early event in the development of serous endometrial cancers and have also been correlated to other unfavorable prognostic factors such as clear-cell histology, higher stage at diagnosis, higher histological grade, and greater depth of myometrial invasion. However, in the case of endometrioid endometrial cancers, p53 alteration seems to be a late event and is indicative of poorer prognosis for patients. Mutations of p53 are not

commonly found in type I low-grade endometrioid tumors further lending to the idea that different molecular subgroupings of endometrial cancers exist (**Figure 6**).

Poly adenosine diphosphate ribose polymerase (PARP) consists of a family of multifunctional enzymes that are located in the nucleus and act as mediators for DNA repair machinery in the base-excision repair (BER) pathway. PARP inhibitors are able to confer their anti-neoplastic activity through enhancement of genomic stability in cancer cells. Many cancer cells harbor intrinsic deficiencies in the homologous recombination (HR) pathway, by targeting DNA repair pathways synthetic lethality is obtained. Loss of PTEN is typically a component of the BRCA-like phenotype. Repair of DNA double-stranded breaks via homologous recombination is impeded, creating a susceptibility to PARP inhibition in these cancer cells. *In vitro* data suggests a role for mutated PTEN status in PARP inhibition susceptibility. This observation provides rationale for utility of PARP inhibitors for type I endometrial cancer cases where about 80% of tumors will harbor an alteration in PTEN (**Figure 6**). Olaparib, veliparib, and iniparib are some PARP inhibitors.

CHAPTER 2: In silico and bioinformatic analysis.

Introduction

Molecular evidence further supports the separation between the two broad (Type I/Type II) groupings as type I tumors rarely have *TP53* mutations while these are frequent in type II cases (**Figure 6**) (80). Type I tumors frequently harbor mutations in the *PTEN* gene and overexpress *K-ras*, and display microsatellite instability whereas these alterations are rare in the type II setting. Type I lesions tend to be diploid while type II lesions display aneuploidy. Further, global gene expression profiles between type I and type II tumors have been shown to be different suggesting utility for this classification system (81).
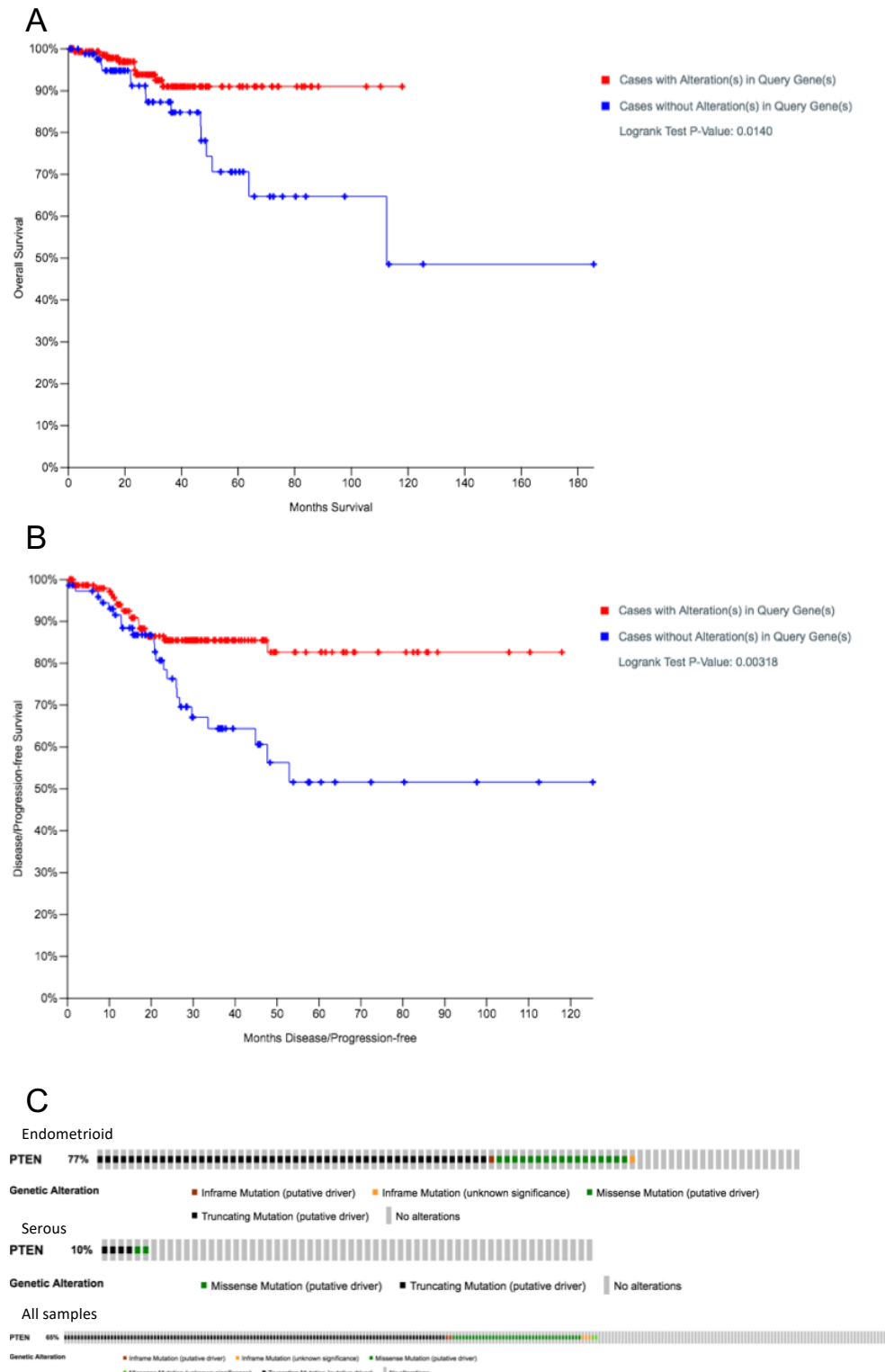
Figure 6. *PTEN* and *TP53* **Mutation Status and Survival from TCGA.**

Figure 6 (cont'd)

D

E

F

Endometrioid

Serous

All samples
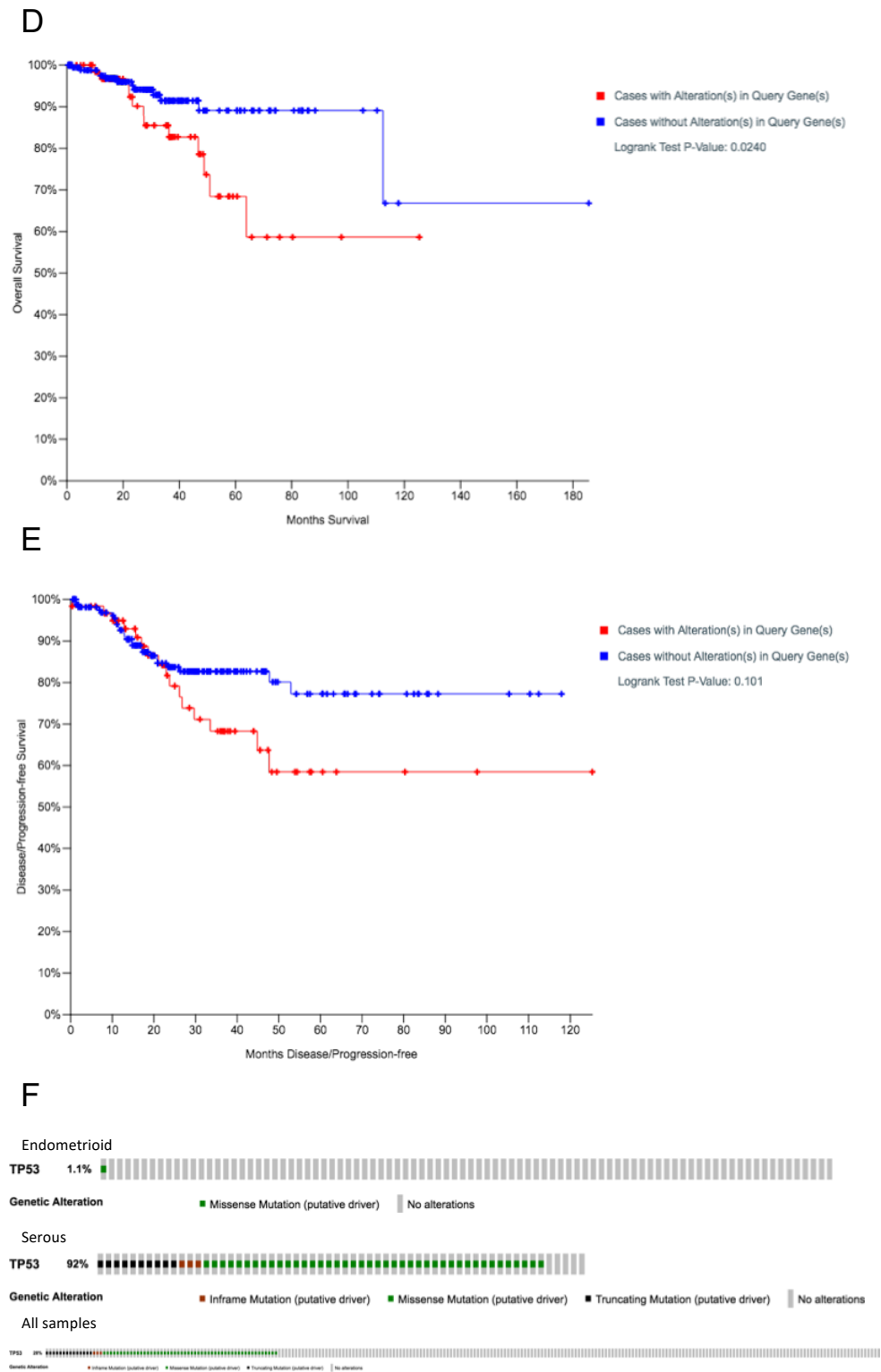
Figure 6 (cont'd)

A. Overall survival for *PTEN* mutation cases. **B.** Progression-free survival for *PTEN* mutation cases. **C.** *PTEN* mutation status based on histotype. **D.** Overall survival for *TP53* mutation cases. **E.** Progression-free survival for *TP53* mutation cases. **F.** *TP53* mutation status based on histotype.

While the historical classification system provides a simple clinical picture of this disease, molecular features of an individual's tumor, such as DNA mutation frequency and copy number changes have been proposed to more accurately predict future tumor behavior. Studies from 373 endometrial cancers in The Cancer Genome Atlas (TCGA) of the United States National Cancer Institute defined four major genomic subtypes (82-84).

As previously mentioned in the introduction, these groups are:

1) Copy number low, typically low-grade endometrioid histotypes that are microsatellite stable (**MSS**), with near diploid genomes. This group has 16 different genes with frequent alterations in the PI3K pathway (92% of tumors), alterations in the RTK/RAS/β-catenin pathway (83% of tumors), and somatic *CTNNB1* mutations (52% of tumors). This group is comprised of low-grade endometrioid, high-grade endometrioid, serous, and mixed-histology tumors at a rate of 60%, 8.7%, 2.3%, and 25% respectively.

2) Copy number high **(CNH)** high-grade (serous-like) cancers have frequent genomic gain and loss typified by serous histology and *TP53* mutation in 90% of samples as well as amplifications of *MYC* and *ERBB2* oncogenes. This group contained

97.7% of serous carcinomas, 75% of the mixed histology carcinomas, 5% of the low-grade endometrioid endometrial cancers, and 19.6% of grade 3 endometrioid endometrial cancers within the entire cohort of samples.

3) The hyper-mutated microsatellite instability-high (**MSI-H**) group of endometrioid type histology have a defect in DNA mismatch repair and low levels of somatic copy number alterations. However, this group typically has mutations in 21 genes including genes in the RTK/RAS/β-catenin pathway (69.5% of tumors) and the PIK3CA/PIK3R1 PTEN pathway (95% of tumors). Frequent MLH1 promoter methylation is present leading to decreased *MLH1* gene expression. 28.6% of low-grade endometrioid and 54.3% of high-grade endometrioid endometrial cancers from the cohort fell into this group. *KRAS* mutations were present in 35% of tumors within this group. MSI status itself has not been shown to correlate as a prognostic factor in clinical outcome (85).

4) The ultra-mutated group is characterized by high-grade endometrioid cancers with defects in the polymerase epsilon (*POLE*) gene exonuclease domain (ultra-mutant **POLE**). Mutation in this gene promotes increased rates of spontaneous mutation leading to tumorigenesis (14). 6.4% of low-grade and 17.4% of high-grade tumors within the cohort fell into this category. POLE tumors are associated with younger age (<60 years of age).

These four molecular classifications, in particular the POLE and MSI-H groups, highlight a significant role for the patient's immune system in controlling spread of their endometrial cancer and define distinctive prognostic markers (119-125). For example,

the ultra-mutant POLE group consists of high-grade cancers which is a pathological feature associated with poor patient outcome. Despite being high-grade, cancers in this group rarely metastasize to cause patient death (82). The favorable outcomes experienced by these patients are thought to be due to active immune recruitment and surveillance of tumor cells. Selected immune genes from TCGA data are summarized in **Figure 7**. Supporting studies have shown that these tumors have increased tumor infiltrating lymphocytes (TIL) and upregulated expression of TIL markers (119, 120).

Gene	MSI	MSS	POLE	POLE/ MSS	POLE / MSI	p vs MSS	p vs MSI
CD8A	166	86	247	2.87	1.491	0.003	0.407
CD3E	277	183	386	2.11	1.393	0.03	0.447
CD3G	13	10	18	1.83	1.431	0.032	0.253
CD2	178	116	242	2.09	1.361	0.013	0.369
CD4	667	762	744	0.98	1.114	0.795	0.61
TBX21	14	11	23	2.06	1.638	0.006	0.171
EOMES	10	8	17	2.29	1.708	0.006	0.071
LCK	160	133	256	1.93	1.596	0.055	0.215
IFNG	8	3	13	4.16	1.565	3E-04	0.142
PRF1	121	94	232	2.48	1.921	0.002	0.042
GZMA	90	88	135	1.53	1.503	0.37	0.525
GZMB	104	56	160	2.84	1.542	0.005	0.219
GZMH	33	24	63	2.62	1.895	0.007	0.067
GZMK	42	35	60	1.70	1.424	0.042	0.301
GZMM	27	21	40	1.94	1.486	0.047	0.246
CXCL9	288	81	802	9.87	2.782	2E-07	0.028
CXCL10	199	111	471	4.25	2.367	1E-04	0.048
PDCD1	50	30	81	2.70	1.606	0.005	0.328
CD274	10	9	20	2.20	2.051	0.015	0.078
LAG3	123	57	238	4.20	1.935	2E-06	0.035
HAVCR2	129	120	180	1.51	1.400	0.041	0.115
TIGIT	51	21	88	4.26	1.732	7E-06	0.194
HLA-DPA1	2253	2702	3127	1.16	1.388	0.836	0.414
HLA-DPB1	2196	2732	3267	1.20	1.488	0.795	0.28
HLA-DQA1	807	911	1504	1.65	1.865	0.12	0.074
HLA-DRA	6955	10020	10497	1.05	1.509	0.94	0.26
HLA-DRB1	4143	6156	6580	1.07	1.588	0.898	0.219
CXCR5	16	9	30	3.35	1.922	3E-04	0.12
CXCL13	79	13	170	12.78	2.156	2E-05	0.34
CTLA4	25	21	50	2.43	1.959	0.02	0.144
FOXP3	62	33	80	2.43	1.280	4E-05	0.29
CD19	14	16	26	1.66	1.879	0.159	0.134
MS4A1	17	7	29	3.98	1.666	0.008	0.409
BLK	8	5	8	1.63	1.019	0.043	0.436
IL1A	9	5	10	2.08	1.046	0.328	0.982
IL1B	66	62	64	1.03	0.964	0.748	0.919
IL8	149	180	159	0.88	1.064	0.871	0.642

Figure 7. Heat Map of TCGA RNA-Seq data for Immune Genes. A direct comparison of the transcriptome of copy number low MSS, to hyper mutant MSI and ultra-mutant POLE mutant cancers identified several significant increases in immune genes to

Figure 7 (cont'd)

include upregulation of CXCL9 p=0.0000002 and CD8 p=0.003 among others. Immunologic gene expressions from TCGA. MSS (n=90), MSI (n=65), POLE (n=17). Heat map shows mean centered expressions. RSEM-normalized mean counts, and POLE vs. MSS and POLE vs. MSI p values of two-sided Mann-Whitney test.

Study Background

Despite advances in treatment of other cancer types, the treatment modalities for endometrial cancer have remained essentially unchanged for several decades. Unlike many other types of cancer, the prevalence of endometrial cancer is increasing overall due to increases in rates of obesity, long-term exposure to exogenous or endogenous estrogen, diabetes, and hypertension (89, 126). Treatment strategies are subject to the experience level and biases of the surgeon, pathologist or radiation oncologist, potentially leading to suboptimal treatment (127-132). Given these factors, there is a need to identify and classify new potential diagnostic and therapeutic targets in the genesis of endometrial cancer in order to more accurately tailor an individualized treatment regime. Additionally, it is necessary to identify markers that predict more aggressive cancers and to develop novel model systems for this disease.

To identify such genetic targets, I conducted a transcriptome analysis of 136 endometrial cancers from women who either experienced an event (meaning they died from their disease or had a recurrence of disease) or from women with cancer that did not experience such an event. As an initial assessment, I performed unsupervised clustering on the 136 transcriptome samples to determine if any gene expression signatures were readily apparent (see Methods section for details). These samples did

not cluster by outcome in an unsupervised analysis (**Figure 8).** In these samples however, I found a clustering of upregulated genes in the women who experienced an event (**Figure 9**). Next, I cross-validated these genes The Cancer Genome Atlas (TCGA) by manually searching each gene and assessing the significance of that gene's expression with endometrial cancer survival or relapse. For a full detailed procedure, please see Chapter 4. From comparison of the two datasets, I narrowed in on a particular gene, *CXXC5* which, when overexpressed in an endometrial tumor, is highly predictive of negative outcome (recurrence or death of the patient) (see **Figure 18** and **Figure 19**). Using a third independent human dataset from our partners at Spectrum Health, I confirmed yet again that high transcript level of *CXXC5* correlates with detrimental outcomes (**Figure 24**). Current literature contains little information on how the protein coded by this gene functions in the endometrium and what possible role CXXC5 could have in contributing to a more aggressive cancer phenotype.

Additionally, it has been recently shown that certain subsets of ultramutable endometrial cancers activate the host immune system to a greater extent than other cancers (133). In this dataset, I have also found an enrichment of immune-associated genes that are strongly up-regulated in ultramutable cancers (**Figure 7**). While correlations between immune activation and favorable survival outcomes have been made, specific mechanisms have yet to be determined as immune-competent animal models are lacking for this particular cancer, especially those developing distant metastatic disease (119, 120, 134).
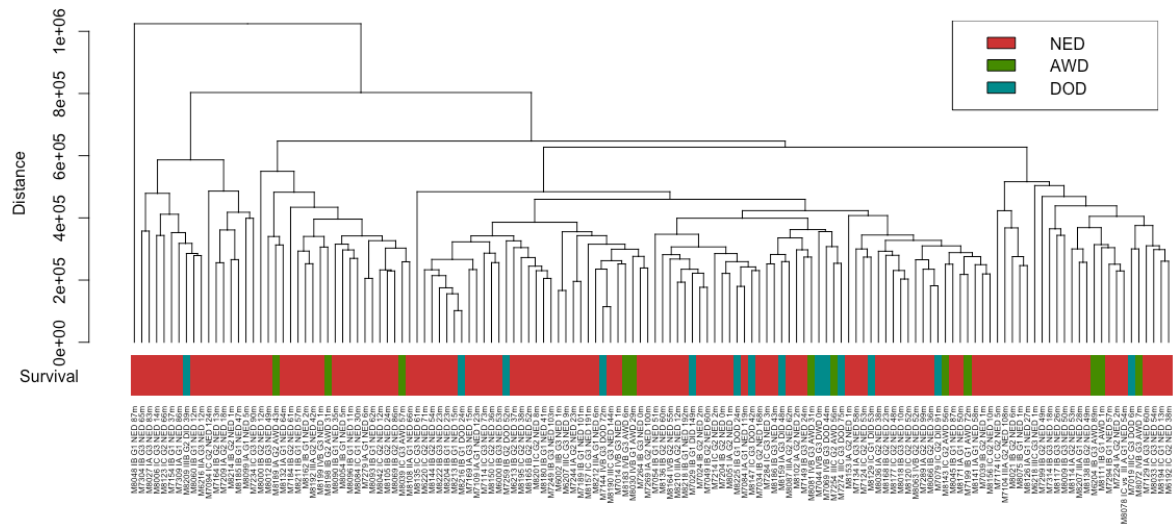
Figure 8. Unsupervised clustering of discovery dataset samples. NED = no evidence of disease, AWD = always with disease, DOD = died of disease. Results indicate random clustering based on disease outcome. N=136. Analysis was conducted as detailed in Methods.
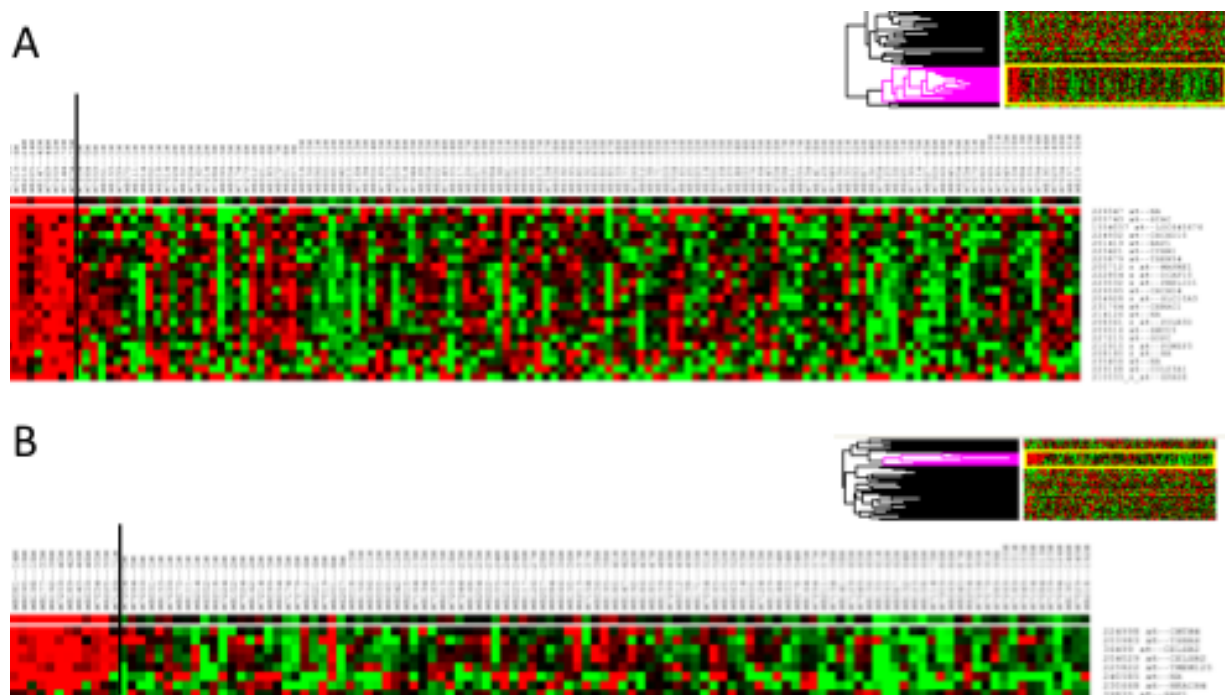
Figure 9. Transcriptional upregulation is associated with overall survival and disease relapse. A. Supervised clustering of overall survival analysis considering cases that died with disease as died cases. N = 9 and 127 in died and other cases respectively. **B.** Supervised clustering showing relapsed and non-relapsed analysis for endometroid histology only samples n=13 in relapsed group and 107 in non-relapsed group.

Due to lack of available information on CXXC5 in relation to the endometrium I aimed to evaluate a potential role for CXXC5 in normal endometrial tissue and in the formation of endometrial cancer. It is well known that gene dosage can have a significant impact on cellular function (135, 136). With this in mind, it might be possible to exploit abnormal gene fingerprints in predicting poor outcome cancers. I chose to focus on genes with a high hazard ratio, which suggests that these genes are associated with poor outcome (**Table 10, Table 11,** and **Table 12**). *CXXC5* is

upregulated on a transcript level and because of this I hypothesize is more likely to be deregulating either one or several cellular pathways. The specific hypothesis tested was whether this gene will modify either one or multiple critical cellular pathways and, when overexpressed, can create permissive growth regulation through protein interactions or chromatin remodeling. We predicted that an upregulated transcript level is leading to increased protein expression and that the protein product of this gene, in particular, is contributing to a more aggressive cancer.

Therapeutic strategies have not significantly improved for decades in treating this disease, particularly in the context of highly advanced metastatic cases. With this in mind we sought to develop and classify a novel murine model of endometrial cancer that forms distant metastatic disease in the lungs under immune-competent conditions. The model we developed is orthotopic and uses a mouse endometrial cancer cell line. It was made based on the flow chart depicted in **Figure 10**. The bioinformatics detailed in the chapter laid the basis for the work surrounding *CXXC5* described later in Chapter 3 while the immune gene component laid the foundation for the mouse modeling work later described in Chapter 4.
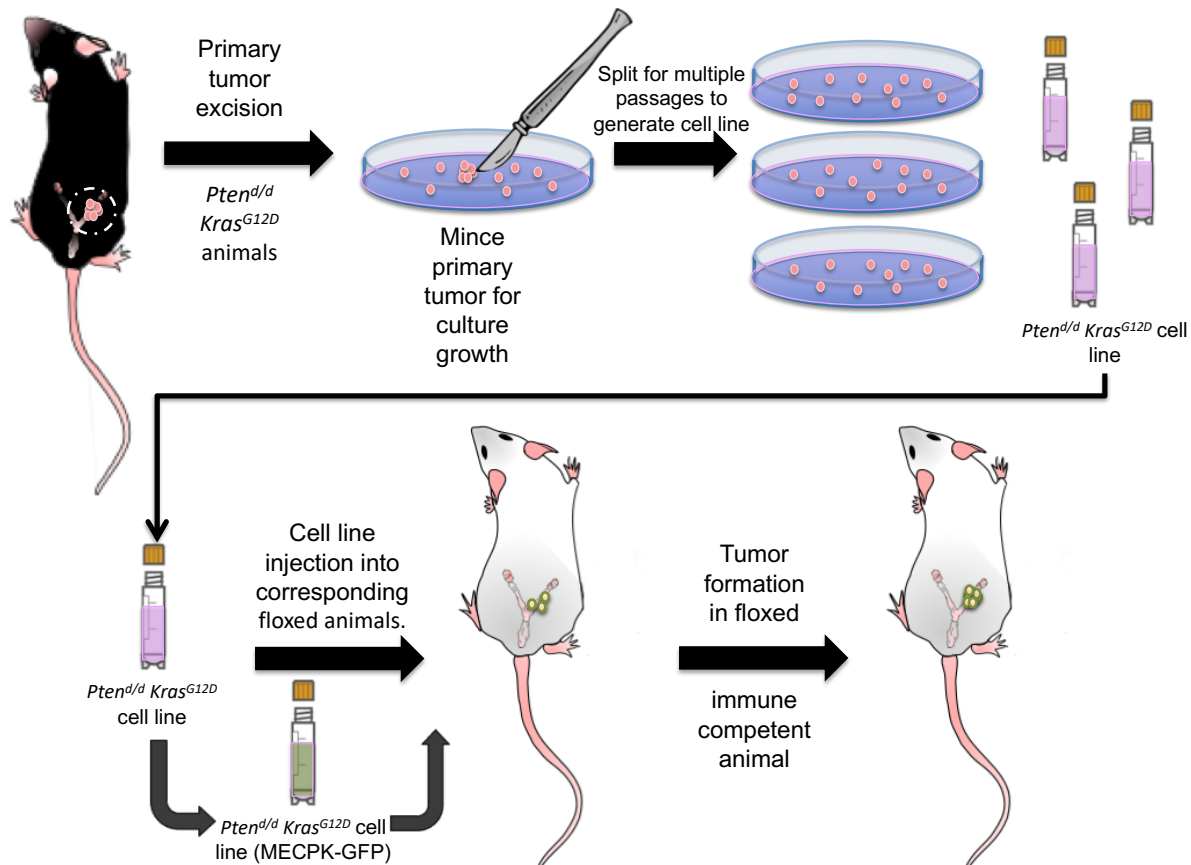
Figure 10. Formation of an Orthotopic Endometrial Cancer Mouse Model. In generation of the orthotopic model, primary tumor tissue was harvested from a genetically modified animal previously characterized in (137). This tissue was cultured to generate cell colonies which were further passaged until a cell line was generated (MECPK) and used in the studies described later in Chapter 4.

Significance

Unlike many other types of cancer, the prevalence of endometrial cancer is increasing overall and despite endometrial cancer having a 5-year survival rate similar to that of breast cancer; it has received far less attention in both research and public

media settings (1). Risk of recurrence and extent of disease are evaluated at the time of surgery, during which tissue samples are gathered and sent to a pathologist for histologic classification. Surgical staging and histologic classification comprise the two main considerations that dictate the treatment regimen for each patient (2, 3, 86-88, 96, 126, 138). While routine, these evaluations are subject to bias and experience level of the physician and may lead to suboptimal treatment of the patient's disease (89-92, 127-132). Thus, this disease in particular would benefit significantly from any sort of prognostic test to predict "bad acting" tumors. Identification of prognostic markers could lead to novel therapeutic targets that would allow advancement in the treatment of this disease (133). I have found that certain gene transcripts, when overexpressed, correlate significantly with relapse and/or death from endometrial cancer (**Table 8, Table 9,** and **Figure 16**). This suggests that high transcription levels of these genes may be driving the cancer's aggressiveness and could lead us to better outcome markers and drug targets. Gene Ontology (GO) Analysis of survival associated transcripts implicates the immune response in better prognosis (**Table 4**). We utilized gene ontology to aid in our understanding of the potential functions of the survival associated genes that we identified by cox regression in the TCGA data set. We identified 273 transcripts associated with overall, disease free survival or both at p<0.001 (**Table 8** and **Table 9**). GO analysis implicated the immune system and specifically the T-cell receptor complex and its low hazard associated transcripts as being associated with favorable OS (**Table 4**). Ontology for DFS implicates high hazard ratio transcripts from a variety of molecular functions or processes as most significant. These data suggest that survival but not recurrence itself is most impacted by immune response. Using data from laser captured

55

samples we have found an overrepresentation of genes related to immune function that act as predictors of cancer survival. An understanding of the immune mechanism that leads to better prognosis could unlock the key to improving prognosis for all endometrial cancer patients. This study was designed to address the most critical problem facing patients with this disease and the clinicians who treat them; discovering better and/or additional markers for survival and possible drug targets for poor prognosis endometrial cancers.

Table 4. Summary of GO Analysis Immune Functioning Genes. 273 transcripts associated with overall, disease free survival or both at p<0.001.

System	Gene Category	Up	Down	Total Significant	List Total	Population Hits	Population Total	EASE score	Genes (Red: HR > 1 , Green HR < 1)
GO Biological Process	immune response	5	20	25	255	731	13292	0.00684	CRH, CRHR1, GAGE2E, MGST3, PTX3, BATF, CTSW, FCGRT, KLRK1, CXCR3, FASLG, KLRB1, LSP1, LTA, LTB, XCL1, XCL2, ZAP70, MADCAM1, TNFRSF14, CD2, CD3D, CD3E, IL32, CD40LG
GO Cellular Component	T-cell receptor complex	0	3	3	250	7	12984	0.00722	CD3D, CD3E, CD247
GO Cellular Component	immunological synapse	0	3	3	250	7	12984	0.00722	CD3D, CD3E, CD247

Methods

TCGA survival curves were created online using data from the Nature 2013 Uterine Corpus Endometrial Carcinoma dataset located at https://www.cbioportal.org/. TP53 and PTEN mutations were selected and run for the endometrioid and serous histotypes individually considering disease free survival and overall survival.

Unsupervised cluster analysis was conducted using the R environment. An Affymetrix array expression dataset of >47,000 transcripts across 136 tumor samples was read in as a CSV file and clustered using the Elbow, Silhouette, and Gap statistic

methods using pre-defined libraries in R. The dataset was collected and described previously in (139). The full code used in the analysis is shown below:

```
library("cluster")

library("factoextra")

library("magrittr")

library("robustbase")

library("NbClust")

library(factoextra)



r<-read.csv('JR_SURAsig.csv',header=T)



affy<-r[1:54675,1:142]

rownames(affy)<-affy[,1] # make the first col of raw data the row names

affy<-affy[,2:142] # just retain columns with data



#affy<-affy[1:100,2:141]



df<-affy
# Elbow method
png('AffyElbowCluster.png')
```

```r
fviz_nbclust(df, kmeans, method = "wss") +

  labs(subtitle = "Elbow method")

dev.off()


# Silhouette method

png('AffySilhouetteCluster.png')

fviz_nbclust(df, kmeans, method = "silhouette")+

  labs(subtitle = "Silhouette method")

dev.off()


# Gap statistic

# nboot = 50 to keep the function speedy.

# recommended value: nboot= 500 for your analysis.

# Use verbose = FALSE to hide computing progression.

set.seed(123)

png('AffyGapStatCluster.png')

fviz_nbclust(df, kmeans, nstart = 25,  method = "gap_stat", nboot = 50)+

  labs(subtitle = "Gap statistic method")

dev.off()


# res.hc <- affy %>%

#   na.omit() %>%
```

```
#   scale() %>%                 # Scale the data

#   dist(method = "euclidean") %>% # Compute dissimilarity matrix

#   hclust(method = "ward.D2")     # Compute hierachical clustering

#

#

# # Cut in 4 groups and color by groups

# (a<-fviz_dend(res.hc, k = 3, # Cut in 3 groups

#           cex = 0.5, # label size

#           k_colors = c("#2E9FDF", "#FC4E07", "#E7B800"),

#           color_labels_by_k = TRUE, # color labels by groups

#           rect = TRUE # Add rectangle around groups

# ))

#
```

Discussion

The survival-associated transcripts in this study are likely to be more predictive of prognostic outcome than other proposed molecular markers as they were specifically selected to predict these outcomes. Several genes highly mutated in endometrial cancers like the PTEN tumor suppressor have consistently been shown to be associated with good outcome in endometrial cancers (140, 141). However, there are few genes reproducibly associated with poor outcome. Of these we were the first to associate the over-expression of the FOLR1 gene in endometrial cancers with poor prognosis following a similar array based discovery effort as later described (142, 143).

Even though this discovery has led to the inclusion of endometrial cancer patients into anti-FOLR1 therapy clinical trials, many women with FOLR1 negative cancers will recur and die. Furthermore, the most consistently cited and dogmatically proposed prognostic biomarker for poor outcome in endometrial cancer is the TP53 tumor suppressor gene. Mutation and subsequent protein stability have been frequently described for TP53 in advanced endometrial cancer (80, 144, 145). However, TP53 mutation has not consistently predicted survival in some studies and does not predict either OS (Logrank Test P-Value: 0.132635) or DFS (Logrank Test P-Value: 0.123667) in the extensive TCGA data. Taken together these data suggest that new and more effective markers are needed. Furthermore, our methods completed both a discovery phase as well as a validation phase involving hundreds of cancers leading to increased reliability and reproducibility.

CHAPTER 3: An immune competent orthotopic model of endometrial cancer with metastasis.

Abstract

Endometrial cancer is the most common gynecologic malignancy in the U.S. with metastatic disease remaining the major cause of patient death. Therapeutic strategies have remained essentially unchanged for decades. A significant barrier to progression in treatment modalities stems from a lack of clinically applicable *in vivo* models to accurately mimic endometrial cancer; specifically, ones that form distant metastases and maintain an intact immune system. To address this problem, we have established the first immune competent orthotopic tumor model for metastatic endometrial cancer by creating a green fluorescent protein labeled cell line from an endometrial cancer that developed in a $Pgr^{cre/+}Pten^{f/f-}Kras^{G12D}$ genetically engineered mouse. These cancer cells (Mouse Endometrial Cancer PTEN deleted K-ras activated - MECPK) were grafted into the mechanically abraded uterine lumen of ovariectomized recipient mice treated with estrogen and subsequently developed local and metastatic endometrial tumors. We noted primary tumor formation in 59% and 86% of mixed background and C57BL/6 animals respectively at 4 weeks and distant lung metastases in 78% of mixed background mice after 2 months. Importantly this model is driven by PTEN and KRAS mutations, which are commonly found in human endometrial cancer. Immunohistochemical analysis indicates that tumors from this model are similar to human endometrial cancers with activated AKT and ERK pathways. This orthotopic tumor model is the first immunocompetent animal model that closely resembles human metastatic endometrial cancer, modeling both local metastasis and hematogenous

spread to lung and has significant potential to advance the study of endometrial cancer and its metastasis.

Introduction

An estimated 61,380 new patients will be diagnosed with endometrial cancer in 2017 making it the most common gynecologic malignancy in the United States and the fourth most common cancer in women (6). Metastatic disease represents the major cause of death with five-year survival predicted to be 16.2% if distant spread is present (9, 146, 147). Although survival is so poor for patients with metastases the treatment modalities have remained essentially unchanged for several decades (148, 149) and unlike many other types of cancer the prevalence of endometrial cancer is increasing overall (9, 146, 150). Currently, surgical staging is used to define the extent of disease as well as the risk of recurrence. In combination with surgical staging, pathologic classification is used to dictate the course of treatment for these women (86-92). Surgical staging and histological evaluation, however, are often imprecise and may be subject to the experience level and biases of the surgeon, pathologist or radiation oncologist, leading to suboptimal treatment (127-132).

Recently, molecular features such as DNA mutation frequency and copy number changes have been proposed to more accurately predict future tumor behavior by dividing this cancer into four subgroups (82). These groups are 1) copy number low, typically low-grade endometrioid histotypes that are microsatellite stable (**MSS**), with near diploid genomes and frequent *PTEN*, *KRAS*, *ARID1A*, *CTNNB1* and *AKT* mutations, 2) copy number high **(CNH)** high-grade cancers with frequent genomic gain

and loss typified by serous histology and *TP53* mutation, 3) the hyper-mutated microsatellite instability-high (**MSI-H**) group of endometrioid type histology with a defect in DNA mismatch repair and 4) an ultra-mutated group characterized by high-grade endometrioid cancers with defects in the polymerase epsilon (*POLE*) gene exonuclease domain (ultra-mutant **POLE**). These four molecular classifications, in particular the POLE and MSI-H groups, highlight a significant role for the patient's immune system in controlling spread of their endometrial cancer and define distinctive prognostic markers (119-125). For example, the ultra-mutant POLE group consists of high-grade cancers which is a pathological feature associated with poor patient outcome. Despite being high-grade, cancers in this group rarely metastasize to cause patient death (82). The favorable outcomes experienced by these patients are thought to be due to active immune recruitment and surveillance of tumor cells. Supporting studies have shown that these tumors have increased tumor infiltrating lymphocytes (TIL) and upregulated expression of TIL markers (119, 120).

Furthermore, recent evidence suggests that some endometrial cancers may respond particularly well to immune therapies and the MSI group is specifically targeted for response to these therapies (122). An understanding of why these particular cancers have a favorable response to immune-based therapies could lead to novel therapeutic strategies for other endometrial cancers. Our model has the potential to be the basis for understanding some of these observations by providing critical insight into interactions between cancer cell and host immune system.

Lack of clinically appropriate animal models, in part, constrains the development of novel therapeutic strategies for endometrial cancer (151). For example, classical

subcutaneous models in nude mice fail to accurately represent the true progression of this disease due to lack of an immune system and incorrect microenvironment (151-155). Genetically engineered animals are an improvement over models that utilize immunodeficient animals in that they maintain an immune system and develop disease in the uterus however, many of these mouse strains have a long latency period and do not develop metastatic disease (137, 156-158). Several uterine specific models reliably develop endometrial cancer (137, 156, 159). These models, while powerful, either fail to develop metastasis or do not lend to extensive study of metastatic disease due to aggressive primary tumor formation and early death of the animal prior to distant metastasis.

The *PTEN* gene is one of the most commonly mutated genes across human cancers and functions as a tumor suppressor (160, 161). PTEN is mutated in >50% of endometrioid endometrial cancers and about 20% (141) of endometrial hyperplasias, a precancerous endometrial lesion, highlighting its central importance in endometrial tumorigenesis (162). In addition, up to 35% of endometrial cancers have activating oncogenic codon 12/13 mutations in the guanine nucleotide binding protein *KRAS* (163). This mutation has also been reported in complex atypical hyperplasia of the endometrium suggesting that as with *PTEN* that it also plays an early role in the progression to endometrial cancer (164). Given their prevalence, propensity of co-occurrence, and pathologic roles we chose to develop a mouse model of endometrial cancer centered around defects in these genes.

In this manuscript, we describe an orthotopic transplant mouse model of endometrial cancer driven by PTEN deletion (*Pten$^{-/-}$*) and K-Ras activation (*K-Ras^{G12D}*)

that originates in the uterus with an intact immune system and correct microenvironment. Tumor growth over time results in local extension and with hematogenous metastases at later time points. The growth characteristics of this model allow for the exciting opportunity to study disease progression over time from primary tumor formation to distant metastasis.

Results

Generation and characterization of MECPK cells

To begin development of an immunocompetent orthotopic model we first created an immortal cell line from the previously characterized endometrial cancer that developed in a 4 week old *Pgr^cre/+^Pten^f/f^K-ras^G12D^* genetically engineered mouse (137). The resultant cell line was named MECPK (<u>M</u>ouse <u>E</u>ndometrial <u>C</u>ancer <u>P</u>TEN deleted <u>K</u>-ras activated) and genotyping confirmed the expected *Pten* and *K-ras* genetic alterations. MECPK cells were transfected with a construct for green fluorescent protein (pSIH-H1-copGFP), and stable GFP expressing cells isolated. We purposely chose to label our cells with a construct lacking a selectable marker to allow for anticipated future experiments in which other genetic alterations necessitating antibiotic selection might be needed (e.g. Crispr/Cas-9).

We further characterized these cells by western blotting. PTEN was absent in MECPK as compared to normal mouse uteri and consistent with the PTEN downregulation in endometrial tumors obtained from female *Pgr^cre/+^Pten^f/f^K-ras^G12D^* animals (**Figure 11 i**). To examine whether PTEN loss resulted in expected downstream effects we assessed levels of phosphorylated AKT (Ser473) a known downstream

effector of activated PI3K signaling. Phospho-AKT was elevated in MECPK with activations similar to $Pgr^{cre/+}Pten^{f/f}K\text{-}ras^{G12D}$ animals and elevated as compared to non-malignant uterus (**Figure 11 ii**) while total AKT remained unchanged between each sample condition (**Figure 11 iii**). MECPK cells do not express estrogen (ESR1) or progesterone (PGR) receptors (**Figure 11 iv, v**).
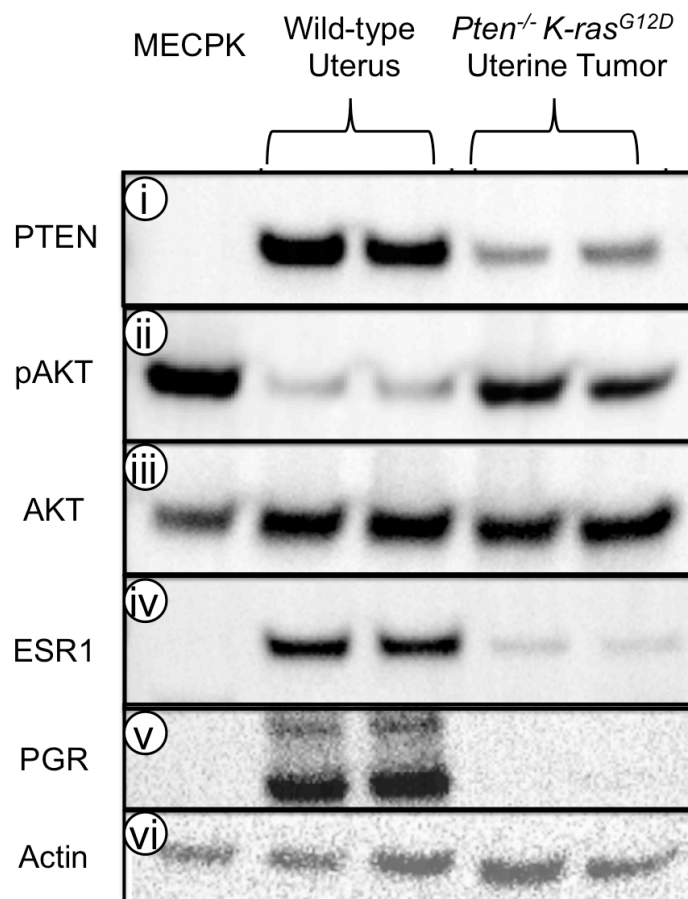
Figure 11. Protein expression profile of MECPK cells, normal uterine tissue, and Pten^{-/-}K-ras^{G12D} uterine tumor. Western blot analysis of PTEN, Phospho-AKT (pAKT), AKT, PGR, and ESR1 in MECPK cell line extract as compared to normal uterine tissue and uterine tumor tissue from $Pten^{-/-}K\text{-}ras^{G12D}$ mice. i) MECPK cells completely lack PTEN as compared to normal tissue and tumor tissue samples indicating purity of the

Figure 11 (cont'd)

cell line and lack of stromal contamination as seen in the faint banding of the tumor samples. ii) MECPK and mouse uterine cancers have elevated levels of pAKT as compared to normal uterine tissue while total AKT (iii) between the samples remained relatively constant. iv-v) Both estrogen and progesterone receptors (ESR1 and PGR) are undetectable in the MECPK cell line. vi) β-actin serves as the loading control. 10 μg protein / lane. Membranes were stripped and re-probed for each antibody.

We next tested whether MECPK cells still retain *in vivo* tumor forming ability. Tumors developed in 3 of 3 animals following subcutaneous injection in athymic nude (Crl:NU(NCr)-Foxn1^{nu}) mice at 2 weeks confirming that the cell line maintained the ability to form tumors (data not shown).

Generation of orthotopic MECPK tumors

To develop better endometrial cancer models, we considered several factors to achieve this goal. First tumors need to originate from the uterus and not be placed subcutaneous, intraperitoneal (I.P.) or in the renal capsule as with previous models (153, 155, 165-172). Further they need to develop in an immune competent background. We theorized that the previous failures of some to establish high rates of human patient-derived xenograft (PDX) engraftment in uterine horns might be for several reasons. Firstly, that the uterus itself might not be in a proliferative state and that this might inhibit engraftment. Additionally, unlike subcutaneous, renal capsule, or I.P. sites, a glycoprotein-rich, mucous-rich layer protects the uterine lumen. We

hypothesized that this mucous layer may inhibit initial attachment of tumor cells to the epithelial layer. We developed and tested the effect of two procedures with the goal to improve orthotopic grafting. Therefore, we evaluated the effect of an abrasion in the uterine lumen which we hypothesized would allow graft cells access through the mucus layer and also evaluated the role of a proliferative endometrium on tumor formation all in the context of an intact immune system.

Enhancement of successful in utero graft establishment through estrogen supplementation and mucosal abrasion.

We conducted experiments on mixed background immune competent animals to evaluate the effect of estrogen supplementation and uterine luminal abrasion on tumor formation. Briefly, three days prior to the start of the experiment, immune competent female mice were injected with exogenous estrogen once daily for three days (0.1 μg/injection). On the date of cell injection (considered day 0) animals were ovariectomized (OVX), the uterine lumen was either abraded using a blunted 25G needle (abrasion) or not abraded (no abrasion) and 500,000 MECPK-GFP cells were injected. We examined uteri and tumor formation in estrogen stimulated (E2) and control (vehicle) mice after 4 weeks (n=5, 8, and 17 for vehicle + abrasion, E2 + no abrasion, and E2 + abrasion respectively). Mice lacking exogenous estrogen supplementation (vehicle + abrasion) failed to develop tumors (0%) while the majority (59%) of luminal abraded mice with estrogen stimulation (E2 + abrasion) developed uterine tumors (p=0.0396). In contrast, mice treated with estrogen but lacking abrasion (E2 + no abrasion) developed tumors in only 1 of 8 mice (13%, **Table 5**). Those

68

abraded uteri were more likely to develop tumors as opposed to non-abraded (p=0.04). Thus, we concluded that mucosal abrasion enhanced graft establishment and likely provides an adherent surface for the injected cells. All future experiments were conducted with the use of exogenous estrogen supplementation and mucosal abrasion (**Figure 12A**). Grossly evident primary tumors developed in 10 of 17 (59%) mice after 1 month in these mixed background mice (**Figure 12B**. i and **Table 5**). Further we utilized a fluorescent dissection microscope to distinguish GFP positive tumor cells (**Figure 12B**. ii). The invasive nature of the cells was also examined by GFP label in frozen sections and GFP labeled cancer cells infiltrated the deeper uterine tissue layers (**Figure 12B**. iii-iv).

Table 5. Summary of 1 month gross tumor formation in mixed background or C57BL/6 mice. *p=0.04 indicating significantly increased take-rate with estrogen supplementation vs. non-estrogen supplemented; 'p=0.04 indicating increased take-rate between estrogen supplemented groups with or without abrasion; #p=0.13 indicating no significant differences between mixed background and C57BL/6 tumor establishment rates.

1 Month - Mixed Background	Tumor	No Tumor	Total Animals Observed	Tumor Development (%)
Vehicle + Abrasion	0	5	5	0% *
E2 + No Abrasion	1	7	8	13% '
E2 + Abrasion	10	7	17	59% *'#

1 Month - C57BL/6J Background	Cancer	No Cancer	Total Animals Observed	Cancer Development (%)
E2 + No Abrasion	0	3	3	0%
E2 + Abrasion	12	2	14	86% #
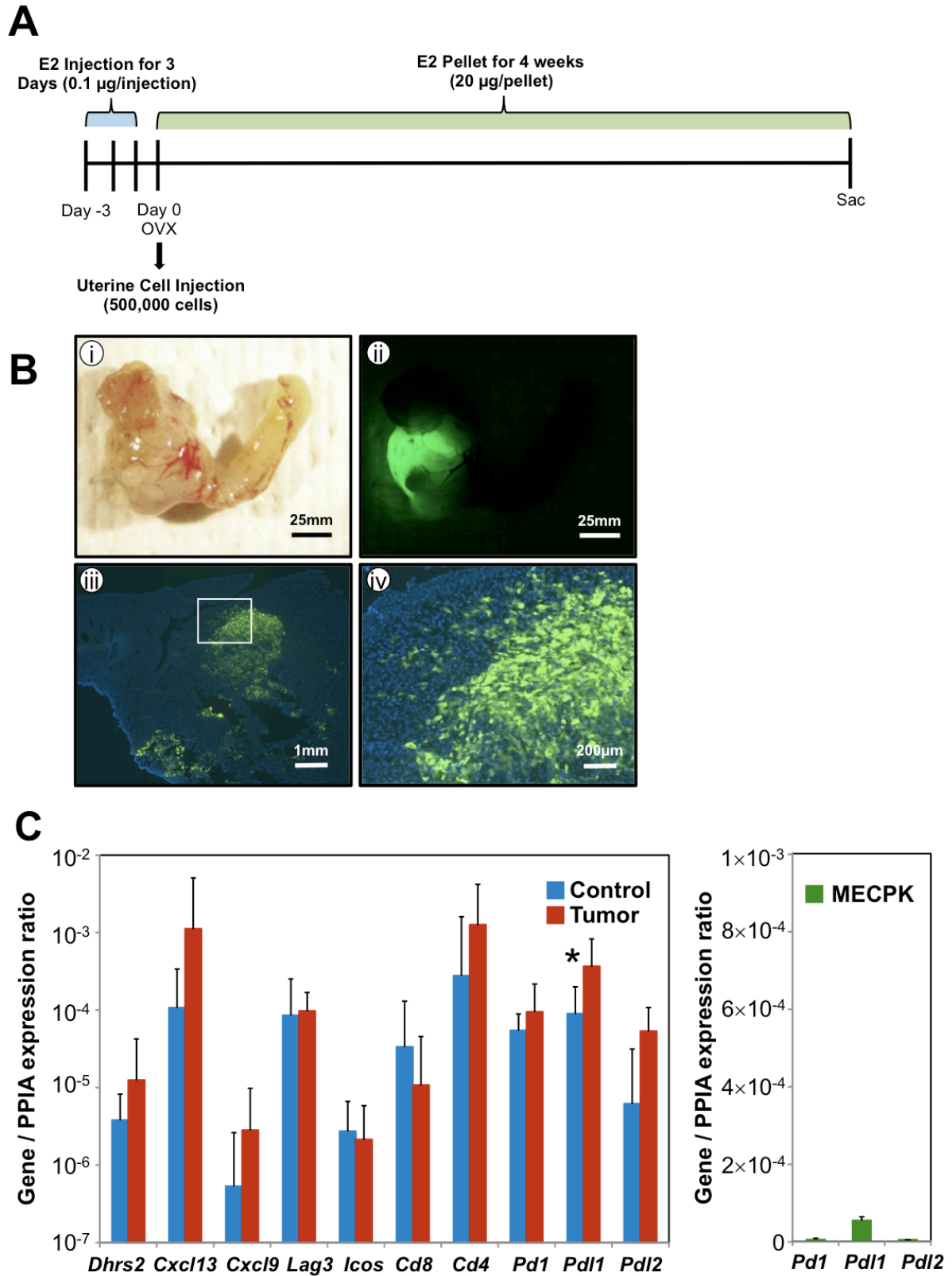
Figure 12. A) Summary of graft protocol. For three consecutive days prior to surgery,

Figure 12 (cont'd)

mice were injected with 0.1 µg of estrogen. The distal ends of the uterine horns were ligated and the ovaries removed (OVX) on the day of surgery. 500,000 cells were injected into one horn suspended in a 1:1 mixture of PBS:Matrigel. The second horn was left as a control and received a sham surgery. **B)** Representative tumor formation in a mixed background immune-competent mouse **(i)** with corresponding detection of GFP labeled cells **(ii)**. GFP labeled cancer cells invade into uterine wall **(iii-iv). C)** Immune gene expression in normal uterine (control) n=3 and tumor bearing uterine tissue (tumor) n=3 (*left*). Selected immune gene expression in MECPK-GFP cells (*right*). Immune gene expression was normalized to *Ppia*, a housekeeping gene. * paired T-test p<0.05.

Characterization of primary MECPK tumors

The MECPK model demonstrates tumor growth in the context of an intact immune system. With this in mind, we chose to examine the expression of several key immune signature genes representing B and T-cell chemo attractants (*Cxcl13, Cxcl9*), MHC Class II ligands (*Lag3, Cd4*), markers of activated T-cells (*Icos*), and MHC class I markers (*Cd8*) that are known to infiltrate human endometrial cancers and which may be drastically elevated in some MSI and many POLE immune-infiltrated and activated cancers (123-125). RNA expression of *Dhrs2*, *Cxcl13*, *Cxcl9*, *Lag3*, *Icos*, *Cd8*, and *Cd4* did not differ significantly between the grafted uterine horn with tumor and the control uterine horn at one-month post cell injection (**Figure 12C**. n=3 independent animal samples per group). Based on these results we concluded that our graft procedure as

well as the MECPK-GFP cells themselves do not inherently induce an immune response or express immune markers. mRNA levels of the key modulators of immune surveillance, *Pd1*, *Pdl1*, and *Pdl2*, were not expressed in the MECPK-GFP cell line (**Figure 12D**. Delta CT values graphed).

We performed a molecular and histological characterization of MECPK uterine tumors (n=3). Histological analysis and Ki67 immunoreactivity confirmed these lesions were highly proliferative high-grade endometrial cancers (**Figure 13A**. i-vi). As expected, PTEN was not detected in tumor cells (**Figure 13A**. vii-ix). PI3K and MAPK pathway activation in tumors were evaluated using phosphor-specific antibodies. Tumor cells expressed phospho-AKT (Ser473) and pERK1/2 (Thr202/Tyr204) (**Figure 13A**. x-xxi). Primary tumor cells were Vimentin variable diffuse positive and CDH1 (E-Cadherin) positive (**Figure 13A**. xii-xxvii). Human-matched IHCs appear in **Figure 13B**.

Tumor histology from our *in vivo* model was evaluated by H&E staining (**Figure 13B**. i). We found that *in vivo* tumor formation displays histological characteristics similar to that of high-grade human disease (**Figure 13B**. ii, iii). Notably, cells were tightly compacted, with absent glandular features, numerous visible mitotic events and near complete loss of stroma.
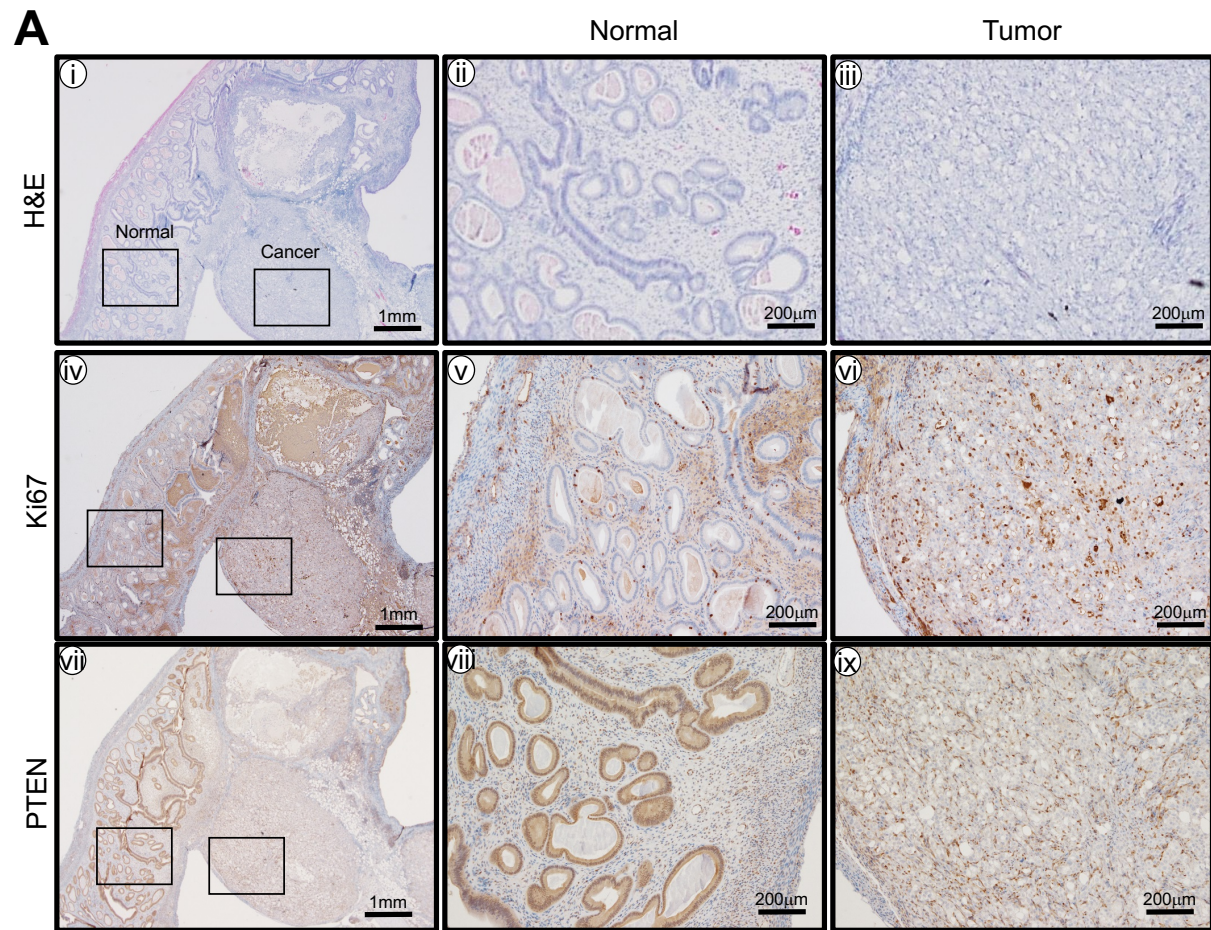
Figure 13. Histological characteristics of endometrial tumors formed in the Pten^{-/-} Kras[G12D] MECPK model.

Figure 13 (cont'd)

Figure 13 (cont'd)

Figure 13 (cont'd)

B

MECPK-GFP   High-grade Human Endometrioid Endometrial Cancer
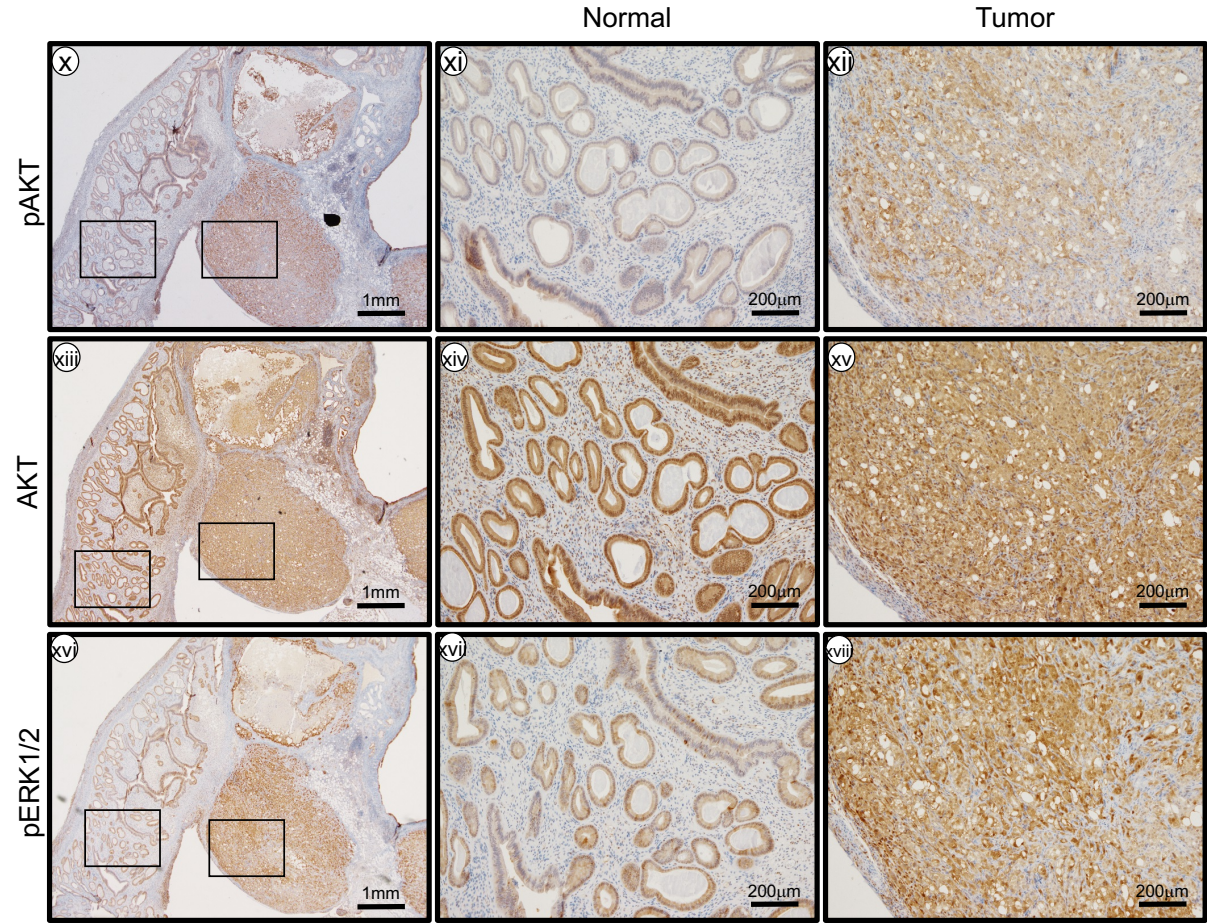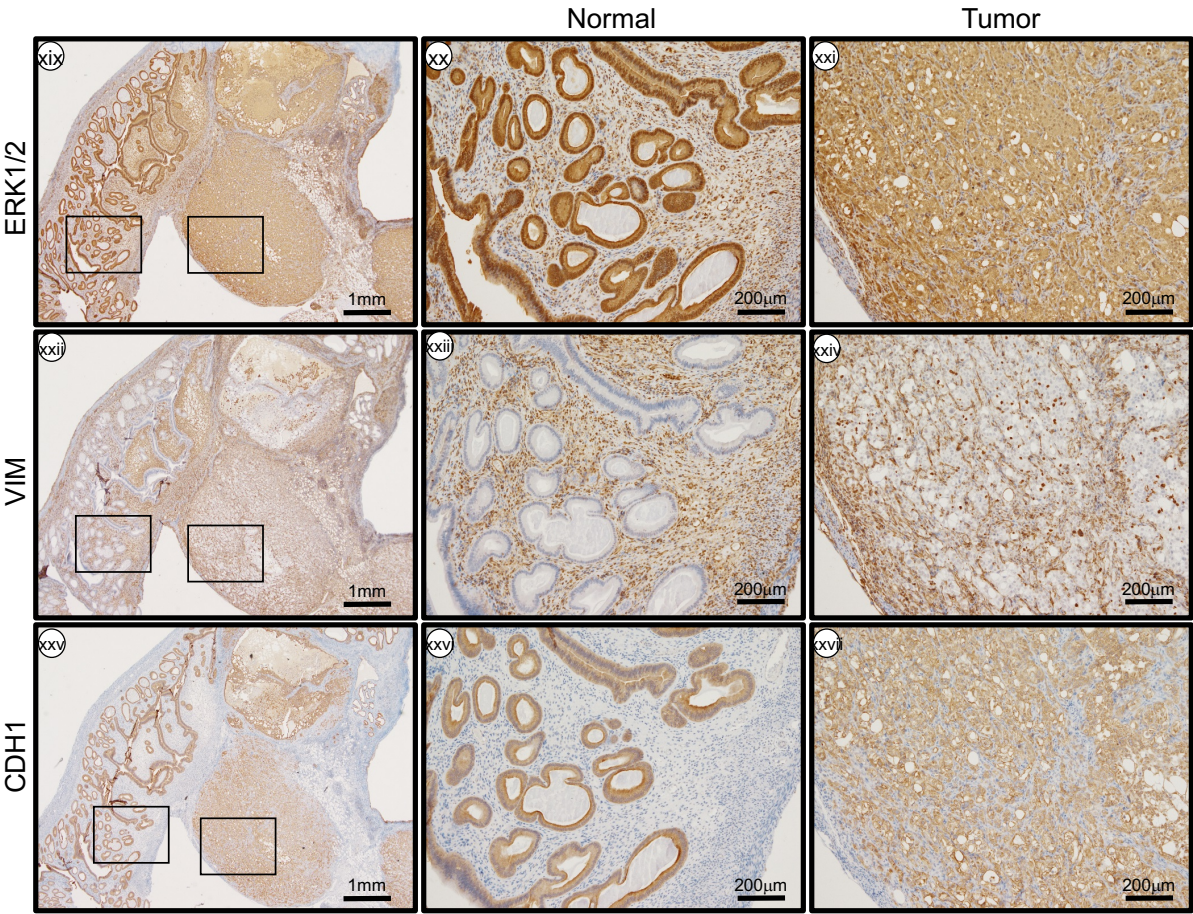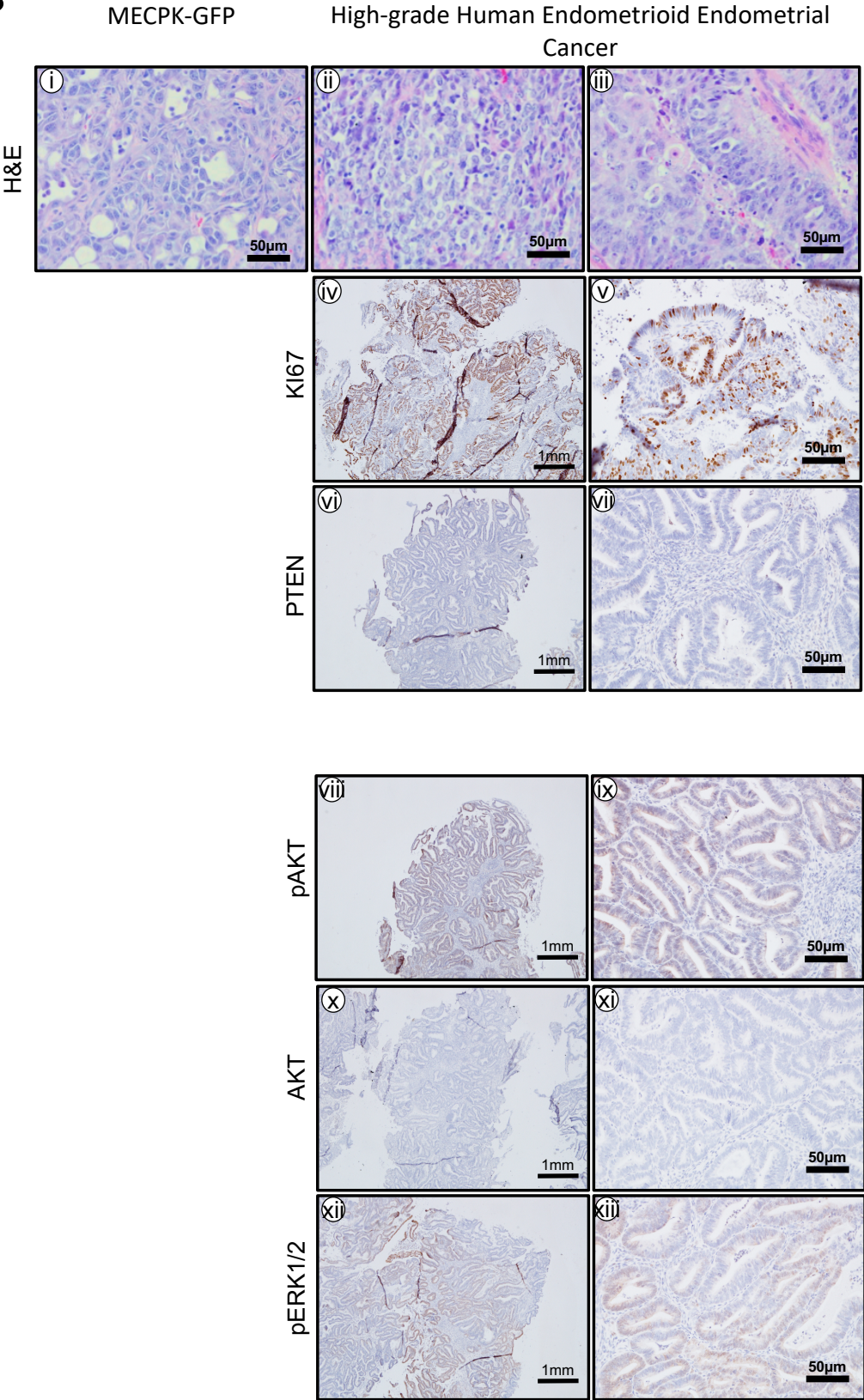
Figure 13 (cont'd)
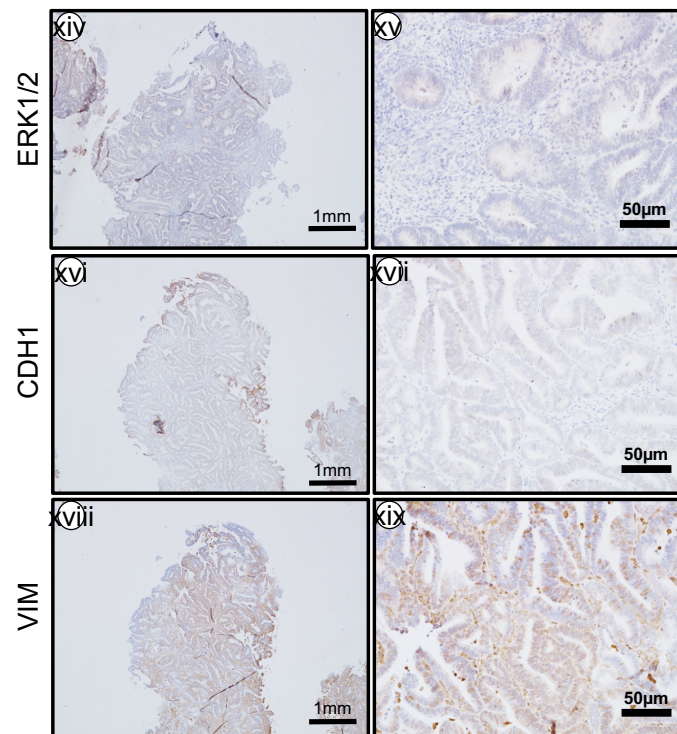
A) i) Low magnification (4X) (left) showing tumor interface with normal tissue and high magnification (20X) of ii) normal (center) and iii) cancer tissues (right) with H&E. H&E of tumors from *Pten$^{-/-}$ Kras^{G12D}* MECPK mice are endometrioid, lack glandular formation, and have minimal stroma. Ki67 confirmed these lesions were highly proliferative (Figure 3A. iv-vi). As expected, PTEN was not detected in the cancer cells of the tumor tissue (vii-ix). Tumors expressed pAKT (x-xii), AKT (xiii-xv), pERK1/2 (xvi-xviii) and ERK1/2 (xix-xxi) important markers of PI3K and MAPK activation. Primary tumors were Vimentin positive in stroma and largely negative in epithelium and cancer cells (xxii-xxiv) and were negative for CDH1 in the stroma and positive in normal epithelium and in cancer cells (xxv-xxvii). n=3 independent tissue samples. B) Comparison of MECPK tumor histology to human endometrial cancer samples. i) Representative H&E of a MECPK

Figure 13 (cont'd)

tumor at 1 month post-injection. *In vivo* tumor formation displays histological characteristics similar to that of grade 3 endometrioid endometrial cancers (ii-iii). Notably, cells are tightly compacted with visible mitotic events and near complete loss of stroma. Scale bar: 50 µm. All other stains show human IHC component for detections on mouse tissues done in A.

MECPK animals die of metastatic cancer

We evaluated the effect of long-term tumor growth of the MECPK model and determined the natural course of disease progression. We initiated MECPK tumors in 9 mixed background, uterine abraded, immune competent animals supplemented with exogenous estrogen and evaluated end of life as determined by either humane endpoint or unexpected death from disease days post injection (DPI). In this experiment, animals expired as early as 35 days and survived as long as 125 DPI (Figure 14B. n=9, two censorships due to unexpected death. Median survival was 76 DPI). Necropsy of expired animals confirmed bulky uterine disease in the 7 animals that were recovered (**Table 6**). In addition, grossly evident and extensive cancer was visualized in the lungs of all animals and was the likely cause of death (**Figure 14**C. ii).
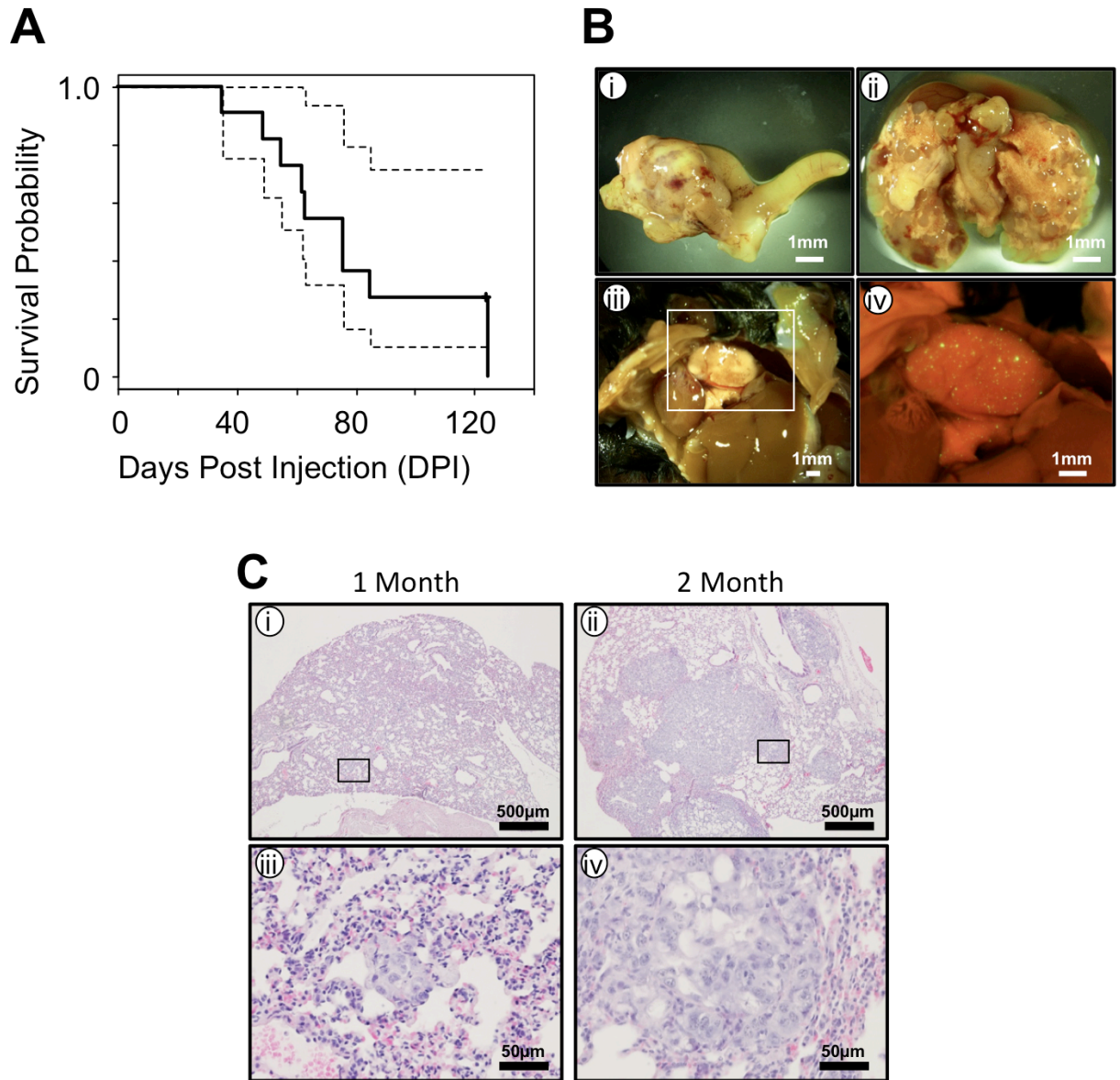
Figure 14. Survival and characterization of metastatic spread for Pten^{-/-}Kras^{G12D}

MECPK model. A) Survival plot showing natural course of disease. N=11 including two censored cases. Median survival = 76 DPI. Dashed lines are 95% confidence limits. B) Representative image of primary uterine tumor and metastatic lung spread at 6 weeks post cell injection (i-ii). GFP detection of non-macroscopic metastatic spread to the lung at four weeks post-injection (iii-iv). C) H&E sections showing progression of lung disease at 1 and 2 months post uterine injection. At one month (i), micro-metastatic is

Figure 14 (cont'd)

detectable through histologic analysis (iii). At two months (ii), larger tumor cell nests are present in the lungs (iv).

Table 6. Summary of metastatic lung disease development over time. Notably, the rate of distant metastatic disease detected in the lung drastically increases if allowed to grow past one month. Experiments were conducted as described in **Figure 12**A. Constant estrogen stimulation was maintained through subcutaneous placement of a 20 µg estrogen beeswax pellet. Pellet was replaced every 4 weeks until a death or a humane endpoint was reached as determined by primary tumor volume or obvious signs of animal distress.

Time Point	Local Metastasis	Distant Metastasis	Total Animals Observed	Chance of Distant Metastasis
Short-Term (1 Month)	8	1	8	13%
Long-Term (Over 1 Month)	9	7	9	78%

Metastatic spread in the MECPK model

Our survival experiment indicated frequent metastases in the lungs of MECPK implanted mice. Therefore, we carefully characterized the rates of the metastatic spread of MECPK cells at one month using samples from a sub-cohort of our previous experiments and in longer-term experiments with the 9 mice described previously. At one month, primary tumor was present in all animals examined from the sub-cohort (**Figure 14**A, sub-cohort n=8 evaluated only from group with cancer; total n=17 in

original experiment, 10 with cancer, 7 without cancer). Of these 8 animals evaluated, all also had local extension spread outside of the uterus. Additionally, in 1 of 8 animals we were able to detect distant spread of disease in the lung (**Figure 14**C-iii, iv). At two months, in addition to primary tumor and local extension of disease (**Figure 14**C-i) we found distant disease in the lung (**Figure 14**C-ii) in all 7 animals evaluated (n=9, 2 censorships mentioned in previous survival study). To further characterize the distant disease, H&E sections were made from the lungs of animals at one month and two months post injection (**Figure 14**D, i-iv). At one month, small nests of micro metastatic disease are present (**Figure 14**D, i,iii, n=3) while at two months and later larger, solid tumor areas had formed (**Figure 14**D, ii, iv). Other rare sites of metastatic disease were present, specifically liver, spleen and cutaneous lesions at a frequency of 8%, 4% and 4% respectively (**Table 7**).

Table 7. Summary of observed metastatic site rates. N=26 animals observed across all time points. Only animals which had confirmed primary tumor formation were considered when calculating percentages.

Metastatic Site	% Observed
Lung	31%
Liver	8%
Spleen	4%
Cutaneous	4%

Tumor formation in C57BL/6 mice.

To test whether MECPK-GFP cells could grow in the commonly available C57BL/6 background, we implanted OVX female C57BL/6 mice supplemented with exogenous estrogen with (n=14) or without luminal abrasion (n=3) (**Table 5**). C57BL/6 mice provided with exogenous estrogen but lacking abrasion failed to develop tumors (n=3). C57BL/6 mice supplemented with exogenous estrogen and abrasion developed cancer in 12 out of 14 animals (n=14; 12 with cancer, 2 without). Cancer development in the uterus of the C57BL/6 strain was not significantly different than development in the mixed background strain ([#]p=0.13).

Discussion

Here we describe the development and characterization of the first immunocompetent orthotopic murine model of endometrial cancer. Our model is based on the implantation of the MECPK cell line, which is derived from primary endometrial tumors of $Pgr^{cre/+}Pten^{f/f}K\text{-}ras^{G12D}$ mice(137). MECPK tumors very closely mimic high-grade human endometrioid type endometrial cancers. Tumors exhibit loss of PTEN, activation of K-Ras, PI3K and MAPK pathway activation, and elevated Ki67 immunoreactivity, thereby confirming these lesions were highly proliferative. These tumor cells are epithelial in nature based on CDH1 staining findings. This being consistent with endometrial cancer versus a stromally-derived malignancy, which was the other possibility due to the PR-cre driver of the original mouse model(137).

Because tumors in MECPK implanted mice possess the well-known genetic defects and established drivers of human endometrioid endometrial cancer, and exhibit

the expected activation of AKT and ERK pathways, we anticipate this model will be useful for the evaluation of targeted therapeutics aimed at modulating these specific pathways.

Primary tumor cells were displayed variable diffuse positivity of Vimentin and were CDH1 positive. E-Cadherin has low to negative by IHC in the grade 3 cancers however is highly positive in endometrial gland epithelium and MECPK tumor IHC. E-cadherin detection in endometrial cancer can be variable based on histotypes (173). Our detection is correct in that glands are the expected positive, stroma is negative, MECPK is positive, and high grade cancers are often negative.

This model develops frequent distant lung metastasis allowing for the preclinical evaluation and treatment of disease spread from early micro-metastatic stages onward. Importantly MECPK tumors grow with equal frequency and exhibit the same tumor proclivity characteristics in the commercially available and fully immunocompetent C57BL/6 mice.

Endometrial cancers from MECPK implanted mice result from defects in well-known and established drivers of human endometrioid endometrial cancer and exhibit the expected activation of AKT and ERK pathways. As such this model should be useful for drug studies examining targets aimed at modulating these specific pathways. Our model circumvents many deficits of other current models of endometrial cancer. Specifically, these models either do not metastasize or are developed in immune deficient mice, which limit the scope of biological processes that can be studied. Further, classical subcutaneous models in nude mice lack an immune system response and maintain tumors in an incorrect microenvironment, which could impact study

outcomes. While genetically engineered animals are an improvement over classic nude animal models, many still have a long latency period and/or do not develop metastatic disease.

Our model resembles high-grade human endometrial cancer histologically as it lacks appreciable stroma and progresses as high-grade human endometrial cancer would *in vivo* specifically metastasizing to the most common site of hematogenous spread; the lung (174, 175). Interestingly MECPK cells lack ESR1 and PGR, which is associated with high-grade disease in humans (15, 176-178). Normal endometrial tissue is both estrogen and progesterone sensitive. We noted enhanced graft take-rates upon exogenous estrogen supplementation despite the lack of detectable protein levels of estrogen receptor in MECPK cell lysate (**Figure 11**. iv). While supplemented estrogen may not be working directly on the injected cells from the cell line, it is likely stimulating stromal tissue as has been shown previously (103) in the normal uterus prior to cell injection increasing its size and potentially enhancing the microenvironment to favor the proliferative tumor cells. Estrogen impacts epithelial permeability through modulation of tight junction proteins in the endometrium and cervix (179-181) leading to increased barrier permeability and allowing injected tumor cells to more easily invade past the epithelium and into deeper tissue layers of the uterus. Additionally, estrogen is a known modulator of vascular growth in the uterus (182) and may be contributing to increased vascularization and favorable growth conditions for resultant tumors as well as an increased potential for hematogenous spread to the lungs. With ovariectomy in our methodology we have eliminated the possibility of ovarian produced progestin, the normal signal for tissue growth to cease thus favoring continuous growth. Together

these factors may potentially provide optimal conditions for unopposed tumor growth in this model and improving overall tumor establishment rates.

One of the most important aspects of this model is that MECPK endometrial tumors and their metastases develop in the presence of an intact immune system. We performed an initial characterization of several immune cell markers previously shown to be upregulated in human endometrial cancers with increased immune infiltrate. We did not note any transcriptional change in key immune markers *Dhrs2*, *Cxcl13*, *Cxcl9*, *Lag3*, *Icos*, *Cd8*, and *Cd4.* MECPK model tumors would be most similar to the copy number low MSS molecular classification group based on the lack of a prominent T-cell infiltrate which is present in endometrioid cancers with MSI and POLE mutation. Consistent with these findings is that MECPK cells express mismatch repair proteins and lack mutation in the exonuclease domain of Polymerase-E (data not shown). We did note that *Pd1*, *Pdl1,* and *Pdl2* were not elevated in our cell line. Levels of Pdl1 are important because the interaction between PD-1 with PD-L1 has been demonstrated to inhibit antigen sensitization in peripheral T cells in this way, protecting normal tissues against self-injury from the immune system. PD-L1 has been shown to be expressed in 11-83% of primary endometrial cancers and in 96% of metastatic samples and thus may serve as an immune target (183, 184). Future studies will address expression of these genes *in vivo*.

Utility of true syngeneic models are limited by the availability of the background strain. Importantly we demonstrated that MECPK cells grow equally as well in C57BL/6 mice using the same protocol as was used in the mixed background animals. Our results indicated similar success rates between the strains. Indeed, this should not be

surprising as the cell line originated from mixed C57BL/6J:129K1 background. It is known that each particular laboratory mouse strain is homozygous and has its own unique major histocompatibility haplotype. C57BL/6J and 129K1 backgrounds harbor the same haplotype and thus graft rejection should not be an issue when switching from the mixed to C57BL/6J background(185). With this in mind, our model should make an impact like other similar models such as the ID8 model for ovarian cancer (186). However, unlike ID8 which spontaneously transformed and lacks known drivers of ovarian cancer our model is driven by PTEN deletion and K-Ras activation: established and well-known drivers that are present and highly prevalent in human endometrial cancers.

We have demonstrated the exciting potential for further utility of our model by adding a GFP label to the MECPK cell line suggesting that *in vitro* manipulation of the cell line can be conducted prior to injecting cells. These cells can then be subject to other manipulations either adding additional oncogenic or deleting specific tumor suppressor or DNA repair gene capabilities which are established factors in defining the newly described molecular sub-groups and perhaps impacting their growth rate or metastatic potential.

Here we have described the first orthotopic mouse model of endometrial cancer in a fully immunocompetent animal. Our model has several significant advantages over current xenograft models. Injection of cancer cells orthotopically allows for tumor cell exposure to the physiologically appropriate microenvironment. Further, the presence of an intact immune system allows for the exciting potential to study immunotherapies and immune interactions with cancer cells. Finally, specific genetic modifications dictated by

the investigator can be made to the cell line *in vitro* prior to grafting, and thus can alter the future *in vivo* tumor for study. These features allow for ease of study of both *in vivo* tumor formation and *in vitro* cell line manipulation.

Materials and Methods

Guidelines for Animal research.

Mice were maintained in the designated animal care facility at the Van Andel Institute according to Michigan State University's institutional guidelines for the care and use of laboratory animals (137).

Mouse Strains

Mixed background: C57BL/6 x 129 females ages 8 weeks or greater received an injection of 500,000 cells into one uterine horn with or without abrasion technique. Sacrifice and evaluation for tumor formation was performed at various time points as described.

C57BL/6: 8-week-old female animals (The Jackson Laboratories. Bar Harbor, ME USA) were injected with 500,000 cells into one uterine horn after abrasion technique was performed. Sacrifice and evaluation for tumor formation was performed 1 month after injection.

Athymic nude (Crl:NU(NCr)-Foxn1nu): Animals were injected (n=3) with 500,000 cells into one uterine horn after abrasion technique was performed. After 2 weeks of growth, animals were sacrificed and evaluated for tumor formation.

MECPK cell line establishment

A small piece of uterine tumor from a 4-week-old female *Pten$^{-/-}$K-Ras^{G12D}* animal was finely minced, placed into a 10-cm plate, and maintained in DMEM supplemented with 10% fetal calf serum, and in the presence of antibiotic/antimycotic (Gibco). Tumor cells were established and fibroblasts were removed over time by gentle scraping. Pure tumor cultures were passaged more than 70 times. The resultant endometrial cancer cell line, Mouse Endometrial Cancer Pten deleted Kras activated (MECPK) was maintained and grown in Dulbecco's Modified Eagle's Medium with F12 (Invitrogen, Grand Island, NY, USA), supplemented with 10% (v/v) fetal bovine serum (Invitrogen), 50 units/ml penicillin and 50 µg/ml streptomycin (Invitrogen) in an atmosphere of 5% CO_2 and 95% air at 37°C. The MECPK-GFP line was generated by transfecting unlabeled MECPK cells with pSIH-H1-copGFP (System Biosciences, Inc., SI501A-1). Since no selection marker is present on this plasmid, single-cell seeding was subsequently performed to obtain a GFP-labeled clone.

Endometrial priming for receipt of tumor cells and in utero cancer cell injection

Female mice (average age 12.5 weeks) were injected with 100 ng of E2 per day for three days prior to cell engraftment. On the day of cellular injection (considered experimental Day 0), a small incision was made on the left flank of the animal anterior to the femur and lateral to the spine. The ovary was visualized through the inner pelvic fascia and a deeper cut into the pelvic cavity was made to expose the ovary. Forceps were used to pull the left uterine horn and ovary outside of the body cavity. A blunted 25G needle was inserted into the uterine lumen and used to mechanically abrade the

luminal mucus layer along the full length of the anti-mesometrial 500,000 MECPK-GFP cells were suspended in 50 ul of a 1:1 mixture of Matrigel (Corning, Bedford, MA) and PBS and injected into the abraded uterine lumen using a 25G needle. We confirmed that our abrasion technique was not directly seeding the injected cancer cells into the blood by comparing abraded animals to tail vein injected animals and looking for GFP labeled cancer cells in the lungs (**Figure 15**). Animals were bilaterally ovariectomized (OVX) at the time of cell injection and a 20 ug estrogen beeswax pellet (replaced every 4 weeks) was placed under the skin at the base of the posterior neck between the shoulder blades. The right uterine horn was left intact as a sham control after OVX. The mice were sacrificed at 1 month for short-term experiments and at a humane endpoint in long-term disease course experiments (as determined by palpable primary tumor volume, external signs of animal distress, or death). Following death, mouse uteri were then excised, weighed and fixed in 4% paraformaldehyde for histological analysis.
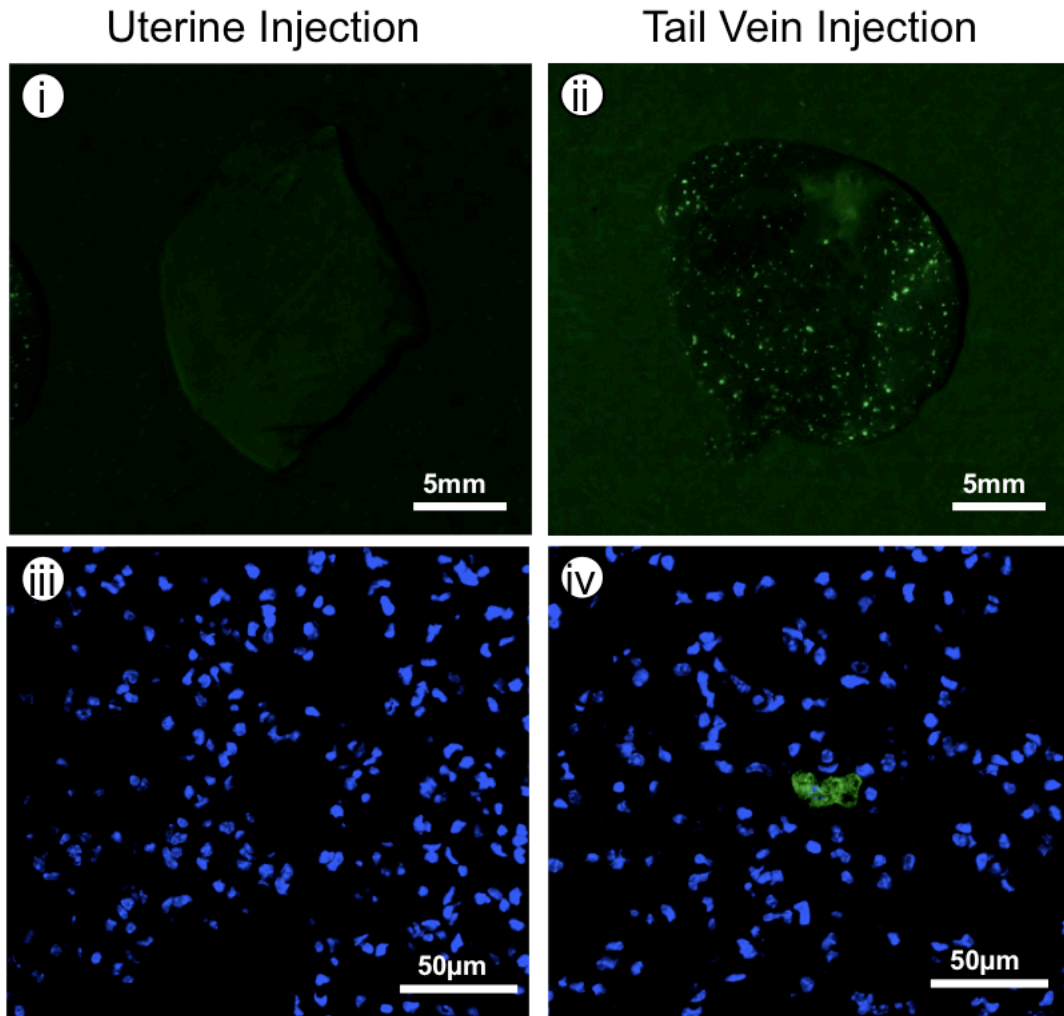
Figure 15. Luminal abrasion does not directly seed cancer cells to circulating blood. Animals were primed with estrogen injections as described in Figure 2A. Cells were prepared as described and injected into either a uterine horn after abrasion or directly into the tail vein. Animals were sacrificed 24 hr after injection and lungs were evaluated for the presence of GFP-labeled cancer cells. Animals with cells injected in an abraded uterus did not have detectable cancer cells in their lungs (i and iii) as compared to tail-vein injected animals (ii and iv) indicating that our methods do not directly seed cancer cells into the bloodstream.

Western Blot Analysis

Tissue and cell line samples containing 15 μg of protein were applied to SDS-PAGE 8-12% Bis-tris gel. The separated proteins were transferred onto a polyvinylidene difluoride membrane (Millipore Corp., Bedford, MA). Membranes were blocked overnight with 0.5% casein (wt/vol) in Phosphate Buffered Saline with 0.1% Tween 20 (vol/vol) (PBS-T) (Sigma-Aldrich, St. Louis, MO) and probed with anti-PTEN (9188, Cell Signaling), pAKT (4060, Cell Signaling), AKT (4691, Cell Signaling), anti-PR (DAKO Corp., Capinteria, CA), or anti-ERα (DAKO Corp., Capinteria, CA) antibodies. Immunoreactivity was visualized by incubation with a horseradish peroxidase-linked secondary antibody and treatment with ECL reagents (Advansta, Menlo Park, CA). To control for loading, the membrane was stripped and probed with anti-actin (Santa Cruz Biotechnology, Inc., Santa Cruz, CA) and developed again.

Immunohistochemistry

Uterine sections from paraffin-embedded tissue were cut at 6 μm and mounted on silane-coated slides, deparafinized, and rehydrated in a graded alcohol series. Sections were pre-incubated with 10% normal horse serum in PBS (pH 7.5) and then incubated with anti-Ki67 antibody (BD550609. BD Pharmingen) or anti-PTEN (9188, Cell Signaling), pAKT (4060, Cell Signaling), AKT (4691, Cell Signaling), ERK1/2 (4695, Cell Signaling), pERK1/2 (4370, Cell Signaling), Vimentin (ab92547, Abcam), E-cadherin (M-106, Takara) in 10% normal serum in PBS (pH 7.5). On the following day, sections were washed in PBS and incubated with a secondary antibody (5 μL/mL;

Vector Laboratories, Burlingame, CA) for 1 hour at room temperature. Immunoreactivity was detected using the DAB kit (Vector Laboratories, Burlingame, CA).

Frozen Sections

Tissue was fixed in 4% paraformaldehyde (PFA) (Fisher O4042-500) in PBS for 6 hr at 4°C. Tissue was then washed in 1X PBS for 5 min followed by cryoprotection in ice cold Hanks' Buffered Salt Solution (HBSS – Gibco 14170) containing increasing concentrations of sucrose (10%, 15%, 20% - Sigma S-1888) at 4°C until evidence of osmotic equilibration as indicated by sinking tissue. Tissue was then embedded directly in base mold (Fisher 22038218) on top of dry ice with OCT (Tissue-Tek 4853) and allowed to solidify for several hours. 6 μm sections were obtained on a cryostat and tissue counterstained with DAPI to detect GFP (VECTASHIELD Mounting Medium with DAPI – VECTOR H-1200).

Quantitative real-time PCR

Flash frozen samples were subject to total RNA isolation with TRIzol Reagent (Ambion, Thermo Fisher Scientific, Waltham, MA) according to manufacturer's recommendation. Two μg of RNA were first treated with OPTIZYME DNase I (Thermo Fisher Scientific, Waltham, MA) for the preparation of DNA-free RNA prior to the transcription into complementary DNA (cDNA) with qScript cDNA Synthesis Kit (Quanta Biosciences, Beverly, MA). These cDNA were used as the template for the quantitative real-time PCR using primers with PerfeCTa SYBR Green FastMix reagent Quanta

Biosciences (Beverly, MA) and the primers with the following sequences for *Dhrs2*

forward 5'-ctgaggaccgccagcaccttgtgac-3', reverse 5'-accagagggttgactccggccaca-3',

Cxcl13 forward 5'-gatcggattcaagttacgcccctg-3', reverse 5'- ataactttcttcatcttggtccaga-3',

Cxcl9 forward 5'-gctgttcttttcctcttgggcatca-3', reverse 5'- ggagcatcgtgcattccttatcact-3',

Lag3 forward 5'-agtgtacgccgcagagtctagctca-3', reverse 5'- acgagatggcctcctttaaggtcac-3', *Icos* forward 5'-aggaaccttagtggaggatatttgc-3', reverse 5'- ccctacgggtagccagagcttcag-3', *Cd8* forward 5'-cggtgatgtacttcagttctgtcgt-3', reverse 5'- ggagttcgcagcactggcttggta-3', *Cd4* forward 5'-caggaaagaggaggtggagttgtgg-3', reverse 5'-ttgcaacaggctggtacccggactg-3', *Pd1* forward 5'-accccaaggcaaaaatcgaggag-3', reverse 5'-gctgggatatcttgttgaggtct-3', *Pdl1* forward 5'-atcagctacggtggtgcggacta-3', reverse 5'-ttctctggttgattttgcggtat-3', and *Pdl2* forward 5'-ccgcctgggactacaagtacctga-3', reverse 5'-acctccaggatcctagtgtctatc-3'. All qPCRs were done on Stratagene MX3000P and the mRNA quantities were normalized using mouse *Ppia* (cyclophilin A) endogenous control.

Statistical Analysis

The statistical significance of tumor formation by E2 in comparison with vehicle was assessed by Fischer's exact test. The numbers of uteri with and without tumors for E2 and vehicle were determined to set up a 2×2 contingency table and two-tailed p-values were calculated by Fischer's exact test. These p-values agreed well with χ^2 test p-values using Monte-Carlo simulations based on 10000 replicates. The p-values were calculated separately for mixed and C57BL/6 backgrounds. Similarly, the p-value for the effect of abrasion was calculated. The p-value for the effect of genetic background was calculated including the E2 cases with and without abrasion. The p-values for

testing abrasion effect by E2 were done by the assessment of tumor formation

probabilities according to binomial distribution and rounding the counts to nearest

integers.

Chapter 4: Elevated CXXC5 is associated with recurrence and poor overall survival in endometrial cancer

Abstract

Endometrial cancer is the fourth most common cancer in women and the most prevalent gynecologic malignancy in the United States; however, there has been little improvement in treatment strategies. This problem will become more eminent in the future as the incidence and prevalence of this disease is increasing overall. As it did decades ago, determination of therapeutic modality still relies heavily on two subjective measures: surgical staging and pathological classification. Thus, new markers are needed to more objectively assess disease state and predict potential progression. We have used three independent datasets (two internal and TCGA) containing quantified measures of the transcriptome derived from both serous and endometrioid endometrial cancers to identify upregulated transcripts that are predictive of overall survival (OS) and/or disease-free survival (DFS). In the initial analysis of our first internal dataset we identified 155 transcripts at $p<0.005$ that were associated with OS, DFS or both by COX regression analysis. We focused on CXXC5 a transcript with elevated hazard ratios and that had impressive association with recurrence ($p=0.000009$) in the endometrial cancer samples of The Cancer Genome Atlas (TCGA). We determined that TCGA cancers that are high CXXC5 expressors (upper quartile) also had worse OS and DFS as compared to those in the low expressor group. Finally, we verified CXXC5 overexpression as being predictive of recurrence by quantitative RT-PCR ($p \leq 0.01$) in an independent set of 73 endometrial cancers. These observations were supported by

immunohistochemistry demonstrating CXXC5 overexpression in tumor samples from patients with adverse clinical events versus patients without events. Based on our results, CXXC5 may serve as a novel marker to identify poor-prognosis endometrial cancer patients.

Introduction

Unlike many other types of cancer, the prevalence of endometrial cancer is increasing overall and despite endometrial cancer having a 5-year survival rate similar to that of breast cancer; it has received far less attention in both research and public media settings (1). Risk of recurrence and extent of disease are evaluated at the time of surgery, during which tissue samples are gathered and sent to a pathologist for histologic classification. Surgical staging and histologic classification comprise the two main considerations that dictate the treatment regimen for each patient (2, 3, 86-88, 96, 126, 138). While routine, these evaluations are subject to bias and experience level of the physician and may lead to suboptimal treatment of the patient's disease (89-92, 127-132). Thus, this disease in particular would benefit significantly from any sort of prognostic test to predict "bad acting" tumors. Identification of prognostic markers could lead to novel therapeutic targets that would allow advancement in the treatment of this disease (133). We have found that certain gene transcripts, when overexpressed, correlate significantly with relapse and/or death from endometrial cancer. This suggests that high transcription levels of these genes may be driving the cancer's aggressiveness and could lead us to better outcome markers and drug targets.

According to the American Cancer Society, approximately 63,230 new cases of endometrial cancer will be diagnosed in 2018 (150). This represents a continuing trend of endometrial cancer increasing in prevalence (9, 150). Of these women, about 11,350 are predicted to die from their disease. Endometrial cancer tends to occur in older women, with about 75% of cases being diagnosed in women over 55 years of age. A woman's lifetime risk of developing endometrial cancer is 2.8% and is more common in white women, but black women are more likely to die from their disease (150). Further, the 5-year-survival for stage IV cases (advanced stage cases) is roughly 15%(9). None of these associations, however, is an accurate predictor of disease outcome for recurrence or survival and is especially lacking in prognostic value for stage I patients.

Most women who will experience a relapse event do so within the first three years after initial diagnosis (10, 11). Women who receive a diagnosis of recurrent or metastatic disease have a poor overall prognosis, regardless of treatment modality. In contrast to initial diagnosis, current data suggests that histology has no predictive value for treatment response in patients with recurrent disease (13). Presently, there are no markers available that reliably predict either disease recurrence or poor survival. Thus, it is crucial that we identify targets for prevention of disease, markers that predict disease outcome, and targets for new therapies.

We have used three independent datasets, two internal (MSU and Spectrum) and one publicly available validation set from the Cancer Genome Atlas (TCGA), containing quantified measures of the transcriptome derived from both serous and endometrioid endometrial cancers to identify upregulated transcripts that are predictive of overall survival (OS) and/or disease-free survival (DFS). We focused on those

98

transcripts from our first internal MSU discovery dataset with elevated hazard ratios and determined whether these transcripts retained similar survival associations with the endometrial cancer samples in TCGA data set. In this study, we focused on the most impressive of the transcripts we have identified, CXXC5, which is an understudied gene in terms of functionality in the endometrium.

CXXC5 is a retinoid-inducible nuclear protein that contains a CXXC zinc finger motif within its structure that is thought to recognize unmethylated CpG dinucleotides (187, 188). The functions of CXXC5 are poorly studied, especially in relation to the endometrium and endometrial cancer, but it has been shown to be involved in p53 induction, Wnt signaling, and may serve as a potential epigenetic modifier through its ability to interact with unmethylated CpGs(187, 189-192). CXXC5 has been shown to have involvement in myleopoiesis through regulation of differentiation of myoblasts into myocytes (193). As we have shown in endometrial cancer, in acute myeloid leukemia (AML), transcriptional upregulation of this gene has been correlated with poor outcome (194). Conversely, AML cases with down regulated transcript level of this gene experienced favorable disease outcomes (195). Additionally, CXXC5 negatively regulates cutaneous wound healing and has been shown to negatively regulate the Wnt/β-catenin pathway in osteoblasts (189). CXXC5 probably regulates WNT signaling by direct interaction with Dishevelled (DVL1) (196, 197). It has also been shown to be required for DNA damage-induced p53 activation (191). Given these interactions identified in other tissues, this transcript and its associated pathways may lead to novel drug targets in the treatment of endometrial cancer either through cell arrest or apoptosis regulation, cell differentiation, or epigenetic modification. Thus, one or more

of these modalities may be contributing to the underlying molecular mechanism for unfavorable outcomes. This study identifies CXXC5 as a gene that may play an important role in predicting endometrial cancer outcome as transcriptional overexpression of CXXC5 and protein overexpression as detected by IHC are both associated with poor prognosis.

Results

Identification of survival associated genes

We used two separate transcriptional analysis datasets to identify possible candidate genes predictive of both poor and favorable survival. The first, our internal discovery dataset, consisted of 136 endometrial cancer samples (MSU discovery set) from women who either experienced a confirmed event, meaning they died from their disease (n=9) or had a recurrence of disease (n=13), compared to those samples from women with cancer but without event. In this analysis, we identified 155 transcripts at p<0.005 that were associated with OS, DFS or both by Cox regression analysis (**Table 8** and **Table 9**). Every sample that was analyzed in this set was a laser-captured, micro-dissected portion of the original tumor. In these cases, the vast majority of mRNA signal comes from the cancer cells. COX regression analysis was performed on Affymetrix Plus 2 gene expression array data to establish which specific transcripts were associated with overall survival, disease relapse, or both (**Figure 16**). Gene expression data for overall survival and relapse prediction of 500 transcripts at p<0.005 clearly shows a predictive association between high and low risk for both overall survival and

relapse of disease as well as histology, stage, grade, and race (**Figure 17**). This indicates that a transcriptional measure can be evaluated as a testable predictor for these outcomes. We then used a second dataset, from the publically available Cancer Genome Atlas (TCGA) RNA Seq V2 RSEM, to validate the findings from our discovery dataset. The TCGA RNA Seq dataset consists of 333 tumor samples obtained by bulk dissection, meaning that tumor cells, immune infiltrate, surrounding stroma and microenvironment contribute to the signal for each case. We further examined those genes most highly associated with OS and DFS endpoints based on their stringent association ($p<0.001$) for similar survival associations in data obtained from 333 endometrial cancers of the TCGA. A total of 7 genes were concordant for recurrence and 9 genes for OS (**Table 10** and **Table 11**, mRNA z-score EXP>2.0). We identified those transcripts with significant cox regression and Kaplan Meijer survival probabilities and with the additional desirable criteria mentioned above to identify a small subset for potential validation (**Table 10** and **Table 11**) in an independent set of cancers with known clinical follow-up and treatment.

Table 8. MSU Discovery Dataset Overall Survival Transcripts. P<0.005

Probe set	Gene symbol	Description	Parametric p-value	FDR	Permutation p-value	Hazard Ratio
233245_at	UHRF1BP1	UHRF1 binding protein 1	0.0000396	0.561	0.0002	0.39
243220_at	NA	NA	0.0000502	0.561	0.0001	0.382
221518_s_at	USP47	ubiquitin specific peptidase 47	0.0000515	0.561	< 1e-07	0.111
207534_at	MAGEB1	melanoma antigen family B, 1	0.0000616	0.561	0.0002	0.508
208180_s_at	NA	NA	0.0000681	0.561	0.0001	2.952
210033_s_at	SPAG6	sperm associated antigen 6	0.0000954	0.561	0.0003	1.782
1563878_a_at	LOC338963	hypothetical protein LOC338963	0.0000961	0.561	< 1e-07	0.382
210910_s_at	POMZP3	POM (POM121 homolog, rat) and ZP3 fusion	0.0001354	0.561	0.0001	2.682
222367_at	NA	NA	0.0001362	0.561	0.0001	0.406
1555729_a_at	CD209	CD209 molecule	0.0001531	0.561	0.0003	0.604
229595_at	CHCHD4	coiled-coil-helix-coiled-coil-helix domain containing 4	0.0001532	0.561	0.0003	3.311
217960_s_at	TOMM22	translocase of outer mitochondrial membrane 22 homolog (yeast)	0.0001557	0.561	0.0002	10.762
235617_x_at	NA	NA	0.000157	0.561	0.0004	0.563
213278_at	MTMR9	myotubularin related protein 9	0.000158	0.561	< 1e-07	0.101
235456_at	NA	NA	0.0001587	0.561	< 1e-07	2.424
206110_at	HIST1H3H	histone cluster 1, H3h	0.000171	0.561	0.0004	2.502
223032_x_at	PRELID1	PRELI domain containing 1	0.0001746	0.561	0.0003	5.52
239567_at	NA	NA	0.0001847	0.561	0.0003	0.54
224932_at	CHCHD10	coiled-coil-helix-coiled-coil-helix domain containing 10	0.0002316	0.63	0.0005	2.551
227916_x_at	EXOSC3	exosome component 3	0.0002456	0.63	0.0002	7.48
203990_s_at	KDM6A	lysine (K)-specific demethylase 6A	0.0002562	0.63	0.001	0.478
1557419_a_at	NA	NA	0.0002992	0.63	0.0003	0.529
230535_s_at	NA	NA	0.0003079	0.63	0.0014	0.505
236955_at	NA	NA	0.0003126	0.63	0.0006	0.627
204148_s_at	NA	NA	0.0003326	0.63	0.0008	2.367
243416_at	NA	NA	0.0003365	0.63	0.0004	0.535
222804_x_at	DCAF10	DDB1 and CUL4 associated factor 10	0.0003564	0.63	0.0006	4.603
243255_at	NA	NA	0.0003829	0.63	0.0005	0.544
225923_at	NA	NA	0.0003908	0.63	0.0015	0.246
233030_at	PNPLA3	patatin-like phospholipase domain containing 3	0.0003981	0.63	0.0005	0.584
205826_at	MYOM2	myomesin (M-protein) 2, 165kDa	0.0004016	0.63	0.0009	0.433
1561423_at	LOC642924	hypothetical protein LOC642924	0.0004208	0.63	0.0013	9.943
222941_at	USP46	ubiquitin specific peptidase 46	0.000437	0.63	0.0009	0.374
1559035_a_at	NA	NA	0.0004813	0.63	0.0001	0.617
232035_at	HIST1H4B	histone cluster 1, H4b	0.0004891	0.63	0.0003	2.203
215507_x_at	NA	NA	0.000491	0.63	0.0012	0.461
241699_at	NA	NA	0.0005014	0.63	0.0017	0.472
241091_at	NA	NA	0.0005171	0.63	0.0003	0.322
238360_s_at	NA	NA	0.0005232	0.63	0.0012	0.396
225930_at	NKIRAS1	NFKB inhibitor interacting Ras-like 1	0.000532	0.63	0.0011	5.406
239849_at	NA	NA	0.000538	0.63	0.0002	0.566
237638_at	NA	NA	0.0005472	0.63	0.0005	0.504
228560_at	NA	NA	0.0005817	0.63	0.0006	0.535
48659_at	MIIP	migration and invasion inhibitory protein	0.0005847	0.63	0.0009	7.783
216162_at	SBNO1	strawberry notch homolog 1 (Drosophila)	0.0005848	0.63	0.0004	0.494
219687_at	HHAT	hedgehog acyltransferase	0.0006146	0.63	0.0005	0.469
202160_at	CREBBP	CREB binding protein	0.0006197	0.63	0.0044	0.382
224601_at	NA	NA	0.0006244	0.63	0.0006	3.106
203297_s_at	JARID2	jumonji, AT rich interactive domain 2	0.0006492	0.63	0.0008	0.101
238870_at	KCNK9	potassium channel, subfamily K, member 9	0.0006729	0.63	0.0003	2.207
1565544_at	RNF141	ring finger protein 141	0.0006784	0.63	0.0004	0.597
213333_at	MDH2	malate dehydrogenase 2, NAD (mitochondrial)	0.0006788	0.63	0.0013	3.234
227497_at	SOX6	SRY (sex determining region Y)-box 6	0.0006838	0.63	0.0005	0.477
242915_at	ZNF682	zinc finger protein 682	0.000715	0.63	0.0013	0.402
227930_at	EIF2C4	eukaryotic translation initiation factor 2C, 4	0.0007306	0.63	0.0011	0.138
224978_s_at	USP36	ubiquitin specific peptidase 36	0.00074	0.63	0.0007	5.706
214011_s_at	NOP16	NOP16 nucleolar protein homolog (yeast)	0.0007782	0.63	0.0009	8.043
232478_at	NA	NA	0.0007796	0.63	0.0014	0.624
201242_s_at	ATP1B1	ATPase, Na+/K+ transporting, beta 1 polypeptide	0.0007906	0.63	0.0004	0.418
205743_at	STAC	SH3 and cysteine rich domain	0.0008061	0.63	0.0017	2.822
220797_at	METT10D	methyltransferase 10 domain containing	0.0008148	0.63	0.001	0.382
230652_at	ARAF	v-raf murine sarcoma 3611 viral oncogene homolog	0.000841	0.63	0.0015	3.896
209077_at	TXN2	thioredoxin 2	0.000843	0.63	0.0009	7.056
200054_at	ZNF259	zinc finger protein 259	0.0008448	0.63	0.0006	5.623
227426_at	SOS1	son of sevenless homolog 1 (Drosophila)	0.0008553	0.63	0.0003	0.14
222796_at	PTCD1	pentatricopeptide repeat domain 1	0.0008806	0.63	0.0012	0.297
237877_at	NA	NA	0.0009219	0.63	0.0003	0.549
203735_x_at	PPFIBP1	PTPRF interacting protein, binding protein 1 (liprin beta 1)	0.0009429	0.63	0.0004	6.628
235840_at	NA	NA	0.0009588	0.63	0.0033	0.307
1553118_at	THEM4	thioesterase superfamily member 4	0.0009884	0.63	0.0024	0.55
229909_at	B4GALNT3	beta-1,4-N-acetyl-galactosaminyl transferase 3	0.0009903	0.63	0.0009	0.547
1556657_at	NA	NA	0.0009927	0.63	0.0019	0.555
221007_s_at	FIP1L1	FIP1 like 1 (S. cerevisiae)	0.0009995	0.63	0.0015	0.252

Table 9. MSU Discovery Dataset Recurrence Free Interval Transcripts. P<0.005

Probe set	Gene symbol	Description	Parametric p-value	FDR	Permutation p-value	Hazard Ratio
206893_at	SALL1	sal-like 1 (Drosophila)	0.0000029	0.159	< 1e-07	0.63
229273_at	SALL1	sal-like 1 (Drosophila)	0.0000098	0.268	< 1e-07	0.617
216860_s_at	GDF11	growth differentiation factor 11	0.0000217	0.395	< 1e-07	0.468
208937_s_at	ID1	inhibitor of DNA binding 1, dominant negative helix-loop-helix protein	0.0000328	0.404	0.0004	0.632
213518_at	PRKCI	protein kinase C, iota	0.0000495	0.404	0.0001	3.413
205499_s_at	SRPX2	sushi-repeat-containing protein, X-linked 2	0.0000625	0.404	0.0002	0.615
237240_at	NA	NA	0.0000748	0.404	0.0004	0.44
236780_at	NA	NA	0.0000761	0.404	0.0002	4.18
231609_at	C10orf82	chromosome 10 open reading frame 82	0.0000824	0.404	0.0001	0.512
1560589_a_at	NA	NA	0.0000866	0.404	0.0004	1.583
243907_at	NA	NA	0.0001006	0.404	< 1e-07	0.484
209678_s_at	PRKCI	protein kinase C, iota	0.0001077	0.404	0.0003	2.944
238724_at	BPGM	2,3-bisphosphoglycerate mutase	0.0001133	0.404	0.0003	0.445
241896_at	MACF1	microtubule-actin crosslinking factor 1	0.000125	0.404	0.0002	0.459
1552785_at	ZNF781	zinc finger protein 781	0.0001262	0.404	0.0004	0.595
232555_at	CREB5	cAMP responsive element binding protein 5	0.0001323	0.404	0.0002	0.468
202150_s_at	NEDD9	neural precursor cell expressed, developmentally down-regulated 9	0.0001338	0.404	0.0005	0.482
215725_at	DGCR11	DiGeorge syndrome critical region gene 11	0.0001423	0.404	0.0003	0.49
205911_at	PTH1R	parathyroid hormone 1 receptor	0.0001431	0.404	0.0007	0.519
230319_at	NA	NA	0.0001477	0.404	0.0001	0.7
36499_at	CELSR2	cadherin, EGF LAG seven-pass G-type receptor 2 (flamingo homolog, Drosophila)	0.0001699	0.438	0.0001	4.572
229303_at	NA	NA	0.0001843	0.438	0.0008	3.578
238748_at	NA	NA	0.0001863	0.438	0.0002	0.538
1559489_a_at	LOC257358	hypothetical LOC257358	0.0001945	0.438	0.0002	0.542
243283_at	NA	NA	0.000225	0.438	0.0003	0.553
232872_at	NA	NA	0.0002286	0.438	0.0005	0.629
230664_at	NA	NA	0.0002371	0.438	0.0006	0.634
244469_at	NA	NA	0.0002406	0.438	0.001	0.532
222598_s_at	NAV2	neuron navigator 2	0.0002498	0.438	0.0003	0.418
206159_at	GDF10	growth differentiation factor 10	0.0002572	0.438	< 1e-07	0.546
236913_at	NA	NA	0.0002582	0.438	0.0006	0.368
221621_at	C17orf86	chromosome 17 open reading frame 86	0.0002617	0.438	0.0003	3.631
234631_at	KRTAP4-8	keratin associated protein 4-8	0.0002656	0.438	0.0003	0.334
227093_at	USP36	ubiquitin specific peptidase 36	0.0002778	0.438	0.0003	6.15
213217_at	ADCY2	adenylate cyclase 2 (brain)	0.0002828	0.438	0.0005	0.56
205454_at	HPCA	hippocalcin	0.0002887	0.438	0.0005	0.514
236982_at	NA	NA	0.0003183	0.468	0.0005	3.024
1553743_at	FAM119A	family with sequence similarity 119, member A	0.0003252	0.468	0.0006	2.913
230668_at	NKAIN4	Na+/K+ transporting ATPase interacting 4	0.000383	0.526	0.0008	1.657
1561653_at	NA	NA	0.000385	0.526	0.0002	0.583
222153_at	MYEF2	myelin expression factor 2	0.0003972	0.53	0.0004	0.593
1562524_at	NA	NA	0.0004327	0.537	0.0008	0.483
1559880_at	NA	NA	0.000438	0.537	0.0002	0.44
232272_at	ZNF624	zinc finger protein 624	0.0004432	0.537	0.0012	0.323
217017_at	OSBPL10	oxysterol binding protein-like 10	0.0004513	0.537	0.0001	0.611
1562909_at	C1orf98	chromosome 1 open reading frame 98	0.0004604	0.537	0.0002	0.546
209171_at	ITPA	inosine triphosphatase (nucleoside triphosphate pyrophosphatase)	0.0004619	0.537	0.0007	7.786
228307_at	EMILIN3	elastin microfibril interfacer 3	0.0004737	0.54	0.0014	0.525
213707_s_at	DLX5	distal-less homeobox 5	0.0004838	0.54	0.0011	0.74
1566517_at	NA	NA	0.0004999	0.547	0.0013	0.246
224516_s_at	CXXC5	CXXC finger 5	0.0005122	0.549	0.0009	3.344
235888_at	LOC728411	glucuronidase, beta pseudogene	0.0005532	0.579	0.0022	1.861
229983_at	TIGD2	tigger transposable element derived 2	0.000561	0.579	0.0011	0.33
233222_at	NA	NA	0.0005952	0.58	0.0003	0.569
207206_s_at	ALOX12	arachidonate 12-lipoxygenase	0.0006045	0.58	0.002	2.142
217242_at	ZNF154	zinc finger protein 154	0.0006136	0.58	0.0005	0.464
1566873_at	NA	NA	0.0006329	0.58	0.0007	0.535
1554057_at	LOC645676	hypothetical LOC645676	0.000634	0.58	0.0005	5.558
229504_at	NA	NA	0.0006356	0.58	0.0005	0.283
229296_at	LOC100128501	hypothetical protein LOC100128501	0.0006361	0.58	0.0002	1.481
208070_s_at	REV3L	REV3-like, catalytic subunit of DNA polymerase zeta (yeast)	0.0006632	0.582	0.0008	0.37
223023_at	BET1L	blocked early in transport 1 homolog (S. cerevisiae)-like	0.000671	0.582	0.0008	2.99
207815_at	PF4V1	platelet factor 4 variant 1	0.000697	0.582	0.0012	0.666
213571_s_at	EIF4E2	eukaryotic translation initiation factor 4E family member 2	0.0007086	0.582	0.0005	0.179
1556734_at	NA	NA	0.0007128	0.582	0.0012	0.407
1553863_at	WDFY4	WDFY family member 4	0.0007312	0.582	0.0015	0.482
1552698_at	MGC16703	tubulin, alpha pseudogene	0.000732	0.582	0.0003	0.572
212759_s_at	TCF7L2	transcription factor 7-like 2 (T-cell specific, HMG-box)	0.0007398	0.582	0.0022	0.602
1560212_a_at	NA	NA	0.0007416	0.582	0.0005	0.45
1564544_x_at	LOC644450	hypothetical protein LOC644450	0.0007447	0.582	0.0005	0.373
211551_at	EGFR	epidermal growth factor receptor (erythroblastic leukemia viral (v-erb-b) oncogene homolog, avian)	0.0007563	0.582	0.0013	0.4
1566442_at	NA	NA	0.0008575	0.632	0.0005	0.632
214844_s_at	DOK5	docking protein 5	0.0008735	0.632	0.0015	1.528
240259_at	FLRT2	fibronectin leucine rich transmembrane protein 2	0.0008762	0.632	0.0016	0.623
223339_at	ATPIF1	ATPase inhibitory factor 1	0.0009228	0.632	0.001	3.847
224821_at	ABHD14B	abhydrolase domain containing 14B	0.0009257	0.632	0.0016	3.074
1556387_at	NA	NA	0.0009348	0.632	0.0025	0.565
1556266_a_at	LOC400831	hypothetical LOC400831	0.0009677	0.632	0.001	0.539
244364_at	MYO3A	myosin IIIA	0.0009702	0.632	0.0013	1.629
232229_at	SETX	senataxin	0.0009768	0.632	0.0022	0.449
217351_at	NA	NA	0.00099	0.632	0.0008	0.569
203700_s_at	DIO2	deiodinase, iodothyronine, type II	0.0009928	0.632	0.0016	0.572

A.

Died (n=9) | Other Cases (n=127)

B.

Relapsed n=13 | Non Relapsed n=107

Figure 16. Heat Map of MSU Discovery Dataset Transcripts. Our MSU internal discovery dataset consisted of 136 endometrial cancer samples. Every sample that was analyzed in this set was a laser-captured, micro-dissected portion of the original tumor.
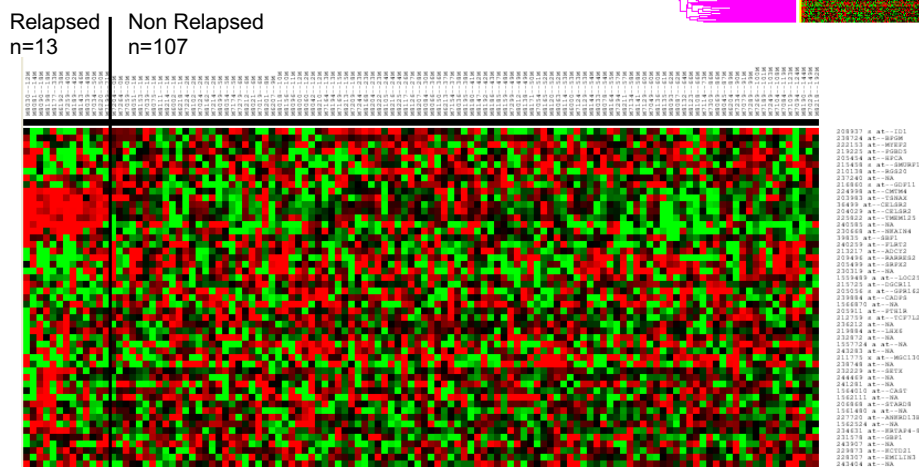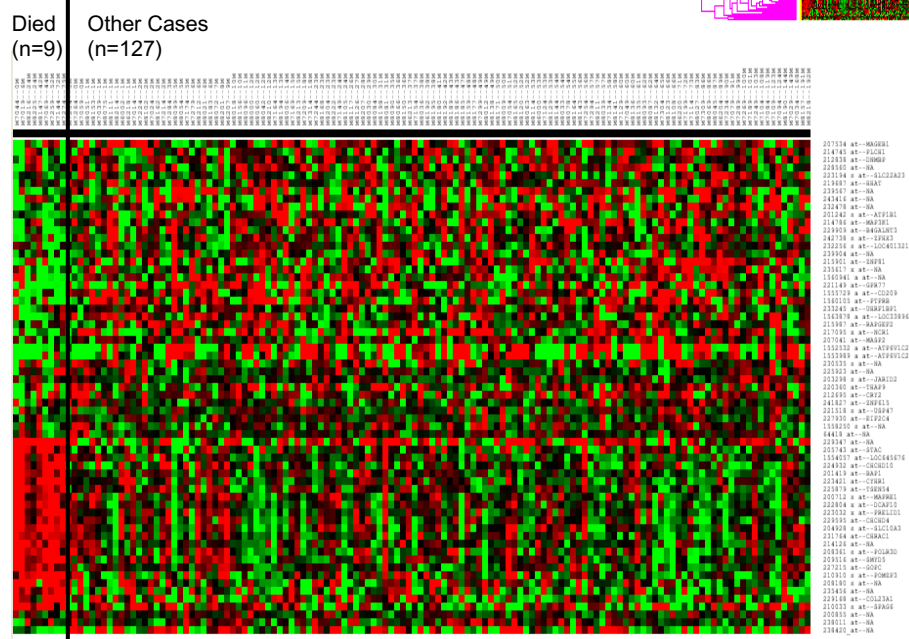
Figure 16 (cont'd)

In these cases, the vast majority of mRNA signal comes from the cancer cells. COX regression analysis was performed on Affymetrix-based gene expression data to establish which specific transcripts were associated with overall survival, disease relapse, or both at $p<0.005$. A. Supervised cluster of overall survival analysis considering patient cases confirmed to have died from their disease. Died n=9, other cases n=127. B. Supervised clustering showing relapsed vs. non-relapsed analysis. Relapsed n=13, non-relapsed n=107.
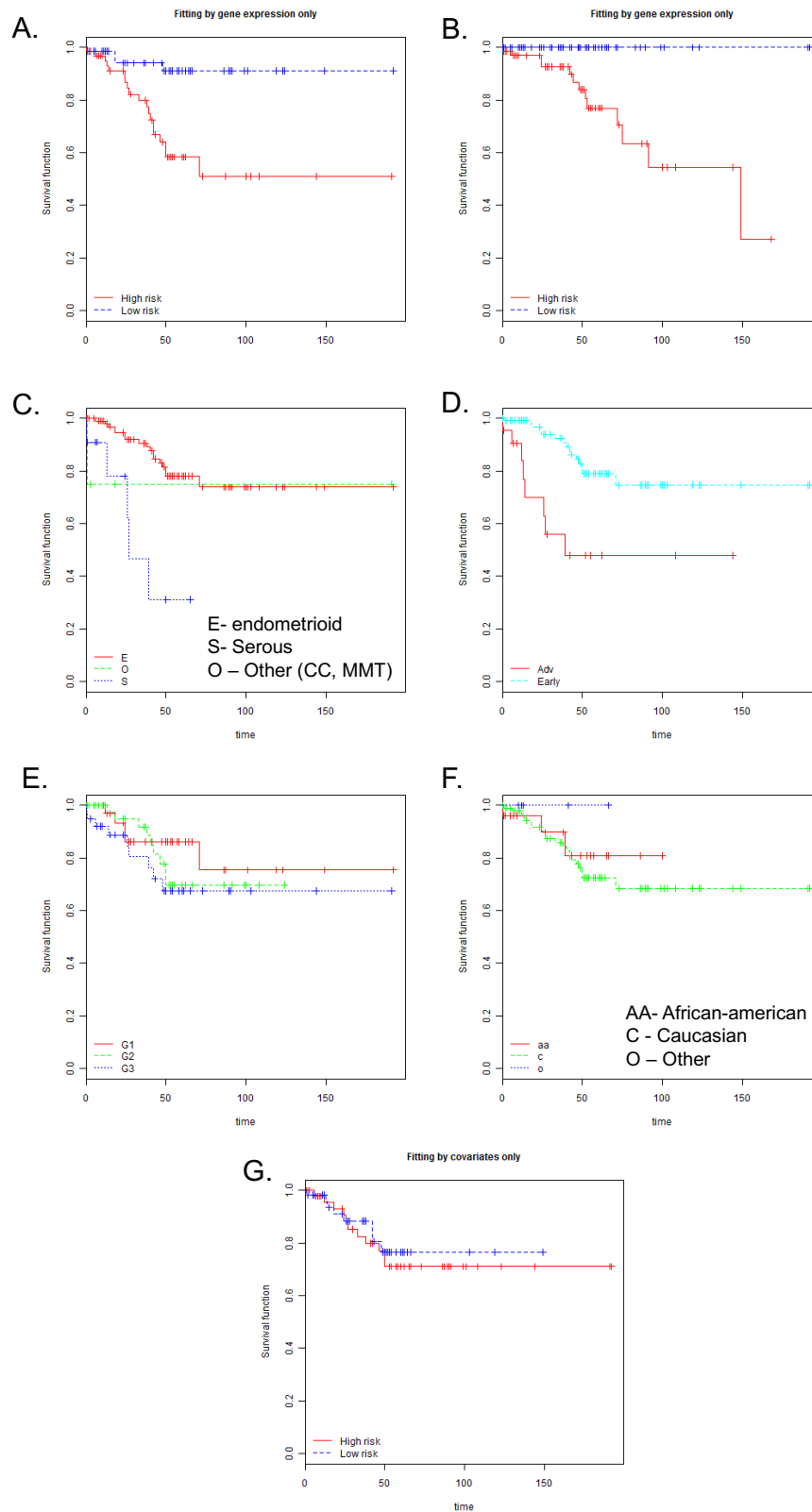
Figure 17. Prediction Modeling. Genes were selected for predictive model based on

Figure 17 (cont'd)

Cox Regression Analysis at p<0.005. Samples were divided into high risk and low risk groups. Kaplan-Meier Plots were made between these groups. A total of 23 recurred and 113 NED cases were used for fitting. All 54K transcripts on the array were examined. Cox Regression Analysis found 437 transcripts at p < 0.005. These are the genes correlated with Recurrence. 360 of these genes were selected for predictive model. Samples were divided into high risk and low risk groups. Kaplan-Meier Plots were made between these groups. Overall survival (A) and Relapse (B) prediction using those transcripts associated with these endpoints at p<0.005 in Cox Regression Analysis. C. Histology as covariate. D. Stage as covariate. E. Grade as covariate. F. Race as covariate. G. BMI as covariate.

Table 10. MSU Discovery Dataset TCGA Validated Overall Survival Transcripts.

Probe set	Gene symbol	Description	Parametric p-value	FDR	Permutation p-value	Hazard Ratio
217960_s_at	TOMM22	translocase of outer mitochondrial membrane 22 homolog (yeast)	0.0001557	0.561	0.0002	10.762
225930_at	NKIRAS1	NFKB inhibitor interacting Ras-like 1	0.000532	0.63	0.0011	5.406
219687_at	HHAT	hedgehog acyltransferase	0.0006146	0.63	0.0005	0.469
238870_at	KCNK9	potassium channel, subfamily K, member 9	0.0006729	0.63	0.0003	2.207
213333_at	MDH2	malate dehydrogenase 2, NAD (mitochondrial)	0.0006788	0.63	0.0013	3.234
227497_at	SOX6	SRY (sex determining region Y)-box 6	0.0006838	0.63	0.0005	0.477
214011_s_at	NOP16	NOP16 nucleolar protein homolog (yeast)	0.0007782	0.63	0.0009	8.043
201242_s_at	ATP1B1	ATPase, Na+/K+ transporting, beta 1 polypeptide	0.0007906	0.63	0.0004	0.418
205743_at	STAC	SH3 and cysteine rich domain	0.0008061	0.63	0.0017	2.822

Table 11. MSU Discovery Dataset TCGA Validated Recurrence Free Interval Transcripts.

Probe set	Gene symbol	Description	Parametric p-value	FDR	Permutation p-value	Hazard Ratio
213518_at	PRKCI	protein kinase C, iota	0.0001077	0.404	0.0003	2.944
230668_at	NKAIN4	Na+/K+ transporting ATPase interacting 4	0.000383	0.526	0.0008	1.657
224516_s_at	CXXC5	CXXC finger 5	0.0005122	0.549	0.0009	3.344
1553863_at	WDFY4	WDFY family member 4	0.0007312	0.582	0.0015	0.482
212759_s_at	TCF7L2	transcription factor 7-like 2 (T-cell specific, HMG-box)	0.0007398	0.582	0.0022	0.602
214844_s_at	DOK5	docking protein 5	0.0008735	0.632	0.0015	1.528
244364_at	MYO3A	myosin IIIA	0.0009702	0.632	0.0013	1.629

Transcriptional analysis of survival associated gene CXXC5

One of the most impressive genes, CXXC5 was chosen as the focus of this study given its highly significant correlation with poor outcome (**Figure 18**A overall survival (p=0.000912) and **Figure 18**B recurrence (p=0.0000234) in TCGA data) and lack of detailed functional classification in the endometrium. Furthermore, we determined that these survival associations were correlated with elevated transcript levels. CXXC5 demonstrated an impressive association with recurrence (**Table 12** and **Figure 18**). We next determined that those TCGA cancers that are high CXXC5 expressing (upper quartile) also had worse OS and DFS as compared to those in the lowest expressing quartile (**Figure 19**). Similar expression profiles were noted for all those genes listed in **Table 10** and **Table 11**(data not shown). We further confirmed these discovery data using qRT-PCR on an internal cohort of endometrial cancers demonstrating that high transcript level of CXXC5 correlates with detrimental outcomes (**Table 12** - columns 7 and 8) by TaqMan in a third independent (Spectrum Health, n=73) cohort of endometrial cancers (**Figure 18**C and D).
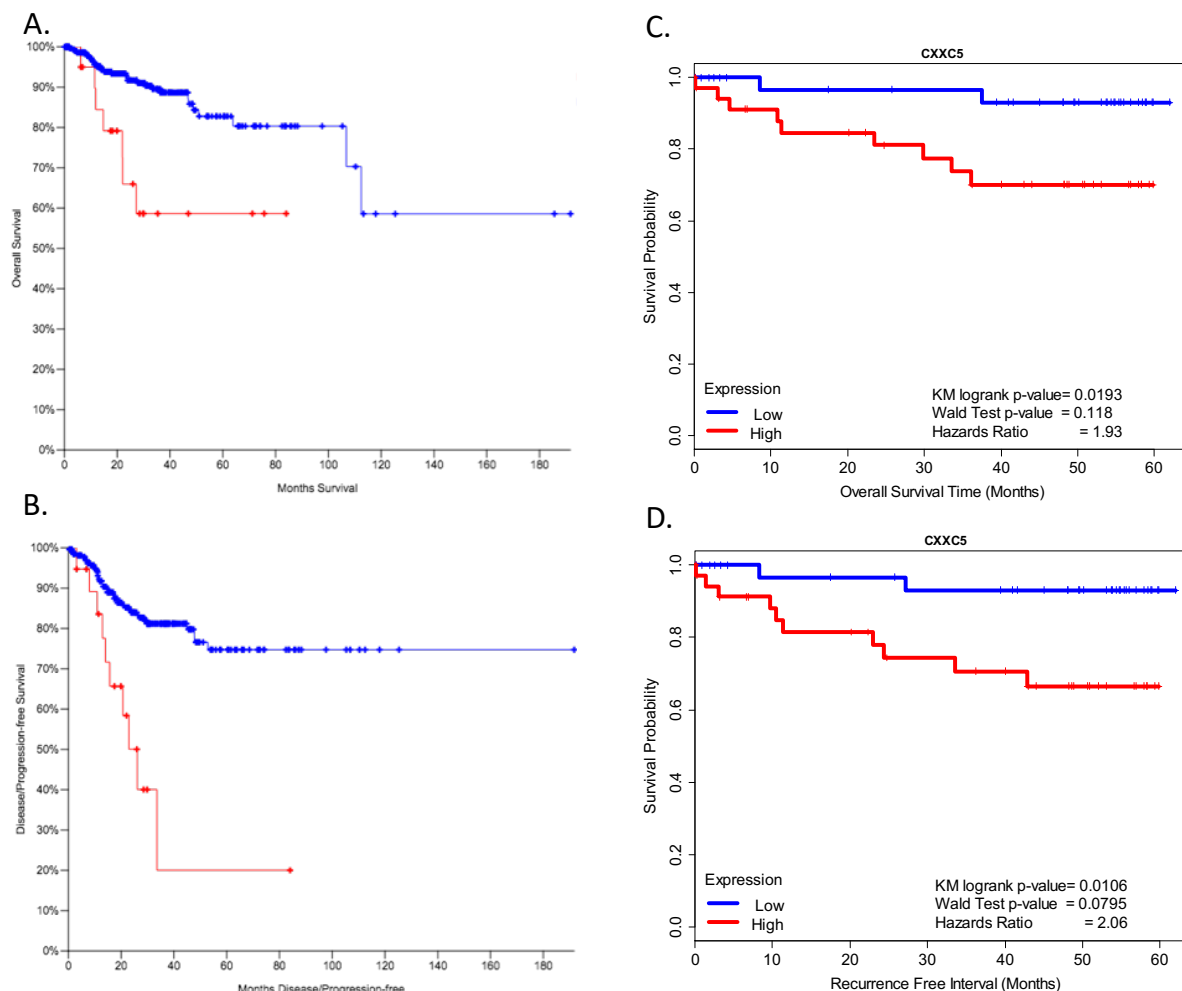
Figure 18. CXXC5 Survival Data. RSEM Normalized RNA-Seq (UNC Illumina HiSeq RNASeq V2, level 3) data was used from TCGA website. 333 cases were considered for the analysis and their clinical parameters were taken from cBioPortal for Uterine Corpus Endometrioid Carcinoma (TCGA, Nature 2013; cBioPortal-generated images: Cerami et al., Cancer Discov. 2012 and Gao et al. Sci. Signal. 2013). Red line indicates cases with alteration (upregulation of transcript level indicated by red line). A.) TCGA OS KM plot. Z=2.0 p-value=0.000912, n=333. B.) TCGA RFI KM plot. Z=2.0 p-value=0.0000234, n=333. C.) OS KM plot of Spectrum data. p=0.0193. No event n=62.

Figure 18 (cont'd)

Died n=11. D.) RFS KM plot of Spectrum data. p=0.0106 No event n=61. Recurred

n=12. E.) Mean relative expression of cases presented in D.

Table 12. Summary of CXXC5 Survival Statistics. CXXC5 expression shows

significant correlation with OS and RFI in three independent datasets.

Gene Symbol	Probe Set	MSU Disease Free Survival		TCGA Overall Survival	TCGA Disease Free Survival	Spectrum Overall Survival	Spectrum Disease Free Survival
		p-value	Hazard Ratio	p-value	p-value	p-value	p-value
CXXC5	224516_s_at	0.0005122	3.344	0.0003	0.000009	0.0193	0.0106
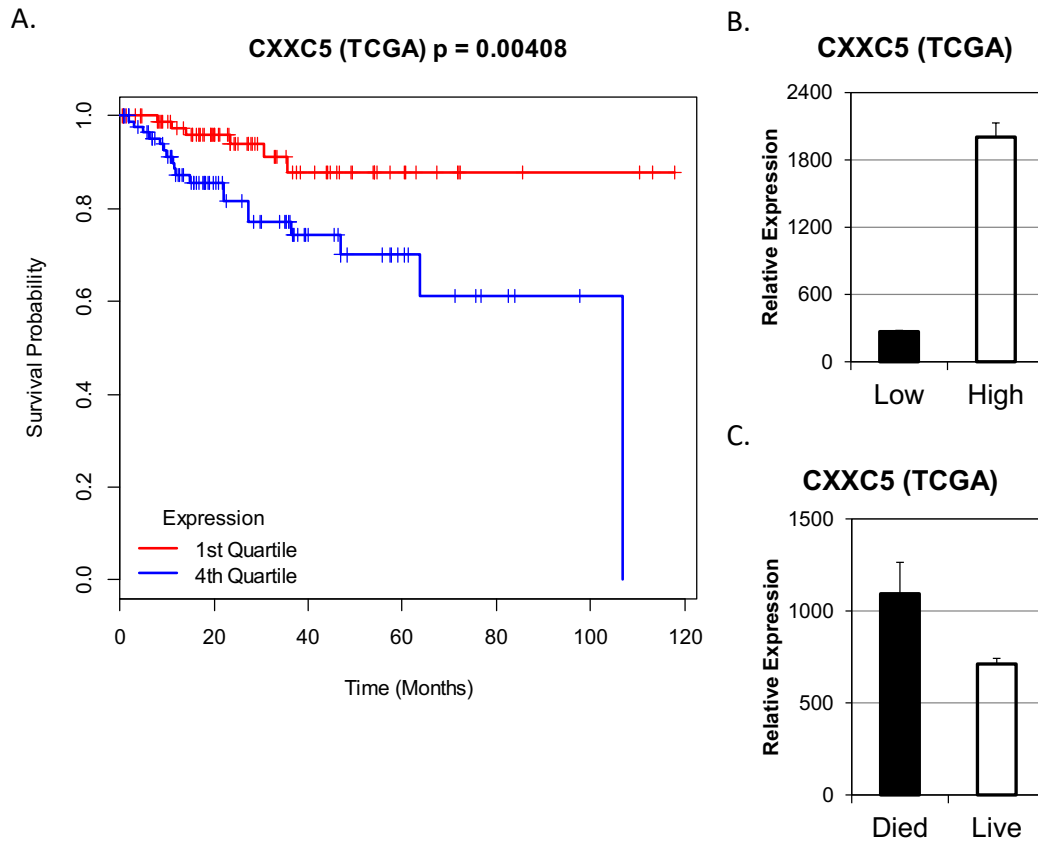
Figure 19. Quartile Expression of CXXC5 from TCGA Serous & Endometrioid. RSEM Normalized RNA-Seq (UNC Illumina HiSeq RNASeq V2, level 3) data was downloaded from TCGA website. From these, 352 cases were considered for the analysis and their clinical parameters were taken from cBioportal for Uterine Corpus Endometrioid Carcinoma (TCGA, Nature 2013). A. Kaplan-Meier plot of low and high expressions in 352 cases including 39 deaths. Cases were divided by expression as 1st and 4th Quartile. 1st quartile includes 88 cases. B. Average 1st and 4th quartile expressions ($p < 0.000001$). C. Average expressions of "Died" and "Live" cases ($p = 0.003$).

Endometrial cancer sub-types and correlation of genetic alterations with high CXXC5 expression

Historically, endometrial cancers have been classified as either Type I or Type II(79). With this in mind, we used TCGA data to assess for correlations between common mutations in these two endometrial cancer subtypes and CXXC5 transcriptional overexpression (**Figure 20**). There is almost no overlap of CTNNB1 and PTEN mutation and CXXC5, an indication that CXXC5 overexpression is not correlated with Type I cases. Furthermore, we noted a strong correlation of CXXC5 with TP53 mutation but not with PTEN mutation indicating that CXXC5 overexpression more commonly occurs in the Type II group. Further the most commonly mutated genes in these cancers included TP53 (**Table 13**). Sensitivity and specificity of CXXC5 overexpression is summarized in **Table 14** by study based on stage, grade, histology, nodes, and invasion status.
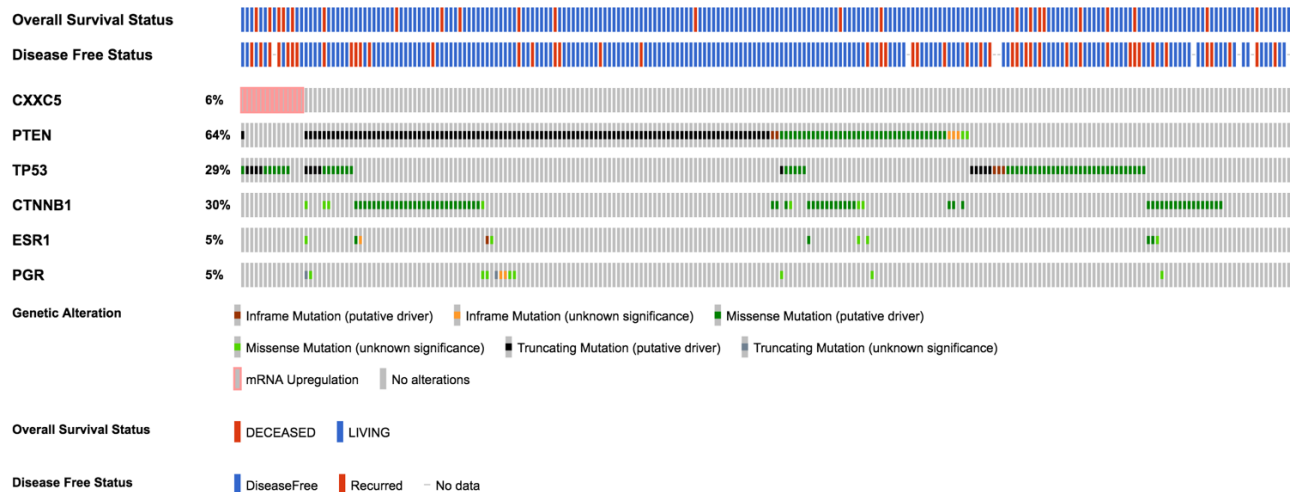
Figure 20. Oncoprint of TCGA data. CXXC5 Z-score set at 2.0. RSEM Normalized RNA-Seq (UNC Illumina HiSeq RNASeq V2, level 3) data were used from TCGA website. CXXC5 overexpression is compared against common mutations in endometrial cancers and overlaid with survival and disease-free status.

Table 13. Top 10 mutation alterations in CXXC5 overexpressing tumors. RSEM Normalized RNA-Seq (UNC Illumina HiSeq RNASeq V2, level 3) data was used from TCGA website. CXXC5 z-score = 2.0. Table indicates top 10 most significantly altered genes that either tend towards mutual exclusivity from CXXC5 overexpression or tend to co-occur with CXXC5 overexpression.

Gene	Cytoband	Samples with alteration in altered group	Samples with alteration in unaltered group	Log Ratio	p-Value	q-Value	Tendency
PTEN	10q23.31	1 (7.14%)	147 (67.43%)	-3.24	9.52E-06	0.165	Mutual exclusivity
TP53	17p13.1	11 (78.57%)	56 (25.69%)	1.61	1.02E-04	0.888	Co-occurrence
WNT8A	5q31.2	2 (14.29%)	0 (0.00%)	>10	3.40E-03	0.94	Co-occurrence
CTNNB1	3p22.1	0 (0.00%)	69 (31.65%)	<-10	6.00E-03	0.94	Mutual exclusivity
RHOXF2B	Xq24	2 (14.29%)	1 (0.46%)	4.96	9.83E-03	0.94	Co-occurrence
TSPEAR	21q22.3	3 (21.43%)	6 (2.75%)	2.96	0.0119	0.94	Co-occurrence
ARID1A	1p36.11	1 (7.14%)	77 (35.32%)	-2.31	0.0229	0.94	Mutual exclusivity
ARMC12	6p21.31	2 (14.29%)	3 (1.38%)	3.38	0.0305	0.94	Co-occurrence
PIK3R1	5q13.1	1 (7.14%)	73 (33.49%)	-2.23	0.031	0.94	Mutual exclusivity
FBXW7	4q31.3	5 (35.71%)	33 (15.14%)	1.24	0.0588	0.94	Co-occurrence

Table 14. CXXC5 Sensitivity and Specificity. Unknown node and invasion status were considered negative. Cases having no survival data were excluded. All calculations were done considering 60-month follow-up time. The events were considered at this cut-off to calculate the 2 x 2 table and specificity and sensitivity.

TCGA		OS	RFI		MSU Discovery		OS	RFI
Histology	sensitivity	27.8%	25.9%		Histology	sensitivity	20.0%	23.5%
	specificity	87.0%	89.0%			specificity	92.9%	94.1%
Stage	sensitivity	58.3%	46.3%		Stage	sensitivity	30.0%	35.3%
	specificity	79.1%	83.3%			specificity	84.9%	86.6%
Grade	sensitivity	75.0%	55.6%		Grade	sensitivity	50.0%	35.3%
	specificity	55.7%	57.8%			specificity	72.2%	71.4%
Node	sensitivity	41.7%	29.6%					
	specificity	86.7%	90.5%					
Invasion	sensitivity	61.1%	51.9%					
	specificity	61.1%	62.0%					

CXXC5 throughout the menstrual cycle

Previous studies have implicated CXXC5 as an estrogen responsive gene in breast tissue (198). Given the estrogen responsive nature of the endometrium, we sought to evaluate for any potential impacts hormone cycling would have on CXXC5 expression levels. To accomplish this goal, we first used the publically available NCBI GEO profiles selecting a study based on gene expression analysis of the endometrium (199). We noted a trend for CXXC5 levels to be elevated during the proliferative phase of endometrial growth as compared to the secretory phase (**Figure 21**).
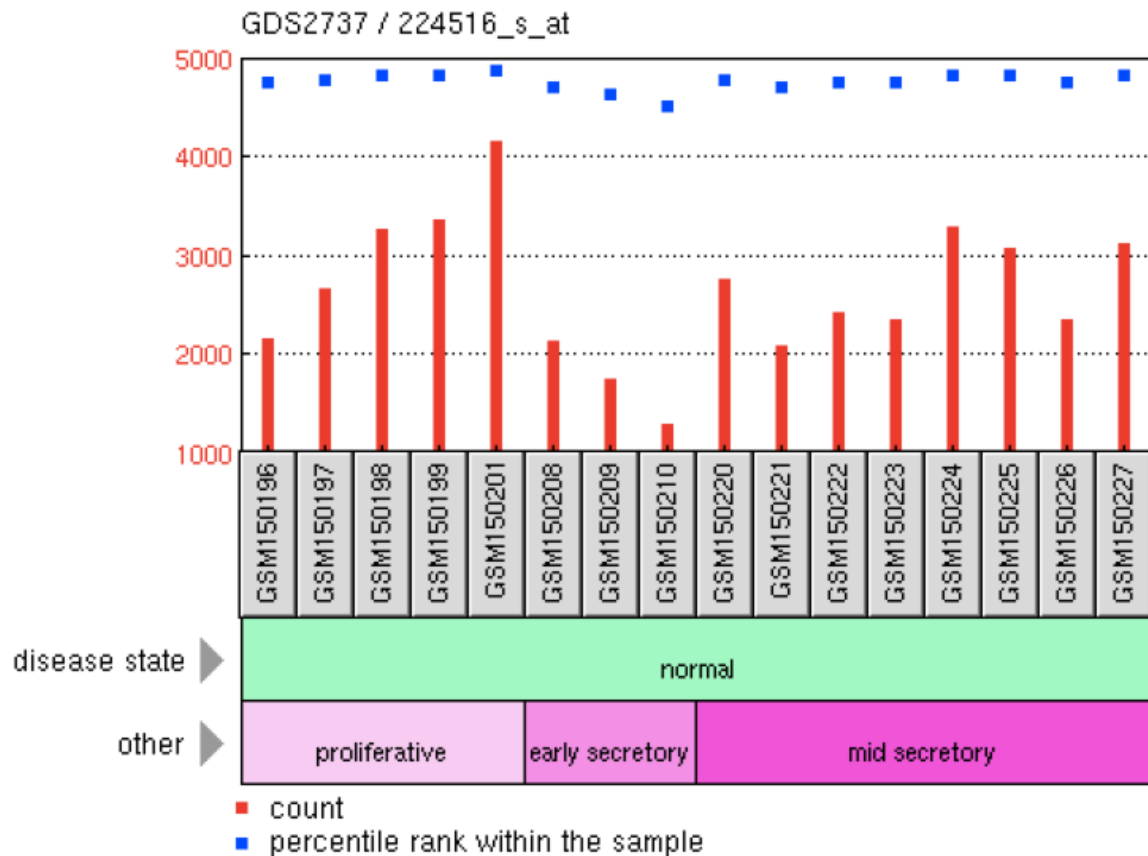
Figure 21. CXXC5 is expressed in the epithelium at a higher level during the proliferative phase. From: https://www.ncbi.nlm.nih.gov/geo/tools/profileGraph.cgi?ID=GDS2737:224516_s_at.

Briefly, this particular study included only women with surgically documented and histologically validated moderate/severe-stage endometriosis as well as biopsies from women who were cycling normally and who were also found to be free of endometriosis at the time of surgery (n=16). The endometriosis-free cohort included women between the ages of 23 and 50 years and indications for their operative procedures included uterine prolapse, uterine leiomyomata, normal volunteers, pelvic pain, and ovarian cyst. All subjects considered for the normal samples were verified as being endometriosis free during laproscopic surgery. Use of any hormonal treatment within 3 months of the

Figure 21 (cont'd)

study biopsy resulted in exclusion from the dataset. Per the study details and methods, specimens were classified as proliferative (PE, d 8–14), early secretory (ESE, d 15–18), midsecretory (MSE, d 19–23), or late secretory (d 24–28) endometrium (199).

Further, CXXC5 expression has not been assessed in normal endometrial tissues. We used immunohistochemistry and determined levels of CXXC5 in normal pre-menopausal proliferative and secretory endometrium to determine whether our *in-silico* findings were applicable in whole human tissues. We found that while not statistically significant, CXXC5 detection trended to be increased during the proliferative phase as compared to the secretory phase and regardless, trended to be expressed more highly in glandular cells as compared to the surrounding stromal cells (**Figure 22** comparison of matched tissue samples in **Figure 25**).
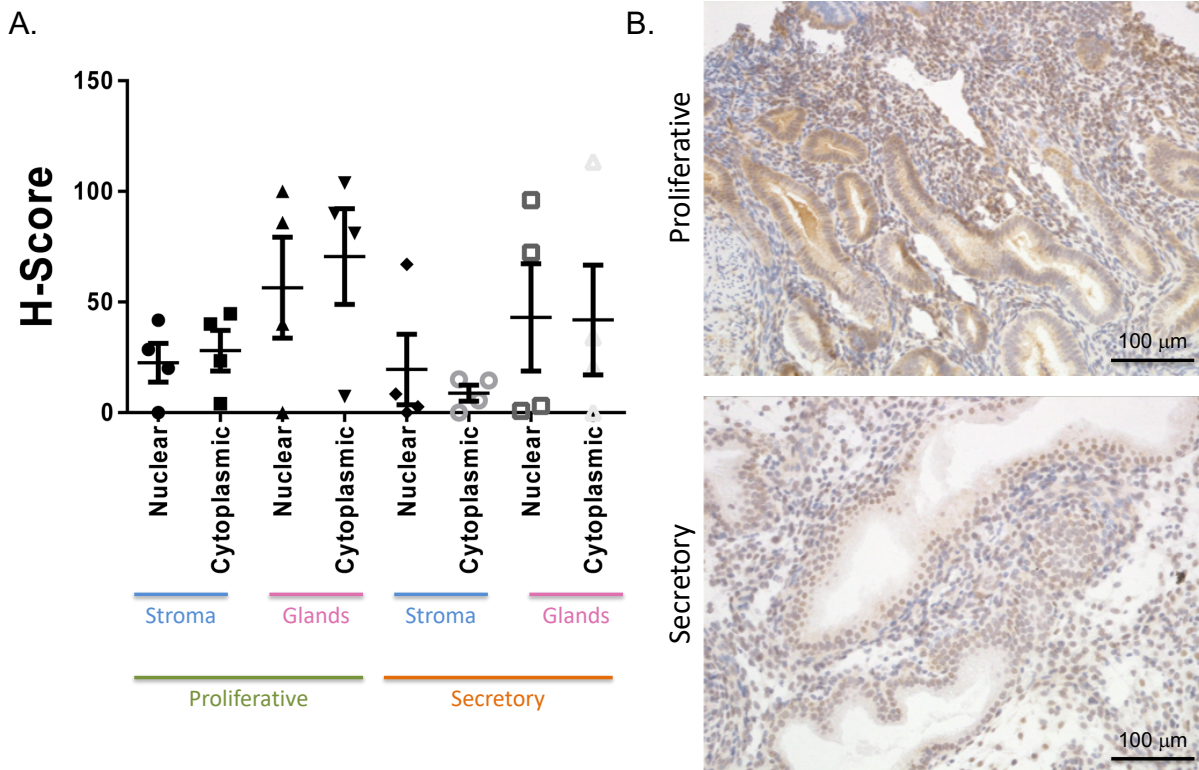
Figure 22. CXXC5 is expressed at a higher level during the proliferative phase. A. H-score quantification of normal endometrial tissues. B. Images of proliferative vs. secretory phase. N=4 specimens per phase. Scale bar = 100 μm.

Evaluation of hormone stimulation of CXXC5 expression in endometrial epithelium and stroma

We next sought to evaluate whether the trends seen in the GEO profiles data could be repeated in vitro and whether glandular or stromal cells were the major contributing factor to changes in expression. To accomplish this goal, we treated hESC-TERT (immortalized endometrial stroma) or EM-TERT (immortalized endometrial epithelium) with varying concentrations of estrogen, progesterone, or both hormones to

mimic menstrual cycle conditions. Stromal cells did not display a quantitative transcriptional change in CXXC5 levels regardless of estrogen or progesterone stimulation as measured by TaqMan qRT-PCR. However, low levels of estrogen treatment alone were able to stimulate an increase in CXXC5 transcriptional levels suggesting an estrogen responsive role in the epithelial component **(Figure 23**).
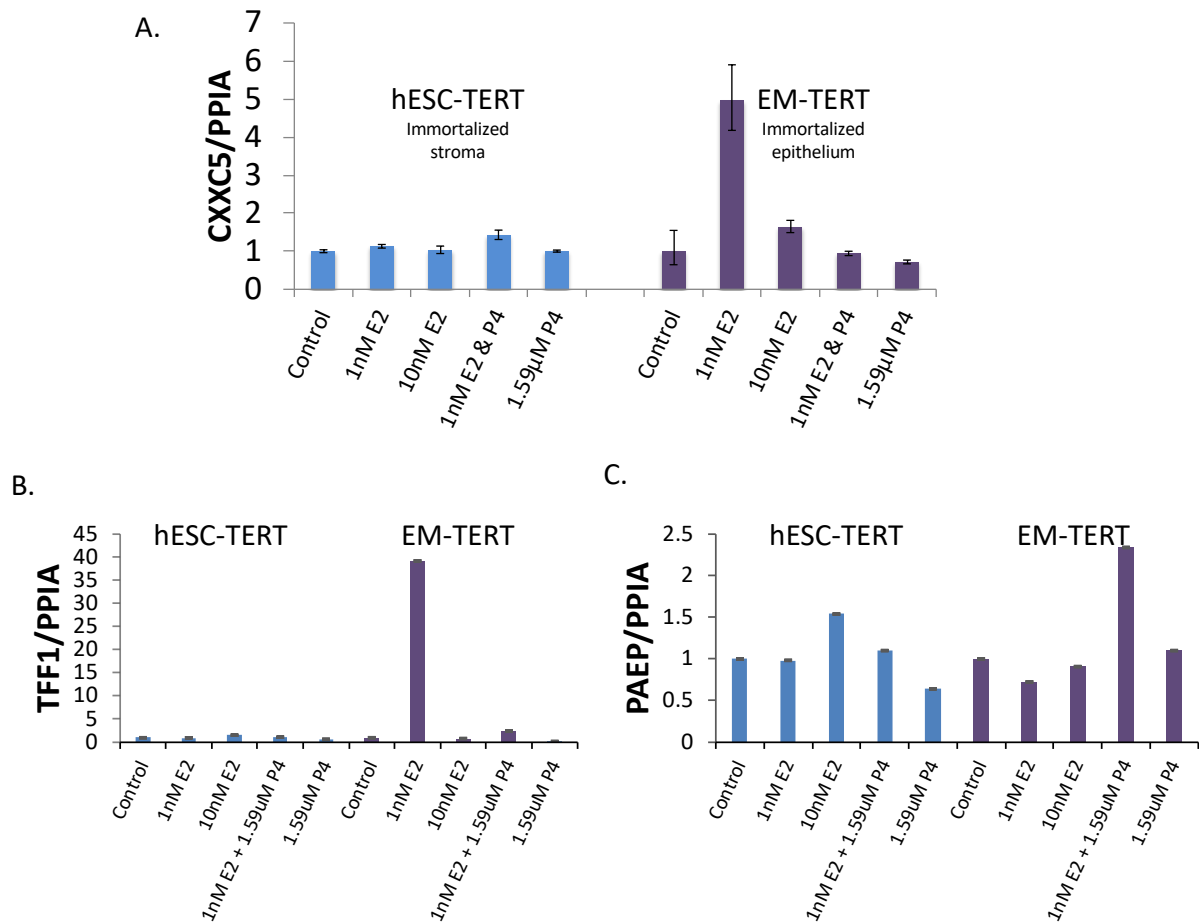

Figure 23. CXXC5 expression in stroma vs. epithelium. A. hESC-TERT (immortalized stromal cells) and EM-TERT (immortalized endometrial epithelial cells) were independently treated with varying concentrations of estrogen along, progesterone alone, or a combination of estrogen and progesterone. EM-TERT cells experienced

Figure 23 (cont'd)

transcriptional upregulation of *CXXC5* upon low estrogen supplementation. B & C. Control estrogen responsive gene *TFF1* and progesterone responsive gene *PAEP*.

Immunohistochemical detection of CXXC5 as a predictor of disease outcome

Additionally, CXXC5 expression has not been assessed in a set of malignant endometrial tissues. We used immunohistochemical detection with H-scoring to quantify levels of CXXC5 in whole tissues from our annotated Spectrum dataset (**Figure 24**A). This set contained endometrial cancers with and without adverse events as well as matched normal endometrial tissues. We found that tumors from patients who experienced an unfavorable outcome (relapse or death) also had significantly elevated tissue CXXC5 levels as compared to tumor cases not experiencing such events (**Figure 24**B, $p < 0.0001$). Interestingly, case-matched normal uterine tissues (non-tumor tissue) from patients who experienced unfavorable outcomes also had elevated levels of CXXC5 detection when compared to normal background uterine tissue from patients who did not experience unfavorable outcomes though this elevation did not reach statistical significance (**Figure 24**B).

Attempts were made at establishing a phenotype for CXXC5 overexpression by knocking down transcriptional activity in endometrial cancer cell lines (**Figure 26**).
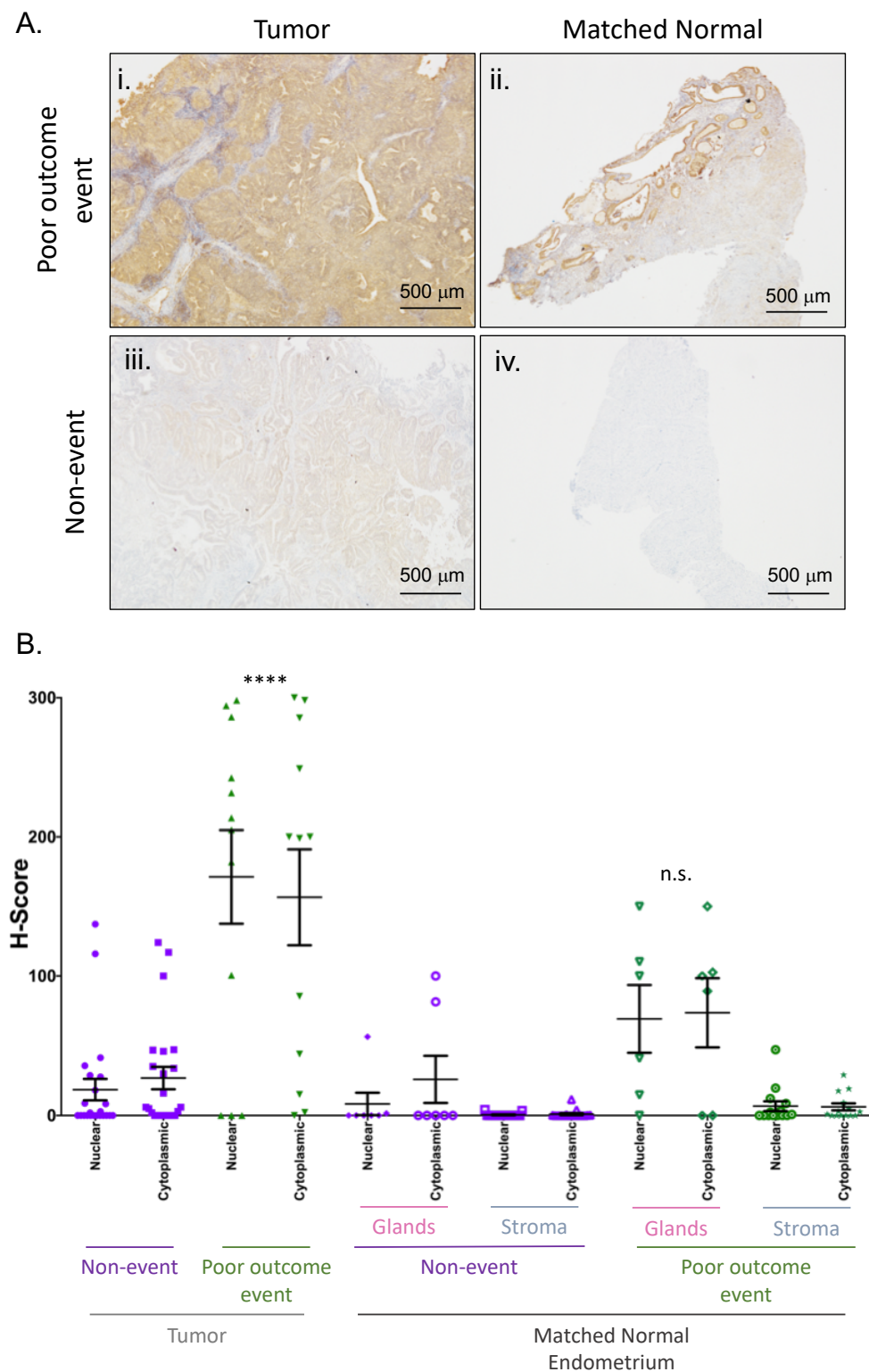
Figure 24. CXXC5 detection by IHC is higher in poor outcome event tumors vs. non-event tumors. A. Representative images of CXXC5 IHC for i. poor outcome event

Figure 24 (cont'd)

tumor, ii. matched normal endometrium from poor outcome event, iii. non-event tumor tissue, and iv. matched normal endometrial tissue from a non-event patient. Scale bar = 500 μm. Glands can be seen with high detection (brown) of CXXC5 while stroma remains hematoxylin stained. B. H-score quantification of IHC detection. Stroma and glands were quantified separately in matched normal tissues. Additionally, cytoplasmic and nuclear detection was quantified separately for each sample. N=12 poor outcome event cases with matched normal tissue and n=23 non-event tissues with matched normal. ****$p<0.0001$.
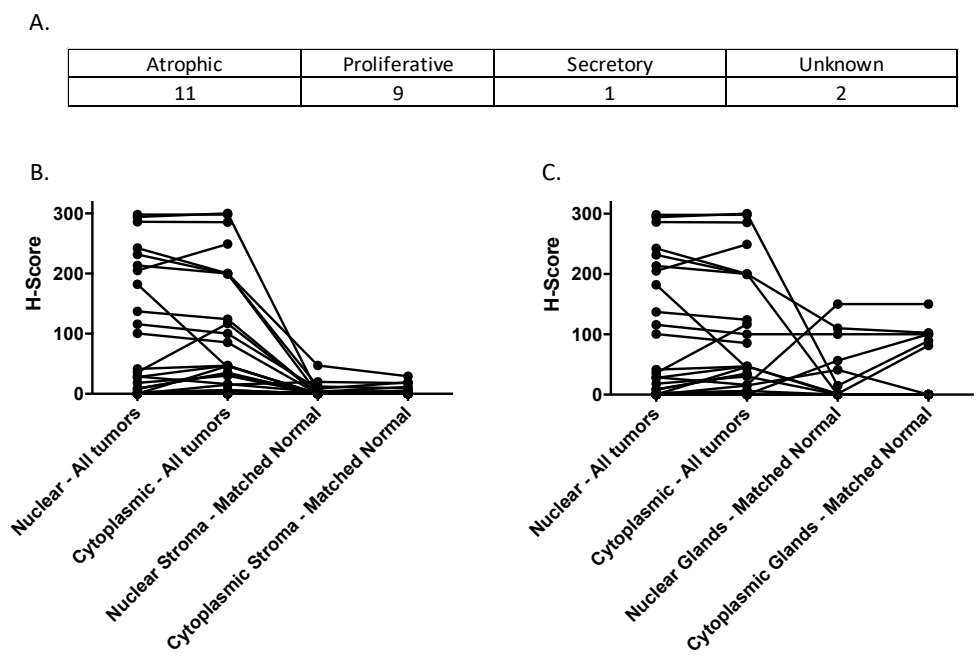
Figure 25. Background tissue phase and sample matched H-scoring. A. Summary of background tissue phases. Of note, 11/23 samples were from post-menopausal (atrophic) uteri. N=23 samples total. B. Tumor vs. matched normal tissue stromal H-scoring. C. Tumor vs. matched normal tissue glandular H-scoring.
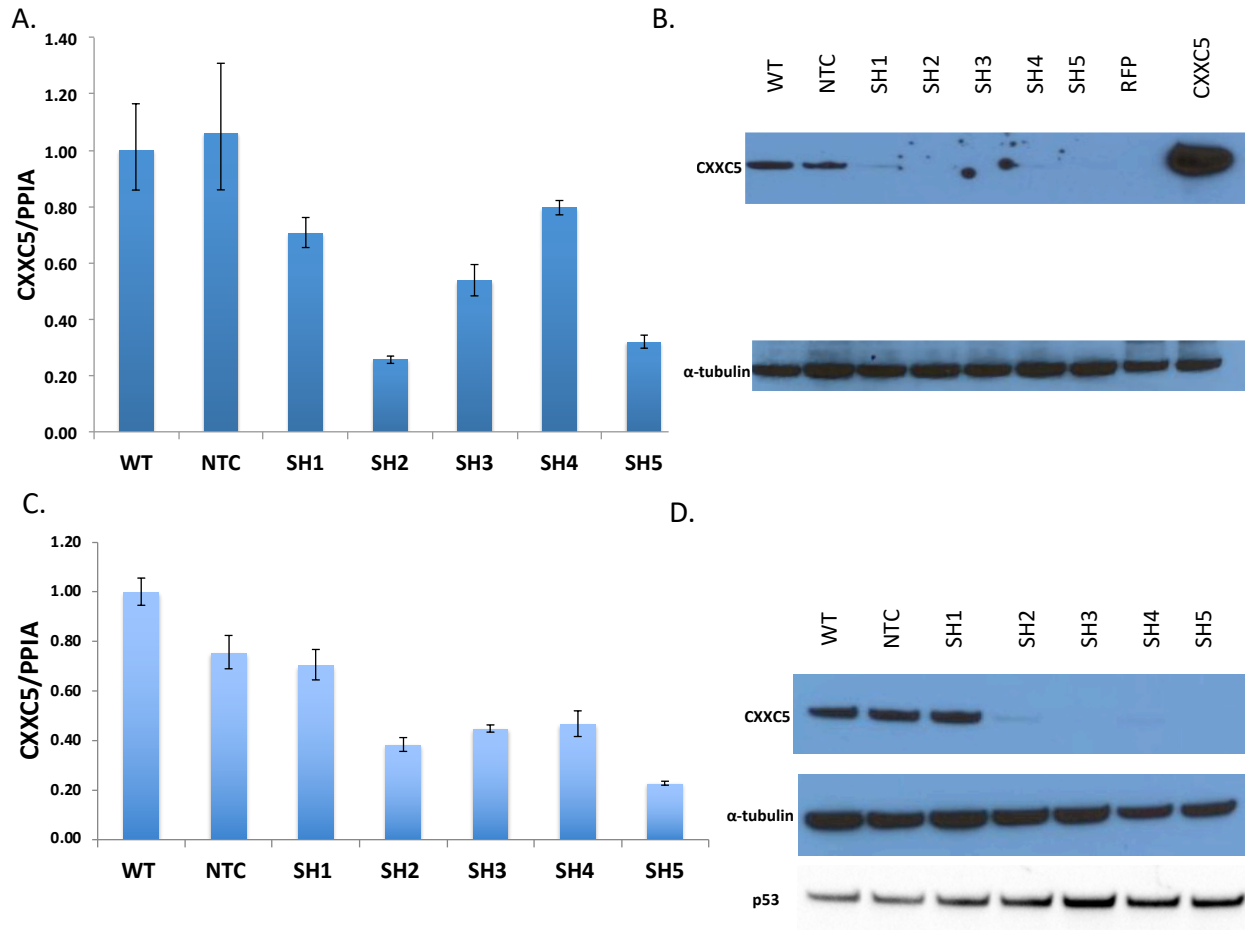
Figure 26. Protein validation and lentiviral knockdown of CXXC5 in selected cell lines. Cells were transfected with lentiviral shRNA from Sigma. 48 hr post-selection with puromycin, cells were harvested for RNA and protein evaluation. Lentiviral shRNA knockdown of CXXC5 in A. ECC1 cells and C. MSU-12 cells shown minimally 25% reduction in transcriptional level across RNA targets. B. CXXC5 protein evaluation in ECC1 cells with corresponding overexpression of the protein. D. Corresponding knockdown of protein expression in MSU-12 cells. p53 included showing modest increase in expression in the CXXC5 knockdown lines.

Discussion

Significant challenges are present when trying to validate such transcriptional survival data. These data were obtained from different gene expression platforms, Affymetrix Oligo Array (MSU) v. RNA-seq (TCGA) and whether RNA was isolated from micro-dissected for tumor cells only (MSU) v. RNA isolated from bulk tissue with numerous non-neoplastic cells of the immune infiltrate and tumor microenvironment contributing to RNA signals (TCGA). Furthermore, the length of follow-up in the TCGA set incomplete. Because of these significant differences we acknowledged up front that many-of our survival-associated genes might not validate in the TCGA data. Particularly those that were diminished in RNA expression for event cases (OS or DFS) as these might have expression masked in RNA-seq data obtained from bulk tissue processed arrays. Despite these concerns we were able to robustly validate many of our transcripts using the TCGA dataset. We chose to prioritize the further analysis of these transcripts based on several factors. These factors included the level of statistically significant association in both the discovery set of cases (MSU) and in the validation cases (TCGA) based on the cox p-value, further whether the gene was associated with both OS and DFS endpoints, and whether there were large fold expression differences between cases with a survival event vs. those cases without. We also examined these genes in our large internal Affymetrix expression data set including 17 laser captured normal endometrial epithelial samples, 36 serous carcinomas and 120 endometrioid carcinomas and assessed their relative expression by histotype and also in normal endometrium (200, 201).

We further examined what information was available about these genes function and whether they were already studied in oncology. For example, transcripts for NOP16 a nucleolar protein were found in our discovery set highly associated with OS p<0.00007 and with a hazard ratio >8. Analysis of TCGA RNA-seq data using a z-score threshold of 2.5 confirmed that elevated NOP16 was associated with OS p=0.00186 and also with DFS p=0.0114. NOP16 itself is not or only weakly expressed in most normal tissues and has been previously described as a potential biomarker for poor prognosis breast cancers. NOP16 is regulated by estrogen and c-Myc and its diminution by shRNAs in breast cancer cells results in reduced cell viability and other oncogenic cell phenotypes that suggest NOP16 might be a good therapeutic target (202, 203). The top candidate transcripts based on these factors and initially identified from the MSU discovery data set and validated in TCGA are shown in **Table 10** and **Table 11**. Indeed, this gene appearing in our discovery and validation datasets reaffirms the utility of our methodology.

Traditionally, endometrial cancers have been classified as either Type I or II (79). Type I cancers constitute about 75% of all cases, are typically lower grade 1-2 and are endometrioid histology, have a younger age of diagnosis, hormone receptor retention, and unopposed estrogen stimulation and in general have a favorable prognosis. Type I cancers are characterized by frequent mutation and deletions of *PTEN*, activating mutation or amplifications of *KRAS, PIK3CA, FGFR2,* or mutation or somatic silencing of DNA mismatch repair genes (79). Type II cancers are typically serous, clear cell, or grade 3-endometrioid histology. These cancers are generally estrogen and progesterone receptor negative and lack unopposed estrogen stimulation and tend to

125

occur in older women. Uterine serous carcinoma is the prototypical type II cancer and is characterized by presence of TP53 mutation occurring in most cases and less frequently mutations in *SPOP, PPP2R1A, PIK3CA and HER2/Neu* overexpression and is often aneuploid (78, 82). Typically, serous cancers are more aggressive than type I, even when diagnosed at an early stage (204). Recently, the TCGA has categorized endometrial cancers based on four heterogeneous somatic mutation or genome copy number status: 1.) polymerase epsilon (POLE)-ultra-mutated, 2.) microsatellite instability hyper-mutated, 3.) copy-number low endometrioid-like, and 4.) copy-number high, serous-like (82).

Downstream modulation of the Wnt/β-catenin pathway by CXXC5 has been shown in regulation of osteoblast differentiation as well as by upstream regulation through *WT1* (189, 197, 205). CXXC5 has been shown to directly bind to *Dishevelled* in the Wnt signaling cascade, which suggests that this could be a potential mechanistic route by which CXXC5 upregulation leads to poor outcomes. *CTNNB1* activating mutation is the major route of WNT disregulation in endometrial cancer (206, 207). This typically occurs in low-grade endometrioid cases not the types with elevated CXXC5 expression. We used cBioPortal and queried endometrial cancers present in the published TCGA cohort and found that those with p53 mutation also had elevated CXXC5 ($p < 0.001$). However, in the case of both CTNNB1 and PTEN, elevated CXXC5 expression was mutually exclusive from mutation ($p = 0.042$ and $p < 0.001$ respectively). Analysis using TCGA data (not shown p<0.001) also confirms strong tendency towards co-occurrence between *CXXC5* upregulation and *WT1*

upregulation suggesting that CXXC5 elevation in poor outcome event tumors may be driven by WT1.

In breast tissue, CXXC5 has been identified as a target gene of the estrogen receptor α pathway via an estrogen response element present in the region upstream of the initial translation codon of the gene (198). We have identified similar preliminary findings in the endometrium by noting expression changes in immortalized endometrial epithelial cells upon estrogen treatment. Additionally, IHC detection of CXXC5 trended towards an increase during the estrogen dominated proliferative phase of the menstrual cycle in uterine tissue specimens. However, based on our analysis using TCGA data, the majority of overexpression cases are associated with features of hormonally insensitive tumors such as p53 mutation and serous histotype. And indeed, TCGA protein enrichment data from these cases shows downregulation of both ESR1 and PGR. This suggests that CXXC5 overexpression in poor outcome event tumors is likely not achieved through a hormone-driven mechanism.

We further attempted to address the trend towards elevated CXXC5 expression in the matched normal tissues of poor outcome event patients by pathological evaluation of the background phase of the tissue to assess for any confounding variables (i.e. whether these tissues happened to be in the proliferative phase of growth). Perhaps unsurprisingly due to the average age of diagnosis, the vast majority of our matched normal tissues were inactive or atrophic eliminating the worry for phasic confounding. This trend, while not significant, suggests that elevated CXXC5 levels in normal uterine tissues could serve as an indicator of aggressive cancer development.

This further necessitates the need for investigation of CXXC5 expression in a larger set of normal uterine tissues and matched tumors.

With growing interest in CXXC5 as a modulator of several well-known pathways, new inhibitors are currently being developed and investigated using computational modeling methods in the context of anabolic osteoporosis therapies (197, 208). Given the nature of CXXC5 overexpression in poor outcome endometrial cancer cases, it remains to be evaluated whether this patient population might reap significant benefits from addition of such inhibitors to their treatment regime.

Materials and Methods

Bioinformatic and Biostatistical Analysis

RSEM Normalized RNA-Seq (UNC Illumina HiSeq RNASeq V2, level 3) data was downloaded from TCGA website. From these, 333 cases were considered for the analysis and their clinical parameters were taken from cBioportal for Uterine Corpus Endometrioid Carcinoma (TCGA, Nature 2013). For Spectrum data, flash frozen prospective validation samples of endometrial cancer were obtained from Spectrum Hospital System recurrence and survival data and qRT-PCR results were analyzed from 73 samples. Laser captured endometrial cancers and glandular epithelium samples were also previously arrayed and published (200, 201, 209). A subset (n = 136) of these cancers had survival characteristics the clinical features for these samples are provided as previously described (139). Cox regression was performed considering proportional hazards model using survival package in R-environment for both overall survival (OS)

and recurrence free survival (RFS). The Affymetrix probeset used for analysis was CXXC5 (224516_s_at).

Statistics

Evaluation of statistical significance for differences between groups will be completed using a Student's t-test and, where appropriate, Two-Way ANOVA with Sidak's multiple comparisons test using Prism (GraphPad Software Inc, San Diego, CA). $P<0.05$ will be considered statistically significant. At least 80% power was targeted in sample size determination.

Identification of survival associated genes

Three separate transcriptional analysis datasets were used to identify and validate possible candidate genes predictive of both poor and favorable survival for endometrial cancer patients. The first, our MSU internal discovery dataset, consisted of 136 endometrial cancer samples. Every sample that was analyzed in this set was a laser-captured, micro-dissected portion of the original tumor. In these cases, the vast majority of mRNA signal comes from the cancer cells. COX regression analysis was performed on Affymetrix-based gene expression data to establish which specific transcripts were associated with overall survival, disease relapse, or both (Figure 1). Gene expression data for overall survival and relapse prediction of 500 transcripts at $p<0.005$ clearly shows a predictive association between high and low risk for both overall survival and relapse of disease (Figure. 2). This indicates that a transcriptional measure can be evaluated as a testable predictor for these outcomes. A second

129

dataset, from the publically available TCGA, was used to validate the findings from our MSU discovery dataset. The TCGA RNA-seq dataset consists of 333 tumor samples obtained by bulk dissection, which includes tumor cells, immune infiltrate, surrounding stroma and microenvironment as contributing factors to the signal for each case. We confirmed the gene array and RNA-seq findings by examining CXXC5 expression in a third independent (Spectrum Health) cohort of endometrial cancers (Figure 3B and C).

mRNA and quantitative real-time PCR

Total RNA was isolated from samples using Trizol (Ambion, Thermo Fisher Scientific, Waltham, MA) according to manufacturer's recommendation and as previously described by our group (200, 201, 210, 211). Two µg of RNA were first treated with OPTIZYME DNase I (Thermo Fisher Scientific, Waltham, MA) for the preparation of DNA-free RNA prior to the transcription into complementary DNA (cDNA) with qScript cDNA Synthesis Kit (Quanta Biosciences, Beverly, MA). These cDNA were used as the template for the quantitative real-time PCR using primers with PerfeCTa FastMix reagent Quanta Biosciences (Beverly, MA) and the primers with the following sequences for *CXXC5* (ThermoFisher, Waltham, MA #4331182). All qPCR were done on Stratagene MX3000P and the mRNA quantities were normalized using Applied Biosystems human PPIA (cyclophilin A) endogenous control (Thermo Fisher Scientific, Waltham, MA).

Cell culture

Cells were obtained from the following sources. Immortalized endometrial epithelial EM-TERT cells were kind gift from Dr. Kyo the originator and described(212). Immortalized human endometrial stromal cell line hESC cells were obtained from the American Type Culture Collection (Rockville MD). All cells were maintained in DMEM/F-12 media supplemented with 10% fetal bovine serum, penicillin, streptomycin and cultured humidified 5% CO_2 condition. Cells were treated with 1nM estrogen, 10 nM estrogen, 1 nM estrogen and 1.59 μM progesterone, or 1.59 μM progesterone alone for 48hr upon which cells were harvested with Trizol.

Immunohistochemistry

Uterine sections from paraffin-embedded tissue were cut at 6 μm and mounted on silane-coated slides, deparafinized, and rehydrated in a graded alcohol series. Sections were pre-incubated with 10% normal horse serum in PBS (pH 7.5) and then incubated with anti-CXXC5 antibody (84546S. Cell Signaling Technology) in 10% normal serum in PBS (pH 7.5). On the following day, sections were washed in PBS and incubated with a secondary antibody (5 μL/mL; Vector Laboratories, Burlingame, CA) for 1 hour at room temperature. Immunoreactivity was detected using the DAB kit (Vector Laboratories, Burlingame, CA). H-Scores were calculated as (3 x the percentage of strongly staining nuclei) + (2 x the percentage of moderately staining nuclei) + (1 x the percentage of weakly staining nuclei), yielding a range from 0 to 300.

Minimally, 5 high-powered fields were quantified per tissue sample with 200< cells counted / field.

Chapter 5: Conclusions and Future Directions

Conclusions, In Brief

The presented work has accomplished several tasks. First, an overview of the literature on endometrial cancer, current treatment strategies, and classification systems was presented. Second, the gaps in progression of treatment modalities for endometrial cancer were addressed as well as the groundwork bioinformatics for the presented studies. Lastly, this work has laid the foundation to address some of the gaps in treatment progression and significant gaps facing clinicians in identifying patients at the greatest risk of poor outcome. In this last regard, we have developed an animal model of endometrial cancer that reliably develops distant metastatic disease in the lungs. Further, this model holds utility in the ability to manipulate the tumor cells in vitro prior to engraftment. This model also maintains an intact immune system allowing for the possibility to study novel immunotherapies in the progression of metastatic endometrial cancer. Finally, we have demonstrated a potential role for the use of CXXC5 immunostaining in identifying which patients are at the greatest risk of experiencing poor outcomes due to their disease. These studies have laid the foundation to advance future work in immunotherapeutics, understanding metastatic disease, identifying more reliable prognostic markers, and identifying potential therapeutic targets all of which have the ability to significantly impact clinical practices.

Future Directions

Determine whether small molecule inhibitors could be effective in CXXC5 knockdown.

As mentioned in Chapter 4, small molecule inhibitors of CXXC5-Dvl are in development for anabolic treatment of osteoporosis. It remains to be determined whether such inhibitors may harbor usefulness in patients whose tumors overexpress CXXC5.

Evaluation of potential protein alterations in primary uterine tumors vs. lung metastases.

During our initial studies in the MECPK mouse model in Chapter 3, I was able to establish several cell lines derived from the uterine tumor as well as isolated cells from cancer nodules in the lungs of the animals. I have been evaluating these cell lines using western blot and qrt-PCR in an attempt to identify altered immune genes of interest that may be allowing certain cells to escape the primary tumor site and migrate to the lungs. Thus far, evaluation of genes such as PD-1 and PD-L1 have not resulted in detection of any such differences in my cells lines or in IHC evaluation of paraffin-embedded tissues. Interestingly, both uterine tumors and lung metastases have detectable PD-1 by IHC. This is curious as typically T-cells themselves express PD-1. Matched uterine tumors and diseased lungs were sent to Dr. Conrads for laser capture microdissection and proteomics. Once we receive the data we will determine whether there are proteins of interest differentially expressed between the sites which may allow for identification of a mechanism for metastatic spread.

Create ultramutable and hypermutable cell lines from mouse endometrium.

The immortalized mouse endometrial cancer cell lines detailed in Chapter 4 have been used in an attempt to model POLE ultramutable and MLH1 knockout hypermutable cell lines. Human POLE P286R mutation is the most common POLE mutation in ultra-mutable endometrial and colon cancer (82, 213). Therefore, a PolE mutant protein was established in the *Pten^{d/d} Kras^{G12D}* cell line by introducing a TET-inducible vector-containing mouse PolE mutated to R at the identical P286 residue in the exo domain. Control cells were an empty vector (no extra PolE) and a vector with wild-type PolE (controlling for extra amounts of PolE). To validate the induction of an ultramutable function of the TET-inducible system, syngeneic cell mutagenesis rates attempts at using a mammalian mutagenesis assay to determine mutagenesis at the *HPRT* locus was made (214). To date, I have encountered several difficulties in using this system. Despite validation of the mutagenesis assay using other endometrial cancer cells with known alterations in DNA repair pathways, the MECPK cell line itself seems to be highly sensitive to reagents used in the assay. I sequenced MECPK *HPRT* to evaluate whether the cell line was already mutated at this locus. Sequencing revealed an intact wild-type sequence. I then further evaluated for thymidine kinase mutation as mutation of this gene produces the same results as *HPRT* mutation. Again, sequencing returned unaltered results. Instead of trying the assay by first cleansing all HPRT mutants, I induced the Pole mutant cells for >20 passages then back selected using 6-thioguanine which should have cleansed off the non-HPRT mutants. I was left with very few sick-looking cell colonies which I sequenced and none returned mutations as they should have.

Crispr/Cas-9 has been attempted on these cells to inactivate MLH1 and produce a hypermutant cell line. I have only had success in knocking out one allele producing a knockdown but not a knockout of MLH1 with no associated hypermutation as knockout of both alleles is necessary. I attempted using donor arms with selectable markers but this did not improve efficiency.

Final Remarks

Endometrial cancer is the most common gynecologic malignancy faced by women. As with most cancers, ability to identify patients at the greatest risk of experiencing a poor outcome remains a significant clinical hurdle. Additionally, treatment of highly advanced and metastatic disease is extremely difficult as there are few treatment options. Molecular profiling of tumors has the exciting potential to objectively classify and pinpoint therapeutic targets on an individualized patient level. The data presented in this work show that this methodology is indeed feasible and has uncovered a new prognostic marker of poor outcome and potential drug target for endometrial cancer patients. Further, we have developed a novel metastatic disease mouse model closely mimicking patients with the most dismal of survival expectations.

APPENDICES

APPENDIX A: Establishment of endometrial cancer cell lines

Immortal cancer cell lines provide a uniform, established and convenient model to study and characterize biological processes in an isolated system. However, given the wide range of uterine cancer subtypes (histotypes, etc.), not all varieties are currently represented by commercially available cell lines and thus a suitable line that satisfies the needs of the investigator may not exist. Furthermore, many endometrial cell lines harbor mutator phenotypes and acquire additional genetic changes not present in the original tumor as the cell line model is passaged over time. Here we describe methods of how to generate endometrial cancer cell lines from primary and metastatic tumor samples including solid and ascites or pleural fluid samples. This process will enable generation of stable cell lines with specific criteria necessary to the investigator's area of study.

Introduction

The first human cancer cells were successfully established in 1955 (215, 216). These cells eventually came to be known as HeLa cells; named for Henrietta Lacks, the woman who died from the cervical cancer that gave rise to the cell line (217-219). This cell line is used extensively in research and has proved to be an indispensable model for investigators. Early endometrial cancer cell lines were established decades ago, in particular the first in vitro cell line of human endometrial adenocarcinoma, human endometrial cancer-1 (HEC-1) cells, were cultured from a 71-year-old female with grade 2 endometrial carcinoma in 1968 (220-222). These and a subsequent handful of

commonly utilized endometrial cells lines were instituted before our current understanding of the importance of histologic and molecular sub-types of endometrial cancer. Significant gaps in available models mimicking the diverse spectrum of histologic and molecular complexities of these cancers suggest there will be a continuing need in forming new and better-characterized models in the development of pharmacologic treatment (223).

Immortalized cell lines can be generated from primary tissues and fluids using several different methods of transformation including viral transformation (224-229) and immortalization through activation of telomerase (212, 218, 230, 231). Here we specifically discuss isolation and growth of uterine cancer cells from tumors or metastatic cells obtained from patients or genetically engineered mouse models without the use of immortalizing agents. This chapter is focused on endometrial cancer but these methods have proven successful for other gynecologic cancers including ovarian cancers and gynecologic sarcomas (232). Generation of a cell line requires acquisition of a viable tumor sample. Important collaborations with clinical pathologists and staff are required such that the tissue used is obtained in a highly controlled manner with rapid transit to the investigator. The sample is subsequently processed using the methods described below shortly after being removed from the patient or after having been maintained in a viable state for no longer than 3 days in cell culture media. Time to loss of viability is variable, as such, tumors should be processed as soon as possible after removal from the patient to prevent sample loss and increase the odds of success. If processing of tissue cannot occur immediately after receipt it is possible to delay preparations for up to 3 days if the sample is stored at 4°C in cell media. Processing of

bulk tumor to isolate cancer cells includes one of two methods: 1.) digestion of bulk tumor by collagenase treatment and/or 2.) mechanical mincing of tumor tissue using scalpels or other sharp instruments such as sterile razor blades. Cells are cultured under both high and low serum conditions to optimize growth. With either method, serial dilution of resultant slurry or ascites must be performed to sufficiently dilute the cell concentration for individual colony growth and clone isolation. While logically it may seem that tissue should be reduced to complete single cell suspensions to achieve the best results, this is not necessarily true. Most of our successfully established lines arose from tumors disrupted to achieve small clusters of cells, which adhered and proliferated.

Materials:

- Viable tumor sample

- Cell culture media (Base media DMEM / F12; Gibco, 11330-032)

- Fetal Bovine Serum (FBS; Omega Scientific, FB-01)

- 100X Penicillin, Streptomycin and Glutamine (100X PSG; Gibco, 10378-016)

- Scalpels

- Forceps

- 10 cm culture dishes

- 15 and 50 mL conical tubes

- Autoclaved/sterile pipette tips

- ACK buffer (Gibco, A10492-01)

- Collagenase I or IV (Sigma-Aldrich, C0130)

- Dispase (Thermo Fischer, 17105041)

- Hyaluronidase (alternative; Sigma-Aldrich, HX0514-1)

- DNAse (optional; Sigma-Aldrich, DN25)

- Hanks' Balanced Salt Solution (HBSS; Thermo Fischer, 14025092)

- 1X Phosphate-buffered saline (PBS; Thermo Fischer, 10010-023)

- Ficoll-Paque Plus (Sigma-Aldrich, GE17-1440-02)

**Note: this protocol was developed for 100-200 mg of tissue. Depending on amount of tissue, its viability and cellularity, the number of serial dilutions may have to be adjusted to proper cell densities at plating. All procedures should be performed in a sterile cell culture hood with sterile materials.

Cell line generation procedure by mechanical isolation:

Cell culture media:

1. Supplement cell culture media (DMEM-F12) for base media, high-serum, and low-serum conditions.

   a. For base media –

      i. Per every 500-mL media add:

         o 5 mL PSG

   b. For high-serum media -

      i. Per every 500-mL media add:

         o 50 mL FBS

$\circ$ 5 mL PSG

c.   For low-serum media –

     i.   Per every 500-mL media add:

        $\circ$ 2.5 mL FBS

        $\circ$ 5 mL PSG

2.   Working in a sterile biosafety cabinet, place tumor sample in 10 cm culture dish with 10 mL base media. Dissect off any unusable connective tissue and separate from usable sample.

3.   Transfer remaining tumor sample to a new 10 cm dish with 12 mL fresh base media.

     a.   Label dish "10^0"

4.   Slice sample into smaller pieces no more than 5-mm using sterile scalpels or scissors.

     a.   Further mince slices until only small chunks are visible. Divide 2 mL between two 15 mL tubes (1 mL/tube) and centrifuge for 3 min at 1,400 rpm.

     b.   Remove base media from tubes.

        i.   Resuspend the cells from one tube in 11 mL of high serum media and the other tube in 11 mL of low serum media.

     c.   Plate 10 mL of each into individual 10 mL plates – "10^{-1} High" and "10^{-1} Low"

5.   Label 6 additional 10 cm dishes. These represent dilutions at high and low serum concentration:

     a.   Two – "10^{-2}"

     b.   Two – "10^{-3}"

c. Two – "10^{-X}" depending on cellularity of the original tumor, more dilutions may be required

6. Add 9 mL of corresponding high serum media to each plate of one set (10^{-2}, 10^{-3}, and 10^{-X}).

   a. Repeat with low serum media for the second set of plates.

   b. Label each set as "high" or "low" to distinguish serum concentrations.

7. Transfer the remaining 1 mL from the sample tubes "10^{0}" to each of the "10^{-1}" plates. See flow diagram **Figure 27**.

   a. Repeat transferring 10^{-1} to 10^{-2}

   b. Repeat again transferring 10^{-2} to 10^{-3}

8. Incubate under normal conditions ($37^{\circ}C$, 5% CO_2).

   a. Cells may take several days to weeks to adhere. Be patient and monitor intermittently so as not to disturb attaching cells (**Figure 28**).
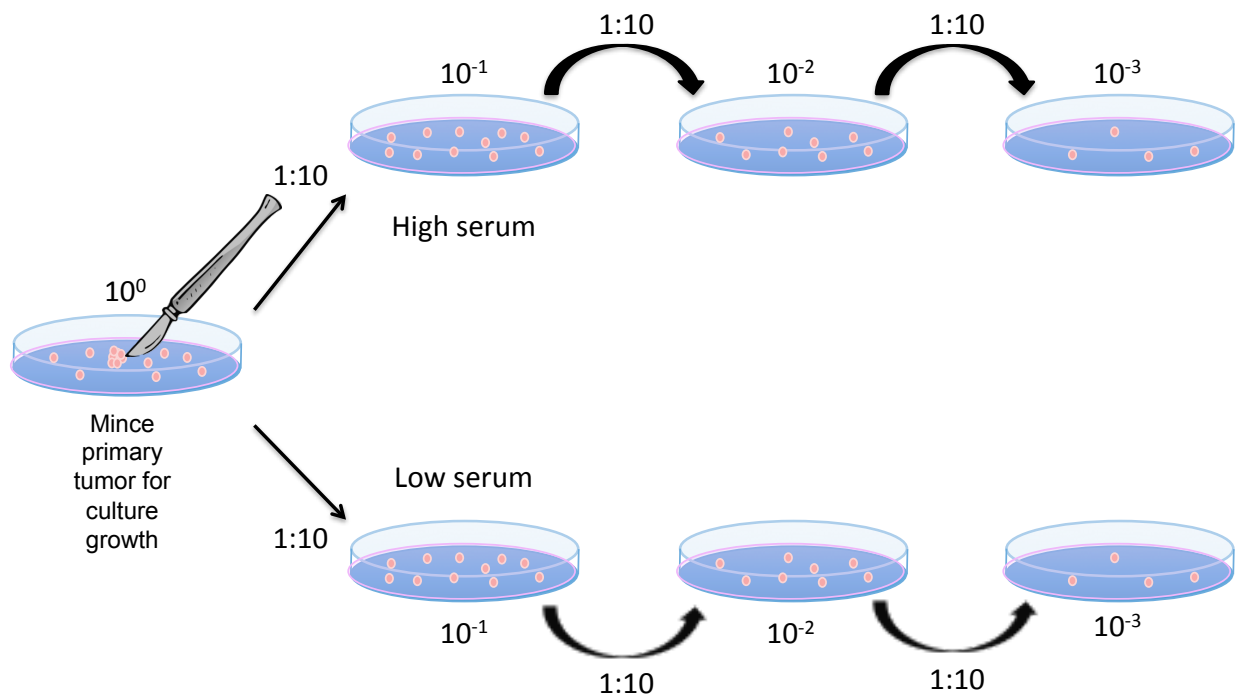
Figure 27. Dilution scheme for plating minced tissues. The number of serial dilutions may have to be adjusted to proper cell densities at plating depending on amount of tissue, its viability and cellularity. Starting with the initial sample minced in base media ("10^0" plate), serially dilute cells in both high- and low-serum platings to optimize growth.
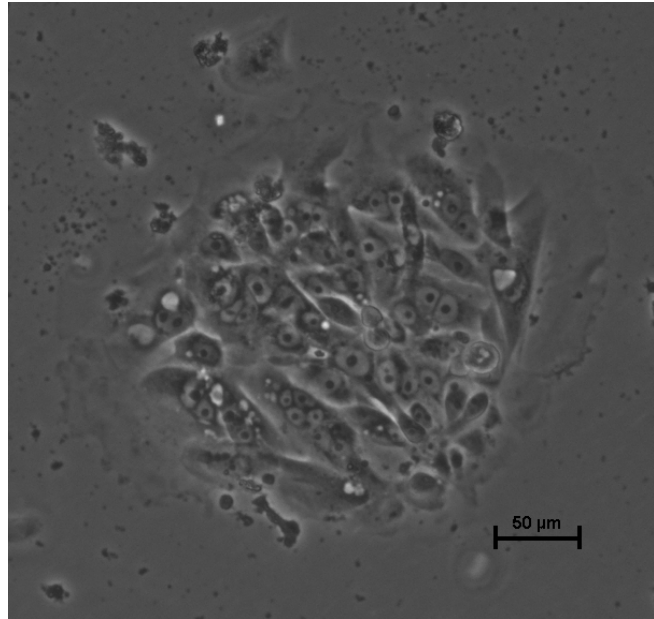
Figure 28. Colony morphology and tumor cell growth after primary sample processing. Growth of a colony 3 days post tumor processing. Primary sample was acquired from a patient with high-grade endometrial cancer.

Cell line generation procedure by mechanical isolation and dissociation with collagenase treatment:

Dissociation Buffer

Prepare the cell dissociation buffer: Dulbecco's modified Eagle medium (DMEM / F-12) supplemented with 10% FBS, penicillin-streptomycin, 200 U/mL Collagenase type IV [50-200 units/mL], and 0.6 U/mL dispase.

Alternate dissociation buffers may include Collagenase type I [50-200 units/mL] and Hyaluronidase [1000 units/mL] with or without DNAse (0.00002 g/mL)

1. Working in a sterile biosafety cabinet, transfer the tumor to a 10-cm culture dish with 1 mL of cell dissociation buffer. Mechanically mince the tumor using sterile razor blades and forceps as described above in Steps 1-3 of mechanical isolation. Agitate the tumor cell suspension through a 5-mL serological pipet 10 times. The tumor pieces should be small enough to not clog the 5-mL serological pipet.

   a. Tissue pieces should be approximately 5 mm (or less).

   b. Wash pieces with HBSS 3 times.

2. Add collagenase to the DMEM / F-12 at a concentration of 50 to 200 units/mL.

Generate a Suspension from tumor or tissue

1. Transfer the tumor cell suspension to a 50-mL conical tube containing the remaining volume of cell dissociation buffer (filled less than 50%) and vortex at maximum speed for 1 minute.

2. Incubate the tumor cell suspension at 37°C for 2 hours to overnight with intermittent vortexing for 1 minute every 20 minutes (3 times/hour).

   a. Incubate tissue in 37°C shaking water bath for a minimum of 2 hr up to 18 hr.

   b. To increase the efficacy of dissociation, 3 mM $CaCl_2$ may be added to the tissue solution before incubation.

3. Transfer the digested slurry to a 50-mL tube and centrifuge to pellet the cells at 400xg for 5 minutes.

4. Remove supernatant.

5. Wash the cell pellet with 1X PBS.

6. Centrifuge to pellet at 400xg for 5 minutes.

7. Remove supernatant.

8. Resuspend the cell pellet in ACK Lysis Buffer for no longer than 5 min, to completely lyse red blood cells.

9. Centrifuge to pellet the remaining tumor cells at 400xg for 5 minutes.

10. Remove supernatant.

11. Resuspend in 2 mL DMEM / F12 without serum.

Deplete Cell Suspension of Tissue Debris and Dead Cells

1. After incubation, vortex the cell suspension at maximum speed for 1 minute.

2. Collect the cell suspension in a fresh 50-mL conical tube and adjust to a final volume of 15 mL per tube.

3. To further separate viable cells from dead cells and tissue debris, separate the tumor cell suspension by density centrifugation using Ficoll-Paque Plus. Create an underlayment of Ficoll-Paque Plus by pipeting 15 mL of Ficoll-Paque Pulse slowly below the cell suspension being careful not to mix the two layers.

4. Centrifuge the cell suspension and Ficoll layers at 500xg for 30 minutes and allow centrifugation to stop with the brakes turned off.

5. Collect cells at the interface of the Ficoll-Paque Plus and cell dissociation buffer and transfer to a fresh 50-mL conical tube.

6. Add fresh DMEM / F12 supplemented with 10% FBS to the cell suspension to dilute it 1:3 (e.g. 20 mL fresh media added to 10 mL of cell suspension).

7. Pellet and resuspend cells in growth media

8. Count and seed cells for further culture. Dilute to single cell colonies as depicted in **Figure 27** through 1:10 serial dilution.

Isolation and growth of cells from ascites:

Ascites or pleural effusions from patients are obtained from pathology usually in aspiration flasks. Volume may vary greatly as will the amount of cellular material in the fluid. These fluids need to be pelleted in an appropriate sized bottle or conical tube. Ascites may be used to establish cell lines from genetically engineered mice or in mice harboring xenografted tumors. The ascites are often ideal sources for cell line generation.

1. Isolate the ascitic fluid from the body cavity through one of two methods.
   a. Using a 25G needle, puncture the body cavity containing the ascites.
      i. Slowly withdraw fluid and move to step 2.
   b. Carefully open the body cavity using a scalpel or dissection scissors.
      i. Using a pipettor, slowly remove fluids from around the cavity contents. After the maximum amount of fluid has been retrieved, move to step 2.
2. For ascites the procedure first involves pelleting cell and debris at 2500xg. Cells are resuspended in 15 mL PBS. These are processed using Ficoll paque plus as above starting at step 3.

Colony selection procedure:

Successful utilization of these protocols requires skill in the identification of diverse cell types present in the tumor tissue. Understanding the differences between these is absolutely necessary to achieve success. Cells isolated from ascites are particularly

amendable for establishment as they are largely free of adherent cell types other than cancer cells. However, bulk uterine tumors contain endometrial stromal cells and cancer associated fibroblasts (CAF). These cells grow rapidly in high serum media and can easily out-compete tumor cells occupying the available space on the plate and eventually pushing them off. The above dilutions are designed to achieve limited cell density, which allows for a few isolated clusters of tumor cells to achieve growth to sufficient size after which they can be transferred to a fresh plate before neighboring fibroblasts invade. In some cases, no plates in high serum are able to have this desired outcome. In these cases, the low serum platings may be successful. At low serum, the stromal and CAF cells may attach but typically fail to grow robustly. Careful monitoring of these plates may reveal tumor cell growths after many weeks. As these establish it may be possible to gradually increase the amount of serum in the media accelerating growth of tumor clusters. Colonies can then be transferred to new plates and grown in high serum media. Failure to successfully isolate cells can result from several different reasons. The most obvious is that the tumor cells fail to adapt to new growth conditions. This is common for most low-grade endometrioid cancers. Other causes of failure include overgrowth of the cultures with stromal fibroblasts as discussed above, failure to transfer tumor cells to new plates (passaging) and plate contamination. Tumor cells in low serum media may take months to expand to a size adequate for transfer to a new plate. Prolonged times in culture require careful refluiding and regular monitoring of cells.

1. Identify an isolated cell colony.

2. Mark the bottom of the cell culture dish to identify the location of the colony you wish to isolate.

3. Using a 1000 μl pipette tip, depress the pipettor then gently scrape the colony from the plate while simultaneously drawing up cells and media.

4. Transfer the cells to a new cell culture dish (24- or 12-well dishes work best).

5. Incubate plate under standard conditions and monitor for growth. Split and passage as necessary.

APPENDIX B: Establishment and long-term storage of endometrial cancer patient derived xenografts (PDX).

Xenografting of human tissues into immunocompromised mice enables *in vivo* study of tumor responses to drug treatments and for development of new therapies (155, 165, 166). Patient derived xenograft (PDX) models more faithfully retain original tumor characteristics than do established cell lines (167). PDX models can be archived in deep freeze, revived and re-implanted to generate large well-timed cohorts of models for *in vivo* studies. Furthermore, these models can be engrafted either subcutaneously, intraperitoneally or orthotopically into the uterine horn to meet specific study objectives (153). In this chapter, we describe the methods to generate uterine cancer PDX models in immune compromised mice as well as long-term graft storage methods. In particular, we focus on detailed procedures for establishing these models in the uterine horn, the most relevant site for detailed studies. These techniques will allow the researcher to address questions about drug efficacy for cancer treatment in a biological system.

Introduction

Xenografting of human tumor tissues involves procurement of a live tumor sample and surgical engraftment of this tissue into or on an immune deficient animal, typically a mouse (170-172). This method has allowed for tremendous impacts on the study of tumor responses to new potential clinical therapies (155, 166). Human tissue grafts are traditionally placed subcutaneously which allows for the convenience of visual

monitoring for progression. Grafts may also be placed elsewhere to more closely mirror the native microenvironment of the tumor's origin and this has been noted to change the course of the spread of the disease (168). Uterine-specific cancer PDX models were first described in 1975 (169). In this initial uterine study, five human endometrial cancer samples were grafted onto nude mice. The subsequent graft establishment rate for this particular study was 60% with two samples maintained by serial transplantation. Orthotopic uterine cancer modeling with established cell lines was described in a study looking at the effectiveness of etoposide administration against cell grafts placed orthotopically (uterus) or subcutaneously (233). Interestingly, the authors of this study found a substantial difference in drug efficacy based on graft placement site. This further reinforces the utility and necessity of studying orthotopically placed grafts as opposed to the traditional subcutaneous placement. Finally, after establishment of a graft line, long-term storage may remain an issue for grafts to reduce animal use in maintaining live tissue. As with cell lines, cold storage represents a method to preserve established grafts for future use.

Selection of graft site:

Given the ease in placement and monitoring of tumor growth, tissue is typically grafted subcutaneously on the flank of the host animal. Based on our experience with gynecological malignancy, we encourage the investigator to consider placing grafts in an area of the animal most closely corresponding to the original site of human growth. We believe that growth in the correct microenvironment allows for the greatest chance at successful PDX establishment in an immune compromised animal and also more

closely mimics the original disease characteristics (**Figure 29**). Additionally, for therapeutic screens others have shown drastic differences in drug effectiveness based on placement site (233).
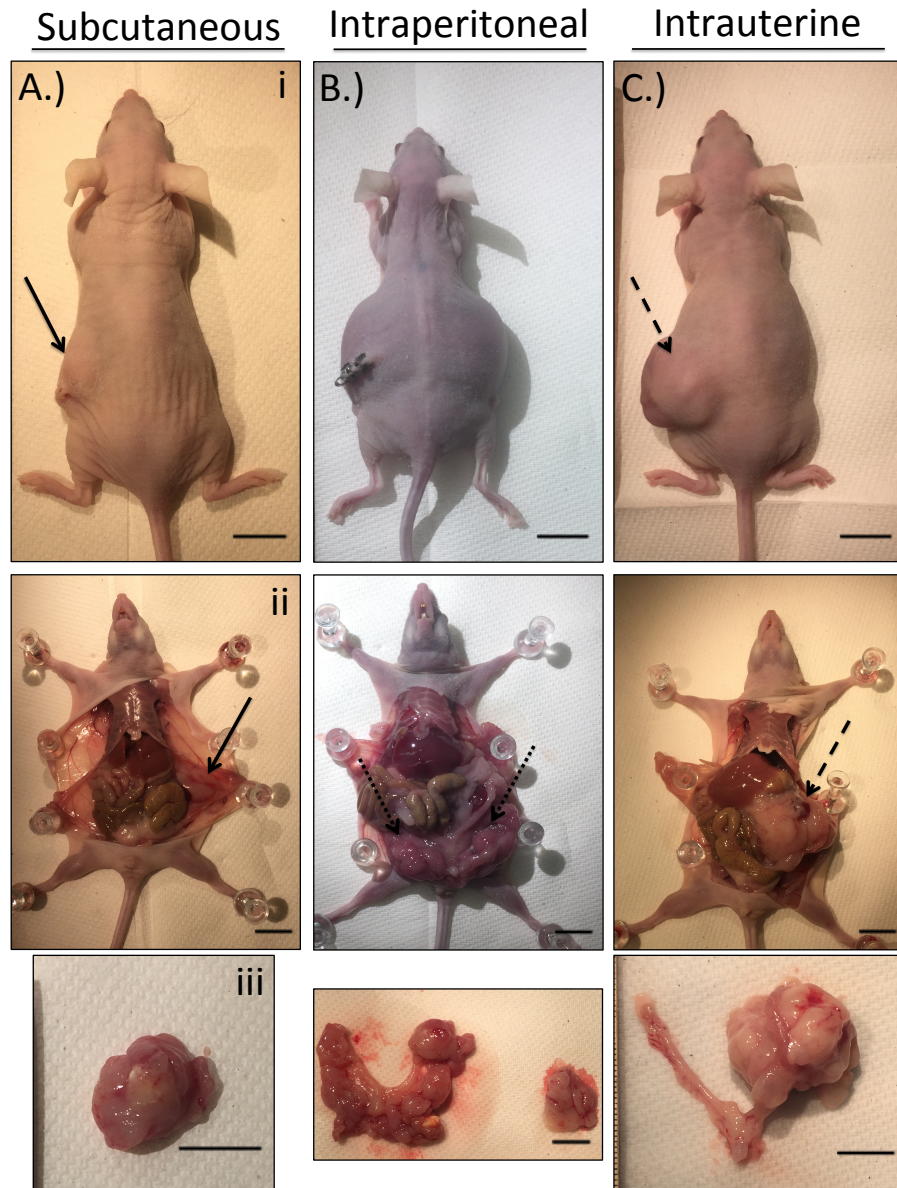

Figure 29. Endometrial cancer patient derived xenograft implantation site impacts tumor growth characteristics: subcutaneous vs. intraperitoneal vs. intrauterine. A high-grade endometrial cancer (approximately 5 mm/piece) was implanted in an eight-

Figure 30 (cont'd)

week-old athymic nude female mouse in one of three separate sites (subcutaneous, intraperitoneal, or intrauterine) and allowed 14 days of growth. A.) Traditional subcutaneous placement. i. Dorsal view shows modest subcutaneous growth on the left side (solid arrow). ii. Ventral view. Subcutaneous tumor displayed on right side of image adherent to the superficial body cavity tissue layers (solid arrow). iii. Bulk tumor removed. B.) Intraperitoneal graft placement. i. Dorsal view shows gross distension of the body cavity by ascites. ii. Ventral view post removal of approximately 5.4 mL of ascitic fluid. Note solid tumor formation in the lower pelvic cavity (dotted arrows bilaterally). iii. Uterus removed with adherent solid tumor growing along connective tissues (left). Additional large tumor removed from inside the abdominal cavity near original graft site (right). C.) Intrauterine (tumor-native) graft placement. i. Dorsal view shows large left-sided protrusion of uterine-confined tumor tissue (dashed arrow). ii. Ventral view with bulky tumor mass confined to the single implanted horn of the uterus (dashed arrow). iii. Surgical removal of the uterus shows dramatic growth of PDX tissue within the lumen of the uterine horn.

Materials:

- Viable tumor sample (trimmed to size appropriate for intended graft site)

- Host animal: typically, Crl:NU(NCr)-*Foxn1^{nu}* (athymic nude) or NOD-*scid* IL2Rgamma^{null} (NSG) strain

- Surgical instruments

  ▪ sterilizer

154

- scissors

- forceps

- surgical staples/suture

- Betadine/alcohol

- Hair clippers

- Anesthetic equipment; vaporizer, snorkel, salvage equipment.

Graft Procedure:

1. Set up surgical area. Autoclave surgical instruments prior to use or have a bead sterilizer available to sterilize instruments prior to surgical procedures. Clean all surfaces with 70% ethanol. Be sure to spray gloves intermittently with 70% ethanol to maintain clean hands.

2. Anesthetize animal according to your approved Animal Use Protocol (AUP). Our lab utilizes 2% isoflurane with supplemented oxygen through a nosecone using a tabletop anesthesia machine with O_2 flush specifically designed for this purpose (Parkland Scientific, Model V3000PS).

3. Clean the surgical site according to your approved AUP. We wash once with 70% ethanol followed by a betadine scrub.

4. For *flank grafts*: Identify the incision site position the animal on its side so that you can clearly see the muscles surrounding the femur. This should make a sort of "bowl shape" where the bottom of the bowl lays between the femur muscles and belly of the animal. When making the incision be sure to only cut the superficial skin layers leaving the internal fascia intact (**Figure 30A**).

5. Using scissors, make a small cut slightly anterior to the femur towards the top portion of the bowl (**Figure 30B**).

6. Insert scissors about 1 inch inward while closed under the skin, open the hinge slowly to form a pocket for graft placement (**Figure 30C**).

7. Pack the graft tissue into the formed pocket (**Figure 30D**).
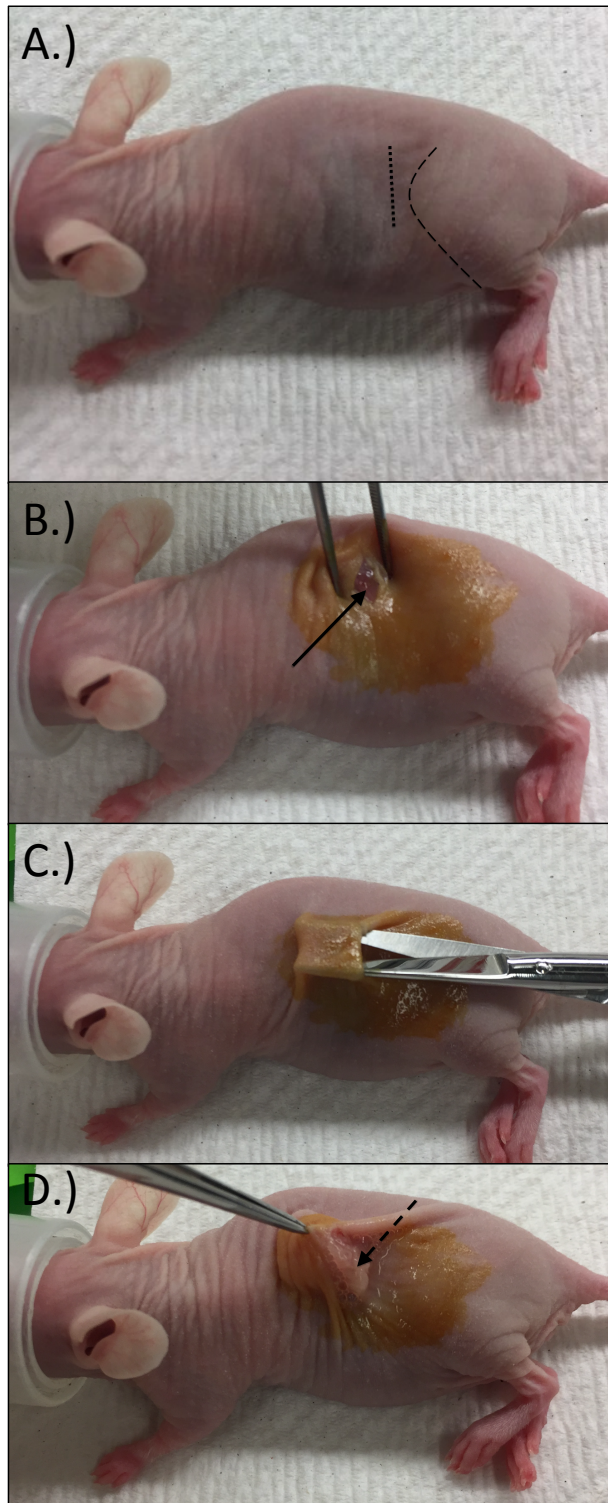
8. Suture or staple the pocket closed.

Figure 30. Anatomical landmarks and fascial layer separation for subcutaneous graft placement. Subcutaneous graft placement requires creation of a pocket between

Figure 31 (cont'd)

fascial layers of the skin. A.) Anatomical landmarks for initial incision. Can be used for subcutaneous flank grafts, intraperitoneal placement, or to locate the uterus for intrauterine grafting. A small (approx. 3 mm) incision (straight dotted line) is made anterior to the knee joint (curved dashed line) when the animal is placed on its side. B.) Cut along the incision line designated in panel A making sure to only cut the superficial skin layers. The underlying tissue layers should remain intact and visible such that the abdominal cavity has not been breached (arrow). C.) Closed scissors are inserted into the incision between tissue layers. The scissors are opened slightly to separate the layers and form a pocket to insert graft tissue. D.) The graft tissue (dashed arrow) is placed into the pocket using forceps.

9. For *intraperitoneal grafts*: Follow protocol as detailed through step 5 above. To access the peritoneal cavity, lift with forceps and cut the deeper fascia. This results in a visible hole into the cavity. With practice, the ovary and attached uterine horn should be visible and easily exposed (**Figure 31**).

10. Place graft tissue into the peritoneal cavity.

11. Suture or staple according to your approved AUP. Some Institutional animal care and use committees (IACUC) require both suturing of the internal fascia as well as stapling the skin. Be sure that no bowel or other organs are contained within your given wound closure materials.

Figure 31. Intraperitoneal graft placement. Intraperitoneal graft placement requires creation of an opening through the skin into the abdominal cavity. For anatomical landmarks for initial incision see A.) Cut into the deeper tissue layers until the inside of the abdominal cavity is visualized (can see bowel, ovary, etc.) B.) Using forceps pull the ovary (arrow) through the incision to ensure entry into the abdominal cavity.

12. For *uterine specific* grafts: Follow the IP graft protocol and expose the ovary and uterine horn (**Figure 31B**). Prior to surgery, cut graft tissue to an appropriate small size about 1-2 mm.

13. Insert a blunted 25G needle into the uterine horn lumen (**Figure 32**).

14. Carefully pull, but do not fully remove, the needle up through the lumen on an angle to abrade the mucosa of the inner uterine wall.

15. When at the top of the insertion site (needle still within the lumen) return the needle to the vertical position and slide back to the starting position to begin a new abrasion.

16. Repeat 4-6 times.

17. Remove the needle.

18. Using forceps, pack graft tissue through the hole created from the 25G needle.

19. Replace ovary and uterus to their correct anatomical location within the body cavity.

20. Close the site as detailed in Step 11.
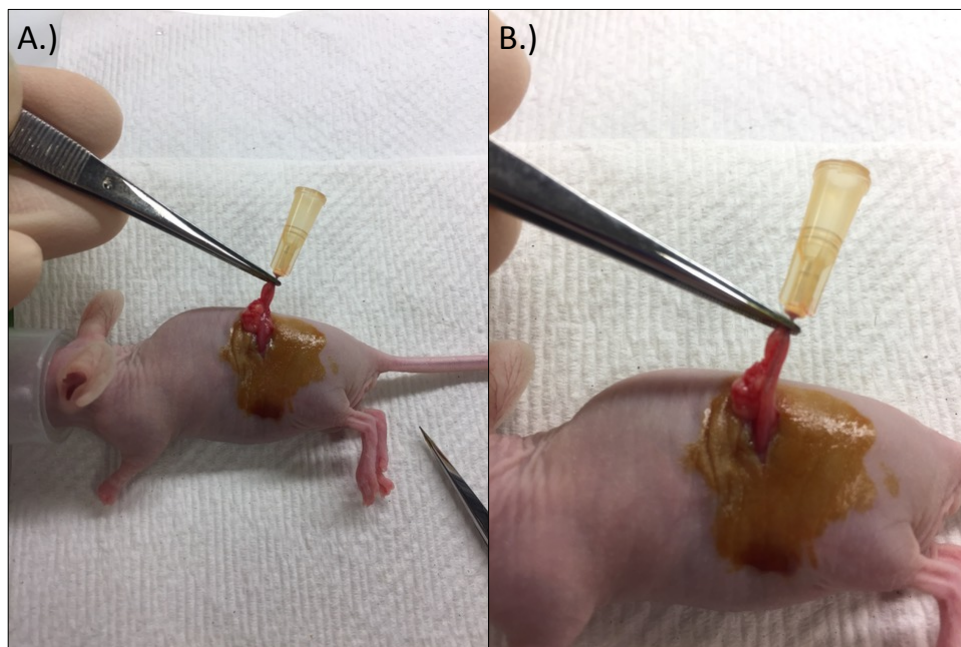
Figure 32. Intrauterine graft placement. Intrauterine graft placement requires abrasion of the uterine luminal surface. Anatomical landmarks for initial incision and exposure as depicted in Figures 2 and 3. A.) Insert a blunted 25G needle into the uterine lumen. Pull against the tissue to create an abrasion. B.) Allow the needle to return to the starting position and repeat.

Graft Storage:

Materials:

- Viable tumor sample (trimmed to size appropriate for cryostorage)

- Cell culture hood

- Cryovials (1.8 mL; Cryo.S, 122279)

- Cell culture media (DMEM / F12; Gibco, 11330-032)

- Fetal bovine serum, (FBS; Omega Scientific, FB-01)

- 100X Penicillin, Streptomycin and Glutamine (100X PSG; Gibco, 10378-016)

- Molecular biology grade dimethyl sulfoxide, (DMSO; Fischer Scientific, BP231-100)

- Sterile forceps

- Sterile scalpels

- Mr. Frosty (Sigma-Aldrich; Nalgene, C1562)

- Immune compromised animal (necessary for graft wake up only).

Graft storage procedure – to be done in cell culture hood:

1. Make 5% DMSO freeze media in FBS.

    a. For 100 mL media add:

        i. 95 mL FBS

        ii. 5 mL DMSO

    b. Only enough 5% DMSO needs to be made for the number of samples to be frozen (ex. ~1.8 mL/sample * X samples to be frozen).

2. Trim tumor sample to a size appropriate for viable cryostorage (approximately 2x2x2 mm).

3. Add enough freeze media to each tube such that the tissue will be covered entirely when submerged (up to 1.8 mL).

4. Use forceps to pick up tumor sample and place inside tube containing freeze media.

5. Replace tube cap, label and place in room temperature Mr. Frosty.

6. Freeze overnight at -80°C.

7. Samples can then be transferred to liquid nitrogen for long-term storage.

Waking up a graft:

1. Have an adult 4-8-week-old tumor naïve female animal available for graft placement.

2. Set up surgical area as detailed in graft establishment protocol.

3. Obtain graft sample vial from liquid nitrogen storage.

    a. Keep in liquid nitrogen or on dry ice for transport.

4. When ready, float sample tube in 37°C water bath until liquid has thawed.

5. Wipe with 70% ethanol and transfer into cell culture hood.

6. Using forceps, remove tissue from storage liquid and place in fresh media supplemented with 10% FBS.

7. Wash once in 10% FBS.

8. Transfer to fresh 10% FBS in a dish or tube for transfer to surgical area.

9. Graft to immune compromised animal by method detailed in graft protocol.

BIBLIOGRAPHY

BIBLIOGRAPHY

1.   Sheikh MA, Althouse AD, Freese KE, Soisson S, Edwards RP, Welburn S, Sukumvanich P, Comerci J, Kelley J, LaPorte RE, Linkov F. USA endometrial cancer projections to 2030: should we be concerned? Future oncology (London, England). 2014;10(16):2561-8. Epub 2014/12/23. doi: 10.2217/fon.14.192. PubMed PMID: 25531045.

2.   AlHilli MM, Mariani A, Bakkum-Gamez JN, Dowdy SC, Weaver AL, Peethambaram PP, Keeney GL, Cliby WA, Podratz KC. Risk-scoring models for individualized prediction of overall survival in low-grade and high-grade endometrial cancer. Gynecologic oncology. 2014;133(3):485-93. Epub 2014/04/03. doi: 10.1016/j.ygyno.2014.03.567. PubMed PMID: 24690476; PMCID: PMC4405150.

3.   Bendifallah S, Canlorbe G, Collinet P, Arsene E, Huguet F, Coutant C, Hudry D, Graesslin O, Raimond E, Touboul C, Darai E, Ballester M. Just how accurate are the major risk stratification systems for early-stage endometrial cancer? British journal of cancer. 2015;112(5):793-801. Epub 2015/02/13. doi: 10.1038/bjc.2015.35. PubMed PMID: 25675149; PMCID: PMC4453957.

4.   Cancer Facts & Figures 2018. Atlanta, GA: 2018.

5.   Key Statistics for Endometrial Cancer 2018 [cited 2018 3-13-18]. Available from: https://www.cancer.org/cancer/endometrial-cancer/about/key-statistics.html.

6.   Cancer Stat Facts: Endometrial Cancer 2017. Available from: https://seer.cancer.gov/statfacts/html/corp.html.

7.   Cancer Stat Facts: Female Breast Cancer. Available from: https://seer.cancer.gov/statfacts/html/breast.html.

8.   Cancer Stat Facts: Prostate Cancer. Available from: https://seer.cancer.gov/statfacts/html/prost.html.

9.   Howlader N NA, Krapcho M, Garshell J, Miller D, Altekruse SF, Kosary CL, Yu M, Ruhl J, Tatalovich Z,Mariotto A, Lewis DR, Chen HS, Feuer EJ, Cronin KA (eds). SEER Cancer Statistics Review1975-2012.

10.   Creutzberg CL, van Putten WL, Koper PC, Lybeert ML, Jobsen JJ, Warlam-Rodenhuis CC, De Winter KA, Lutgens LC, van den Bergh AC, van der Steen-Banasik E, Beerman H, van Lent M. Survival after relapse in patients with endometrial cancer: results from a randomized trial. Gynecologic oncology. 2003;89(2):201-9. Epub 2003/04/26. PubMed PMID: 12713981.

11.   Del Carmen MG, Boruta DM, 2nd, Schorge JO. Recurrent endometrial cancer. Clinical obstetrics and gynecology. 2011;54(2):266-77. Epub 2011/04/22. doi: 10.1097/GRF.0b013e318218c6d1. PubMed PMID: 21508696.

12.   Rauh-Hain JA, Del Carmen MG. Treatment for advanced and recurrent endometrial carcinoma: combined modalities. The oncologist. 2010;15(8):852-61. Epub 2010/07/28. doi: 10.1634/theoncologist.2010-0091. PubMed PMID: 20660059; PMCID: PMC3228028.

13.   McMeekin DS, Filiaci VL, Thigpen JT, Gallion HH, Fleming GF, Rodgers WH. The relationship between histology and outcome in advanced and recurrent endometrial cancer patients participating in first-line chemotherapy trials: a Gynecologic Oncology Group study. Gynecologic oncology. 2007;106(1):16-22. Epub 2007/06/19. doi: 10.1016/j.ygyno.2007.04.032. PubMed PMID: 17574073.

14.   Billingsley CC, Cohn DE, Mutch DG, Stephens JA, Suarez AA, Goodfellow PJ. Polymerase varepsilon (POLE) mutations in endometrial cancer: clinical outcomes and implications for Lynch syndrome testing. Cancer. 2015;121(3):386-94. Epub 2014/09/17. doi: 10.1002/cncr.29046. PubMed PMID: 25224212; PMCID: PMC4304930.

15.   Saito N. [Biochemical analysis of estrogen receptor and progesterone receptor in normal uterus and endometrial carcinoma]. Nihon Naibunpi Gakkai zasshi. 1987;63(2):87-101. Epub 1987/02/20. PubMed PMID: 3569607.

16.   Sherman BM, Korenman SG. Hormonal characteristics of the human menstrual cycle throughout reproductive life. The Journal of clinical investigation. 1975;55(4):699-706. Epub 1975/04/01. doi: 10.1172/jci107979. PubMed PMID: 1120778; PMCID: PMC301805.

17.   Treloar AE, Boynton RE, Behn BG, Brown BW. Variation of the human menstrual cycle through reproductive life. International journal of fertility. 1967;12(1 Pt 2):77-126. Epub 1970/01/01. PubMed PMID: 5419031.

18.   Hall JE, Schoenfeld DA, Martin KA, Crowley WF, Jr. Hypothalamic gonadotropin-releasing hormone secretion and follicle-stimulating hormone dynamics during the luteal-follicular transition. The Journal of clinical endocrinology and metabolism. 1992;74(3):600-7. Epub 1992/03/11. doi: 10.1210/jcem.74.3.1740493. PubMed PMID: 1740493.

19.   Fleischer AC, Kalemeris GC, Entman SS. Sonographic depiction of the endometrium during normal cycles. Ultrasound in medicine & biology. 1986;12(4):271-7. Epub 1986/04/01. PubMed PMID: 3521022.

20.   Gipson IK, Moccia R, Spurr-Michaud S, Argueso P, Gargiulo AR, Hill JA, 3rd, Offner GD, Keutmann HT. The Amount of MUC5B mucin in cervical mucus peaks at midcycle. The Journal of clinical endocrinology and metabolism. 2001;86(2):594-600. Epub 2001/02/07. doi: 10.1210/jcem.86.2.7174. PubMed PMID: 11158014.

21.   Adams JM, Taylor AE, Schoenfeld DA, Crowley WF, Jr., Hall JE. The midcycle gonadotropin surge in normal women occurs in the face of an unchanging gonadotropin-releasing hormone pulse frequency. The Journal of clinical endocrinology and metabolism. 1994;79(3):858-64. Epub 1994/09/01. doi: 10.1210/jcem.79.3.7521353. PubMed PMID: 7521353.

22.   Noyes RW, Hertig AT, Rock J. Dating the endometrial biopsy. American journal of obstetrics and gynecology. 1975;122(2):262-3. Epub 1975/05/01. PubMed PMID: 1155504.

23.   Akhmedkhanov A, Zeleniuch-Jacquotte A, Toniolo P. Role of exogenous and endogenous hormones in endometrial cancer: review of the evidence and research perspectives. Annals of the New York Academy of Sciences. 2001;943:296-315. Epub 2001/10/12. PubMed PMID: 11594550.

24.   Cline JM. Neoplasms of the reproductive tract: the role of hormone exposure. ILAR journal. 2004;45(2):179-88. Epub 2004/04/28. PubMed PMID: 15111737.

25.   Henderson BE, Feigelson HS. Hormonal carcinogenesis. Carcinogenesis. 2000;21(3):427-33. Epub 2000/02/26. PubMed PMID: 10688862.

26.   Endometrial carcinoma: Epidemiology and risk factors [Internet]2019. Available from: https://www.uptodate.com/contents/endometrial-carcinoma-epidemiology-and-risk-factors?search=endometrial&topicRef=16924&source=see_link.

27.   Smith DC, Prentice R, Thompson DJ, Herrmann WL. Association of exogenous estrogen and endometrial carcinoma. The New England journal of medicine. 1975;293(23):1164-7. Epub 1975/12/04. doi: 10.1056/nejm197512042932302. PubMed PMID: 1186789.

28.   Ziel HK, Finkle WD. Increased risk of endometrial carcinoma among users of conjugated estrogens. The New England journal of medicine. 1975;293(23):1167-70. Epub 1975/12/04. doi: 10.1056/nejm197512042932303. PubMed PMID: 171569.

29.   Schottenfeld D. Epidemiology of endometrial neoplasia. Journal of cellular biochemistry Supplement. 1995;23:151-9. Epub 1995/01/01. PubMed PMID: 8747390.

30.   Gallup DG, Stock RJ. Adenocarcinoma of the endometrium in women 40 years of age or younger. Obstetrics and gynecology. 1984;64(3):417-20. Epub 1984/09/01. PubMed PMID: 6462572.

31.   Cancer incidence in five continents. Volume VII. IARC scientific publications. 1997(143):i-xxxiv, 1-1240. Epub 1997/01/01. PubMed PMID: 9505086.

32.   Yap OW, Matthews RP. Racial and ethnic disparities in cancers of the uterine corpus. Journal of the National Medical Association. 2006;98(12):1930-3. Epub 2007/01/18. PubMed PMID: 17225836; PMCID: PMC2569671.

33.   Trimble EL, Harlan LC, Clegg LX, Stevens JL. Pre-operative imaging, surgery and adjuvant therapy for women diagnosed with cancer of the corpus uteri in community practice in the United States. Gynecologic oncology. 2005;96(3):741-8. Epub 2005/02/22. doi: 10.1016/j.ygyno.2004.11.041. PubMed PMID: 15721420.

34.   Maxwell GL, Tian C, Risinger J, Brown CL, Rose GS, Thigpen JT, Fleming GF, Gallion HH, Brewster WR. Racial disparity in survival among patients with advanced/recurrent endometrial adenocarcinoma: a Gynecologic Oncology Group study. Cancer. 2006;107(9):2197-205. Epub 2006/09/27. doi: 10.1002/cncr.22232. PubMed PMID: 17001661.

35.   Ferguson SE, Olshen AB, Levine DA, Viale A, Barakat RR, Boyd J. Molecular profiling of endometrial cancers from African-American and Caucasian women. Gynecologic oncology. 2006;101(2):209-13. Epub 2005/12/29. doi: 10.1016/j.ygyno.2005.11.028. PubMed PMID: 16380157.

36.   Watson P, Lynch HT. Extracolonic cancer in hereditary nonpolyposis colorectal cancer. Cancer. 1993;71(3):677-85. Epub 1993/02/01. PubMed PMID: 8431847.

37.   Committee opinion no. 634: Hereditary cancer syndromes and risk assessment. Obstetrics and gynecology. 2015;125(6):1538-43. Epub 2015/05/23. doi: 10.1097/01.Aog.0000466373.71146.51. PubMed PMID: 26000542.

38.   Lu KH, Dinh M, Kohlmann W, Watson P, Green J, Syngal S, Bandipalliam P, Chen LM, Allen B, Conrad P, Terdiman J, Sun C, Daniels M, Burke T, Gershenson DM, Lynch H, Lynch P, Broaddus RR. Gynecologic cancer as a "sentinel cancer" for women with hereditary nonpolyposis colorectal cancer syndrome. Obstetrics and gynecology. 2005;105(3):569-74. Epub 2005/03/02. doi: 10.1097/01.AOG.0000154885.44002.ae. PubMed PMID: 15738026.

39.   Garg K, Leitao MM, Jr., Kauff ND, Hansen J, Kosarin K, Shia J, Soslow RA. Selection of endometrial carcinomas for DNA mismatch repair protein immunohistochemistry using patient age and tumor morphology enhances detection of mismatch repair abnormalities. The American journal of surgical pathology. 2009;33(6):925-33. Epub 2009/02/25. doi: 10.1097/PAS.0b013e318197a046. PubMed PMID: 19238076.

40.   Schmeler KM, Lynch HT, Chen LM, Munsell MF, Soliman PT, Clark MB, Daniels MS, White KG, Boyd-Rogers SG, Conrad PG, Yang KY, Rubin MM, Sun CC, Slomovitz BM, Gershenson DM, Lu KH. Prophylactic surgery to reduce the risk of gynecologic cancers in the Lynch syndrome. The New England journal of medicine. 2006;354(3):261-9. Epub 2006/01/20. doi: 10.1056/NEJMoa052627. PubMed PMID: 16421367.

41.   Subramaniam DS, Isaacs C. Does prophylactic surgery reduce the risk of gynecologic cancers arising from the Lynch syndrome? Nature clinical practice Oncology. 2006;3(8):426-7. Epub 2006/08/09. doi: 10.1038/ncponc0562. PubMed PMID: 16894387.

42.   Peter P Stanich MML, MD. PTEN hamartoma tumor syndromes, including Cowden syndrome. UpToDate. 2019. Epub Mar 8, 2018.

43.   NIH. Cowden syndrome: Genetics Home Reference; 2018 [updated May 15, 2018; cited 2018 May 18]. Available from: https://ghr.nlm.nih.gov/condition/cowden-syndrome.

44.   Zhou B, Yang L, Sun Q, Cong R, Gu H, Tang N, Zhu H, Wang B. Cigarette smoking and the risk of endometrial cancer: a meta-analysis. The American journal of medicine. 2008;121(6):501-8.e3. Epub 2008/05/27. doi: 10.1016/j.amjmed.2008.01.044. PubMed PMID: 18501231.

45.   Maxwell GL, Schildkraut JM, Calingaert B, Risinger JI, Dainty L, Marchbanks PA, Berchuck A, Barrett JC, Rodriguez GC. Progestin and estrogen potency of combination oral contraceptives and endometrial cancer risk. Gynecologic oncology. 2006;103(2):535-40. Epub 2006/06/03. doi: 10.1016/j.ygyno.2006.03.046. PubMed PMID: 16740300.

46.   Horn LC, Meinel A, Handzel R, Einenkel J. Histopathology of endometrial hyperplasia and endometrial carcinoma: an update. Annals of diagnostic pathology. 2007;11(4):297-311. Epub 2007/07/17. doi: 10.1016/j.anndiagpath.2007.05.002. PubMed PMID: 17630117.

47.   Esteller M, Garcia A, Martinez-Palones JM, Xercavins J, Reventos J. Clinicopathologic features and genetic alterations in endometrioid carcinoma of the uterus with villoglandular differentiation. American journal of clinical pathology. 1999;111(3):336-42. Epub 1999/03/17. PubMed PMID: 10078108.

48.   Kurman RJ, Norris HJ. Evaluation of criteria for distinguishing atypical endometrial hyperplasia from well-differentiated carcinoma. Cancer. 1982;49(12):2547-59. Epub 1982/06/15. PubMed PMID: 7074572.

49.   Hunter JE, Tritz DE, Howell MG, DePriest PD, Gallion HH, Andrews SJ, Buckley SB, Kryscio RJ, van Nagell JR, Jr. The prognostic and therapeutic implications of cytologic atypia in patients with endometrial hyperplasia. Gynecologic oncology. 1994;55(1):66-71. Epub 1994/10/01. PubMed PMID: 7959270.

50.   Sherman ME, Bitterman P, Rosenshein NB, Delgado G, Kurman RJ. Uterine serous carcinoma. A morphologically diverse neoplasm with unifying clinicopathologic features. The American journal of surgical pathology. 1992;16(6):600-10. Epub 1992/06/01. PubMed PMID: 1599038.

51.   Spiegel GW. Endometrial carcinoma in situ in postmenopausal women. The American journal of surgical pathology. 1995;19(4):417-32. Epub 1995/04/01. PubMed PMID: 7694943.

52.   Zheng W, Khurana R, Farahmand S, Wang Y, Zhang ZF, Felix JC. p53 immunostaining as a significant adjunct diagnostic method for uterine surface

carcinoma: precursor of uterine papillary serous carcinoma. The American journal of surgical pathology. 1998;22(12):1463-73. Epub 1998/12/16. PubMed PMID: 9850172.

53.   Soslow RA, Pirog E, Isacson C. Endometrial intraepithelial carcinoma with associated peritoneal carcinomatosis. The American journal of surgical pathology. 2000;24(5):726-32. Epub 2000/05/09. PubMed PMID: 10800992.

54.   Ambros RA, Sherman ME, Zahn CM, Bitterman P, Kurman RJ. Endometrial intraepithelial carcinoma: a distinctive lesion specifically associated with tumors displaying serous differentiation. Human pathology. 1995;26(11):1260-7. Epub 1995/11/01. PubMed PMID: 7590702.

55.   Creasman WT, Morrow CP, Bundy BN, Homesley HD, Graham JE, Heller PB. Surgical pathologic spread patterns of endometrial cancer. A Gynecologic Oncology Group Study. Cancer. 1987;60(8 Suppl):2035-41. Epub 1987/10/15. PubMed PMID: 3652025.

56.   Zaino RJ, Kurman RJ, Brunetto VL, Morrow CP, Bentley RC, Cappellari JO, Bitterman P. Villoglandular adenocarcinoma of the endometrium: a clinicopathologic study of 61 cases: a gynecologic oncology group study. The American journal of surgical pathology. 1998;22(11):1379-85. Epub 1998/11/10. PubMed PMID: 9808130.

57.   Kusuyama Y, Yoshida M, Imai H, Hosomichi T, Mabuchi Y, Yokota H. Secretory carcinoma of the endometrium. Acta cytologica. 1989;33(1):127-30. Epub 1989/01/01. PubMed PMID: 2916359.

58.   Hendrickson MR, Kempson RL. Ciliated carcinoma--a variant of endometrial adenocarcinoma: a report of 10 cases. International journal of gynecological pathology : official journal of the International Society of Gynecological Pathologists. 1983;2(1):1-12. Epub 1983/01/01. PubMed PMID: 6874221.

59.   Salazar OM, DePapp EW, Bonfiglio TA, Feldstein ML, Rubin P, Rudolph JH. Adenosquamous carcinoma of the endometrium. An entity with an inherent poor prognosis? Cancer. 1977;40(1):119-30. Epub 1977/07/01. PubMed PMID: 880545.

60.   Silverberg SG, Bolin MG, DeGiorgi LS. Adenoacanthoma and mixed adenosquamous carcinoma of the endometrium. A clinicopathologic study. Cancer. 1972;30(5):1307-14. Epub 1972/11/01. PubMed PMID: 5083064.

61.   Zaino RJ, Kurman R, Herbold D, Gliedman J, Bundy BN, Voet R, Advani H. The significance of squamous differentiation in endometrial carcinoma. Data from a Gynecologic Oncology Group study. Cancer. 1991;68(10):2293-302. Epub 1991/11/15. PubMed PMID: 1913465.

62.   Carcangiu ML, Chambers JT. Uterine papillary serous carcinoma: a study on 108 cases with emphasis on the prognostic significance of associated endometrioid carcinoma, absence of invasion, and concomitant ovarian carcinoma. Gynecologic oncology. 1992;47(3):298-305. Epub 1992/12/01. PubMed PMID: 1473741.

63.   Chan JK, Loizzi V, Youssef M, Osann K, Rutgers J, Vasilev SA, Berman ML. Significance of comprehensive surgical staging in noninvasive papillary serous carcinoma of the endometrium. Gynecologic oncology. 2003;90(1):181-5. Epub 2003/06/25. PubMed PMID: 12821361.

64.   Goff BA. Uterine papillary serous carcinoma: what have we learned over the past quarter century? Gynecologic oncology. 2005;98(3):341-3. Epub 2005/08/23. doi: 10.1016/j.ygyno.2005.07.006. PubMed PMID: 16111527.

65.   Melhem MF, Tobon H. Mucinous adenocarcinoma of the endometrium: a clinico-pathological review of 18 cases. International journal of gynecological pathology : official journal of the International Society of Gynecological Pathologists. 1987;6(4):347-55. Epub 1987/01/01. PubMed PMID: 2826354.

66.   Maier RC, Norris HJ. Coexistence of cervical intraepithelial neoplasia with primary adenocarcinoma of the endocervix. Obstetrics and gynecology. 1980;56(3):361-4. Epub 1980/09/01. PubMed PMID: 7422175.

67.   McCluggage WG, Roberts N, Bharucha H. Enteric differentiation in endometrial adenocarcinomas: a mucin histochemical study. International journal of gynecological pathology : official journal of the International Society of Gynecological Pathologists. 1995;14(3):250-4. Epub 1995/07/01. PubMed PMID: 8600077.

68.   Webb GA, Lagios MD. Clear cell carcinoma of the endometrium. American journal of obstetrics and gynecology. 1987;156(6):1486-91. Epub 1987/06/01. PubMed PMID: 3591862.

69.   Lax SF, Pizer ES, Ronnett BM, Kurman RJ. Clear cell carcinoma of the endometrium is characterized by a distinctive profile of p53, Ki-67, estrogen, and progesterone receptor expression. Human pathology. 1998;29(6):551-8. Epub 1998/07/04. PubMed PMID: 9635673.

70.	Tagsjo EB, Rosenberg P, Simonsen E. Primary squamous cell carcinoma of the endometrium. Case report. European journal of gynaecological oncology. 1993;14(4):308-10. Epub 1993/01/01. PubMed PMID: 8344325.

71.	Yamashina M, Kobara TY. Primary squamous cell carcinoma with its spindle cell variant in the endometrium. A case report and review of literature. Cancer. 1986;57(2):340-5. Epub 1986/01/15. PubMed PMID: 3942966.

72.	Kumar A, Schneider V. Metastases to the uterus from extrapelvic primary tumors. International journal of gynecological pathology : official journal of the International Society of Gynecological Pathologists. 1983;2(2):134-40. Epub 1983/01/01. PubMed PMID: 6313532.

73.	Creasman WT, Odicino F, Maisonneuve P, Quinn MA, Beller U, Benedet JL, Heintz AP, Ngan HY, Pecorelli S. Carcinoma of the corpus uteri. FIGO 26th Annual Report on the Results of Treatment in Gynecological Cancer. International journal of gynaecology and obstetrics: the official organ of the International Federation of Gynaecology and Obstetrics. 2006;95 Suppl 1:S105-43. Epub 2006/12/13. doi: 10.1016/s0020-7292(06)60031-3. PubMed PMID: 17161155.

74.	Pecorelli S. Revised FIGO staging for carcinoma of the vulva, cervix, and endometrium. International journal of gynaecology and obstetrics: the official organ of the International Federation of Gynaecology and Obstetrics. 2009;105(2):103-4. Epub 2009/04/16. PubMed PMID: 19367689.

75.	Bucy GS, Mendenhall WM, Morgan LS, Chafe WE, Wilkinson EJ, Marcus RB, Jr., Million RR. Clinical stage I and II endometrial carcinoma treated with surgery and/or radiation therapy: analysis of prognostic and treatment-related factors. Gynecologic oncology. 1989;33(3):290-5. Epub 1989/06/01. PubMed PMID: 2722051.

76.	Guntupalli SR, Zighelboim I, Kizer NT, Zhang Q, Powell MA, Thaker PH, Goodfellow PJ, Mutch DG. Lymphovascular space invasion is an independent risk factor for nodal disease and poor outcomes in endometrioid endometrial cancer. Gynecologic oncology. 2012;124(1):31-5. Epub 2011/10/28. doi: 10.1016/j.ygyno.2011.09.017. PubMed PMID: 22030404; PMCID: PMC3936402.

77.	Hanson MB, van Nagell JR, Jr., Powell DE, Donaldson ES, Gallion H, Merhige M, Pavlik EJ. The prognostic significance of lymph-vascular space invasion in stage I endometrial cancer. Cancer. 1985;55(8):1753-7. Epub 1985/04/15. PubMed PMID: 3978563.

78.	Hendrickson M, Ross J, Eifel P, Martinez A, Kempson R. Uterine papillary serous carcinoma: a highly malignant form of endometrial adenocarcinoma. The American journal of surgical pathology. 1982;6(2):93-108. Epub 1982/03/01. PubMed PMID: 7102898.

79.	Bokhman JV. Two pathogenetic types of endometrial carcinoma. Gynecologic oncology. 1983;15(1):10-7. Epub 1983/02/01. PubMed PMID: 6822361.

80.	Kovalev S, Marchenko ND, Gugliotta BG, Chalas E, Chumas J, Moll UM. Loss of p53 function in uterine papillary serous carcinoma. Human pathology. 1998;29(6):613-9. Epub 1998/07/04. PubMed PMID: 9635683.

81.	Cao QJ, Belbin T, Socci N, Balan R, Prystowsky MB, Childs G, Jones JG. Distinctive gene expression profiles by cDNA microarrays in endometrioid and serous carcinomas of the endometrium. International journal of gynecological pathology : official journal of the International Society of Gynecological Pathologists. 2004;23(4):321-9. Epub 2004/09/24. PubMed PMID: 15381901.

82.	Cancer Genome Atlas Research N, Kandoth C, Schultz N, Cherniack AD, Akbani R, Liu Y, Shen H, Robertson AG, Pashtan I, Shen R, Benz CC, Yau C, Laird PW, Ding L, Zhang W, Mills GB, Kucherlapati R, Mardis ER, Levine DA. Integrated genomic characterization of endometrial carcinoma. Nature. 2013;497(7447):67-73. doi: 10.1038/nature12113. PubMed PMID: 23636398; PMCID: 3704730.

83.	Le Gallo M, Bell DW. The Emerging Genomic Landscape of Endometrial Cancer. Clinical chemistry. 2014;60(1):98-110. PubMed PMID: 24170611.

84.	McConechy MK, Ding J, Cheang MC, Wiegand K, Senz J, Tone A, Yang W, Prentice L, Tse K, Zeng T, McDonald H, Schmidt AP, Mutch DG, McAlpine JN, Hirst M, Shah SP, Lee CH, Goodfellow PJ, Gilks CB, Huntsman DG. Use of mutation profiles to refine the classification of endometrial carcinomas. The Journal of pathology. 2012;228(1):20-30. Epub 2012/06/02. doi: 10.1002/path.4056. PubMed PMID: 22653804; PMCID: PMC3939694.

85.	Diaz-Padilla I, Romero N, Amir E, Matias-Guiu X, Vilar E, Muggia F, Garcia-Donas J. Mismatch repair status and clinical outcome in endometrial cancer: a systematic review and meta-analysis. Critical reviews in oncology/hematology. 2013;88(1):154-67. Epub 2013/04/09. doi: 10.1016/j.critrevonc.2013.03.002. PubMed PMID: 23562498.

86. Keys HM, Roberts JA, Brunetto VL, Zaino RJ, Spirtos NM, Bloss JD, Pearlman A, Maiman MA, Bell JG. A phase III trial of surgery with or without adjunctive external pelvic radiation therapy in intermediate risk endometrial adenocarcinoma: a Gynecologic Oncology Group study. Gynecologic oncology. 2004;92(3):744-51. Epub 2004/02/27. doi: 10.1016/j.ygyno.2003.11.048. PubMed PMID: 14984936.

87. Kong TW, Chang SJ, Paek J, Lee Y, Chun M, Ryu HS. Risk group criteria for tailoring adjuvant treatment in patients with endometrial cancer: a validation study of the Gynecologic Oncology Group criteria. Journal of gynecologic oncology. 2015;26(1):32-9. Epub 2014/11/08. doi: 10.3802/jgo.2015.26.1.32. PubMed PMID: 25376915; PMCID: PMC4302283.

88. Mariani A, Dowdy SC, Cliby WA, Gostout BS, Jones MB, Wilson TO, Podratz KC. Prospective assessment of lymphatic dissemination in endometrial cancer: a paradigm shift in surgical staging. Gynecologic oncology. 2008;109(1):11-8. Epub 2008/02/29. doi: 10.1016/j.ygyno.2008.01.023. PubMed PMID: 18304622; PMCID: PMC3667391.

89. Fanning J, Gangestad A, Andrews SJ. National Cancer Data Base/Surveillance Epidemiology and End Results: potential insensitive-measure bias. Gynecologic oncology. 2000;77(3):450-3. Epub 2000/06/01. doi: 10.1006/gyno.2000.5815. PubMed PMID: 10831358.

90. Greven KM. Tailoring radiation to the extent of disease for uterine-confined endometrial cancer. Seminars in radiation oncology. 2000;10(1):29-35. Epub 2000/02/15. doi: 10.1053/srao01000029. PubMed PMID: 10671656.

91. Kwon JS, Francis JA, Qiu F, Weir MM, Ettler HC. When is a pathology review indicated in endometrial cancer? Obstetrics and gynecology. 2007;110(6):1224-30. Epub 2007/12/07. doi: 10.1097/01.AOG.0000287618.86078.6c. PubMed PMID: 18055713.

92. Papadia A, Azioni G, Brusaca B, Fulcheri E, Nishida K, Menoni S, Simpkins F, Lucci JA, 3rd, Ragni N. Frozen section underestimates the need for surgical staging in endometrial cancer patients. International journal of gynecological cancer : official journal of the International Gynecological Cancer Society. 2009;19(9):1570-3. Epub 2009/12/04. doi: 10.1111/IGC.0b013e3181bff64b. PubMed PMID: 19955939.

93. Marziale P, Atlante G, Pozzi M, Diotallevi F, Iacovelli A. 426 cases of stage I endometrial carcinoma: a clinicopathological analysis. Gynecologic oncology. 1989;32(3):278-81. Epub 1989/03/01. PubMed PMID: 2920947.

94.   Sorbe B, Nordstrom B, Maenpaa J, Kuhelj J, Kuhelj D, Okkan S, Delaloye JF, Frankendal B. Intravaginal brachytherapy in FIGO stage I low-risk endometrial cancer: a controlled randomized study. International journal of gynecological cancer : official journal of the International Gynecological Cancer Society. 2009;19(5):873-8. Epub 2009/07/04. doi: 10.1111/IGC.0b013e3181a6c9df. PubMed PMID: 19574776.

95.   Fung-Kee-Fung M, Dodge J, Elit L, Lukka H, Chambers A, Oliver T. Follow-up after primary therapy for endometrial cancer: a systematic review. Gynecologic oncology. 2006;101(3):520-9. Epub 2006/03/25. doi: 10.1016/j.ygyno.2006.02.011. PubMed PMID: 16556457.

96.   Creutzberg CL, van Putten WL, Koper PC, Lybeert ML, Jobsen JJ, Warlam-Rodenhuis CC, De Winter KA, Lutgens LC, van den Bergh AC, van de Steen-Banasik E, Beerman H, van Lent M. Surgery and postoperative radiotherapy versus surgery alone for patients with stage-1 endometrial carcinoma: multicentre randomised trial. PORTEC Study Group. Post Operative Radiation Therapy in Endometrial Carcinoma. Lancet (London, England). 2000;355(9213):1404-11. Epub 2000/05/03. PubMed PMID: 10791524.

97.   Miller D, Filiaci V, Fleming G, Mannel R, Cohn D, Matsumoto T, Tewari K, DiSilvestro P, Pearl M, Zaino R. Late-Breaking Abstract 1: Randomized phase III noninferiority trial of first line chemotherapy for metastatic or recurrent endometrial carcinoma: A Gynecologic Oncology Group study. Gynecologic oncology.125(3):771. doi: 10.1016/j.ygyno.2012.03.034.

98.   Fleming GF. Systemic chemotherapy for uterine carcinoma: metastatic and adjuvant. Journal of clinical oncology : official journal of the American Society of Clinical Oncology. 2007;25(20):2983-90. Epub 2007/07/10. doi: 10.1200/jco.2007.10.8431. PubMed PMID: 17617530.

99.   Vale CL, Tierney J, Bull SJ, Symonds PR. Chemotherapy for advanced, recurrent or metastatic endometrial carcinoma. The Cochrane database of systematic reviews.   2012(8):Cd003915.   Epub   2012/08/17.   doi: 10.1002/14651858.CD003915.pub4. PubMed PMID: 22895938.

100.   Fleming GF, Brunetto VL, Cella D, Look KY, Reid GC, Munkarah AR, Kline R, Burger RA, Goodman A, Burks RT. Phase III trial of doxorubicin plus cisplatin with or without paclitaxel plus filgrastim in advanced endometrial carcinoma: a Gynecologic Oncology Group Study. Journal of clinical oncology : official journal of the American Society of Clinical Oncology. 2004;22(11):2159-66. Epub 2004/06/01. doi: 10.1200/jco.2004.07.184. PubMed PMID: 15169803.

101.	Obel JC, Friberg G, Fleming GF. Chemotherapy in endometrial cancer. Clinical advances in hematology & oncology : H&O. 2006;4(6):459-68. Epub 2006/09/20. PubMed PMID: 16981669.

102.	Temkin SM, Fleming G. Current treatment of metastatic endometrial cancer. Cancer control : journal of the Moffitt Cancer Center. 2009;16(1):38-45. Epub 2008/12/17. doi: 10.1177/107327480901600106. PubMed PMID: 19078928.

103.	Singh M, Zaino RJ, Filiaci VJ, Leslie KK. Relationship of estrogen and progesterone receptors to clinical outcome in metastatic endometrial carcinoma: a Gynecologic Oncology Group Study. Gynecologic oncology. 2007;106(2):325-33. Epub 2007/05/29. doi: 10.1016/j.ygyno.2007.03.042. PubMed PMID: 17532033.

104.	Decruze SB, Green JA. Hormone therapy in advanced and recurrent endometrial cancer: a systematic review. International journal of gynecological cancer : official journal of the International Gynecological Cancer Society. 2007;17(5):964-78. Epub 2007/04/20. doi: 10.1111/j.1525-1438.2007.00897.x. PubMed PMID: 17442022.

105.	Markman M. Hormonal therapy of endometrial cancer. European journal of cancer (Oxford, England : 1990). 2005;41(5):673-5. Epub 2005/03/15. doi: 10.1016/j.ejca.2004.12.008. PubMed PMID: 15763641.

106.	Ma BB, Oza A, Eisenhauer E, Stanimir G, Carey M, Chapman W, Latta E, Sidhu K, Powers J, Walsh W, Fyles A. The activity of letrozole in patients with advanced or recurrent endometrial cancer and correlation with biological markers--a study of the National Cancer Institute of Canada Clinical Trials Group. International journal of gynecological cancer : official journal of the International Gynecological Cancer Society. 2004;14(4):650-8. Epub 2004/08/12. doi: 10.1111/j.1048-891X.2004.14419.x. PubMed PMID: 15304161.

107.	Rose PG, Brunetto VL, VanLe L, Bell J, Walker JL, Lee RB. A phase II trial of anastrozole in advanced recurrent or persistent endometrial carcinoma: a Gynecologic Oncology Group study. Gynecologic oncology. 2000;78(2):212-6. Epub 2000/08/06. doi: 10.1006/gyno.2000.5865. PubMed PMID: 10926805.

108.	Piulats JM, Matias-Guiu X. Immunotherapy in Endometrial Cancer: In the Nick of Time. Clinical cancer research : an official journal of the American Association for Cancer Research. 2016;22(23):5623-5. Epub 2016/10/05. doi: 10.1158/1078-0432.Ccr-16-1820. PubMed PMID: 27697995.

109.	Howitt BE, Shukla SA, Sholl LM, Ritterhouse LL, Watkins JC, Rodig S, Stover E, Strickland KC, D'Andrea AD, Wu CJ, Matulonis UA, Konstantinopoulos PA. Association of Polymerase e-Mutated and Microsatellite-Instable Endometrial Cancers With Neoantigen Load, Number of Tumor-Infiltrating Lymphocytes, and Expression of PD-1 and PD-L1. JAMA oncology. 2015;1(9):1319-23. Epub 2015/07/17. doi: 10.1001/jamaoncol.2015.2151. PubMed PMID: 26181000.

110.	FDA approves first cancer treatment for any solid tumor with a specific genetic feature Silver Spring, MD: FDA; 2017 [cited 2018 April 13th]. Available from: https://www.fda.gov/NewsEvents/Newsroom/PressAnnouncements/ucm560167.htm.

111.	Le DT, Uram JN, Wang H, Bartlett BR, Kemberling H, Eyring AD, Skora AD, Luber BS, Azad NS, Laheru D, Biedrzycki B, Donehower RC, Zaheer A, Fisher GA, Crocenzi TS, Lee JJ, Duffy SM, Goldberg RM, de la Chapelle A, Koshiji M, Bhaijee F, Huebner T, Hruban RH, Wood LD, Cuka N, Pardoll DM, Papadopoulos N, Kinzler KW, Zhou S, Cornish TC, Taube JM, Anders RA, Eshleman JR, Vogelstein B, Diaz LA, Jr. PD-1 Blockade in Tumors with Mismatch-Repair Deficiency. The New England journal of medicine. 2015;372(26):2509-20. Epub 2015/06/02. doi: 10.1056/NEJMoa1500596. PubMed PMID: 26028255; PMCID: PMC4481136.

112.	Ott PA, Bang YJ, Berton-Rigaud D, Elez E, Pishvaian MJ, Rugo HS, Puzanov I, Mehnert JM, Aung KL, Lopez J, Carrigan M, Saraf S, Chen M, Soria JC. Safety and Antitumor Activity of Pembrolizumab in Advanced Programmed Death Ligand 1-Positive Endometrial Cancer: Results From the KEYNOTE-028 Study. Journal of clinical oncology : official journal of the American Society of Clinical Oncology. 2017;35(22):2535-41. Epub 2017/05/11. doi: 10.1200/jco.2017.72.5952. PubMed PMID: 28489510.

113.	Ueda Y, Miyake T, Egawa-Takata T, Miyatake T, Matsuzaki S, Yokoyama T, Yoshino K, Fujita M, Enomoto T, Kimura T. Second-line chemotherapy for advanced or recurrent endometrial carcinoma previously treated with paclitaxel and carboplatin, with or without epirubicin. Cancer chemotherapy and pharmacology. 2011;67(4):829-35. Epub 2010/06/22. doi: 10.1007/s00280-010-1384-z. PubMed PMID: 20563809; PMCID: PMC3064891.

114.	Moore KN, Tian C, McMeekin DS, Thigpen JT, Randall ME, Gallion HH. Does the progression-free interval after primary chemotherapy predict survival after salvage chemotherapy in advanced and recurrent endometrial cancer?: a Gynecologic Oncology Group ancillary data analysis. Cancer. 2010;116(23):5407-14. Epub 2010/08/26. doi: 10.1002/cncr.25480. PubMed PMID: 20737572.

115. Yeramian A, Moreno-Bueno G, Dolcet X, Catasus L, Abal M, Colas E, Reventos J, Palacios J, Prat J, Matias-Guiu X. Endometrial carcinoma: molecular alterations involved in tumor development and progression. Oncogene. 2013;32(4):403-13. Epub 2012/03/21. doi: 10.1038/onc.2012.76. PubMed PMID: 22430211.

116. Jozwiak P, Forma E, Brys M, Krzeslak A. O-GlcNAcylation and Metabolic Reprograming in Cancer. Frontiers in endocrinology. 2014;5:145. Epub 2014/09/25. doi: 10.3389/fendo.2014.00145. PubMed PMID: 25250015; PMCID: PMC4158873.

117. Dedes KJ, Wetterskog D, Ashworth A, Kaye SB, Reis-Filho JS. Emerging therapeutic targets in endometrial cancer. Nature reviews Clinical oncology. 2011;8(5):261-71. Epub 2011/01/12. doi: 10.1038/nrclinonc.2010.216. PubMed PMID: 21221135.

118. Fremin C, Meloche S. From basic research to clinical development of MEK1/2 inhibitors for cancer therapy. Journal of hematology & oncology. 2010;3:8. Epub 2010/02/13. doi: 10.1186/1756-8722-3-8. PubMed PMID: 20149254; PMCID: PMC2830959.

119. Bellone S, Bignotti E, Lonardi S, Ferrari F, Centritto F, Masserdotti A, Pettinella F, Black J, Menderes G, Altwerger G, Hui P, Lopez S, de Haydu C, Bonazzoli E, Predolini F, Zammataro L, Cocco E, Ferrari F, Ravaggi A, Romani C, Facchetti F, Sartori E, Odicino FE, Silasi DA, Litkouhi B, Ratner E, Azodi M, Schwartz PE, Santin AD. Polymerase epsilon (POLE) ultra-mutation in uterine tumors correlates with T lymphocyte infiltration and increased resistance to platinum-based chemotherapy in vitro. Gynecologic oncology. 2017;144(1):146-52. Epub 2016/11/30. doi: 10.1016/j.ygyno.2016.11.023. PubMed PMID: 27894751; PMCID: PMC5183545.

120. Bellone S, Centritto F, Black J, Schwab C, English D, Cocco E, Lopez S, Bonazzoli E, Predolini F, Ferrari F, Silasi DA, Ratner E, Azodi M, Schwartz PE, Santin AD. Polymerase epsilon (POLE) ultra-mutated tumors induce robust tumor-specific CD4+ T cell responses in endometrial cancer patients. Gynecologic oncology. 2015;138(1):11-7. doi: 10.1016/j.ygyno.2015.04.027. PubMed PMID: 25931171; PMCID: 4469551.

121. Bilbao-Sieyro C, Ramirez R, Rodriguez-Gonzalez G, Falcon O, Leon L, Torres S, Fernandez L, Alonso S, Diaz-Chico N, Perucho M, Diaz-Chico JC. Microsatellite instability and ploidy status define three categories with distinctive prognostic impact in endometrioid endometrial cancer. Oncotarget. 2014;5(15):6206-17. Epub 2014/07/16. doi: 10.18632/oncotarget.2187. PubMed PMID: 25026289; PMCID: PMC4171623.

122.   Gargiulo P, Della Pepa C, Berardi S, Califano D, Scala S, Buonaguro L, Ciliberto G, Brauchli P, Pignata S. Tumor genotype and immune microenvironment in POLE-ultramutated and MSI-hypermutated Endometrial Cancers: New candidates for checkpoint blockade immunotherapy? Cancer treatment reviews. 2016;48:61-8. Epub 2016/07/01. doi: 10.1016/j.ctrv.2016.06.008. PubMed PMID: 27362548.

123.   Mehnert JM, Panda A, Zhong H, Hirshfield K, Damare S, Lane K, Sokol L, Stein MN, Rodriguez-Rodriquez L, Kaufman HL, Ali S, Ross JS, Pavlick DC, Bhanot G, White EP, DiPaola RS, Lovell A, Cheng J, Ganesan S. Immune activation and response to pembrolizumab in POLE-mutant endometrial cancer. The Journal of clinical investigation. 2016;126(6):2334-40. Epub 2016/05/10. doi: 10.1172/jci84940. PubMed PMID: 27159395; PMCID: PMC4887167.

124.   Piulats JM, Guerra E, Gil-Martin M, Roman-Canal B, Gatius S, Sanz-Pamplona R, Velasco A, Vidal A, Matias-Guiu X. Molecular approaches for classifying endometrial carcinoma. Gynecologic oncology. 2017;145(1):200-7. Epub 2017/01/04. doi: 10.1016/j.ygyno.2016.12.015. PubMed PMID: 28040204.

125.   van Gool IC, Eggink FA, Freeman-Mills L, Stelloo E, Marchi E, de Bruyn M, Palles C, Nout RA, de Kroon CD, Osse EM, Klenerman P, Creutzberg CL, Tomlinson IPM, Smit V, Nijman HW, Bosse T, Church DN. POLE proofreading mutations elicit an anti-tumor immune response in endometrial cancer. Clinical cancer research : an official journal of the American Association for Cancer Research. 2015;21(14):3347-55. PubMed PMID: 25878334.

126.   Colombo N, Preti E, Landoni F, Carinelli S, Colombo A, Marini C, Sessa C. Endometrial cancer: ESMO Clinical Practice Guidelines for diagnosis, treatment and follow-up. Annals of oncology : official journal of the European Society for Medical Oncology / ESMO. 2013;24 Suppl 6:vi33-8. Epub 2013/10/23. doi: 10.1093/annonc/mdt353. PubMed PMID: 24078661.

127.   Papadia A, Bellati F, Ditto A, Bogani G, Gasparri ML, Di Donato V, Martinelli F, Lorusso D, Benedetti-Panici P, Raspagliesi F. Surgical Treatment of Recurrent Endometrial Cancer: Time for a Paradigm Shift. Annals of surgical oncology. 2015. Epub 2015/03/18. doi: 10.1245/s10434-015-4504-5. PubMed PMID: 25777095.

128.   Boruta DM, 2nd, Growdon WB, McCann CK, Garrett LA, del Carmen MG, Goodman A, Schorge JO. Evolution of surgical management of early-stage endometrial cancer. American journal of obstetrics and gynecology. 2011;205(6):565 e1-6. Epub 2011/08/23. doi: 10.1016/j.ajog.2011.06.081. PubMed PMID: 21855843.

129.   Gilks CB, Oliva E, Soslow RA. Poor interobserver reproducibility in the diagnosis of high-grade endometrial carcinoma. The American journal of surgical pathology. 2013;37(6):874-81. Epub 2013/05/01. doi: 10.1097/PAS.0b013e31827f576a. PubMed PMID: 23629444.

130.   Hoang LN, McConechy MK, Kobel M, Han G, Rouzbahman M, Davidson B, Irving J, Ali RH, Leung S, McAlpine JN, Oliva E, Nucci MR, Soslow RA, Huntsman DG, Gilks CB, Lee CH. Histotype-genotype correlation in 36 high-grade endometrial carcinomas. The American journal of surgical pathology. 2013;37(9):1421-32. Epub 2013/10/01. doi: 10.1097/PAS.0b013e31828c63ed. PubMed PMID: 24076778.

131.   Guan H, Semaan A, Bandyopadhyay S, Arabi H, Feng J, Fathallah L, Pansare V, Qazi A, Abdul-Karim F, Morris RT, Munkarah AR, Ali-Fehmi R. Prognosis and reproducibility of new and existing binary grading systems for endometrial carcinoma compared to FIGO grading in hysterectomy specimens. International journal of gynecological cancer : official journal of the International Gynecological Cancer Society. 2011;21(4):654-60. Epub 2011/05/06. doi: 10.1097/IGC.0b013e31821454f1. PubMed PMID: 21543931.

132.   Han G, Sidhu D, Duggan MA, Arseneau J, Cesari M, Clement PB, Ewanowich CA, Kalloger SE, Kobel M. Reproducibility of histological cell type in high-grade endometrial carcinoma. Modern pathology : an official journal of the United States and Canadian Academy of Pathology, Inc. 2013;26(12):1594-604. Epub 2013/06/29. doi: 10.1038/modpathol.2013.102. PubMed PMID: 23807777.

133.   da Silva JL, Paulino E, Dias MF, de Melo AC. Endometrial cancer: redefining the molecular-targeted approach. Cancer chemotherapy and pharmacology. 2015;76(1):1-11. Epub 2015/05/04. doi: 10.1007/s00280-015-2758-z. PubMed PMID: 25935126.

134.   Drescher KM, Sharma P, Watson P, Gatalica Z, Thibodeau SN, Lynch HT. Lymphocyte recruitment into the tumor site is altered in patients with MSI-H colon cancer. Familial cancer. 2009;8(3):231-9. Epub 2009/01/24. doi: 10.1007/s10689-009-9233-0. PubMed PMID: 19165625.

135.   Veitia RA, Bottani S, Birchler JA. Cellular reactions to gene dosage imbalance: genomic, transcriptomic and proteomic effects. Trends in genetics : TIG. 2008;24(8):390-7. Epub 2008/07/01. doi: 10.1016/j.tig.2008.05.005. PubMed PMID: 18585818.

136.   Rice AM, McLysaght A. Dosage-sensitive genes in evolution and disease. BMC biology. 2017;15(1):78. Epub 2017/09/03. doi: 10.1186/s12915-017-0418-y. PubMed PMID: 28863777; PMCID: PMC5580218.

137.   Kim TH, Wang J, Lee KY, Franco HL, Broaddus RR, Lydon JP, Jeong JW, Demayo FJ. The Synergistic Effect of Conditional Pten Loss and Oncogenic K-ras Mutation on Endometrial Cancer Development Occurs via Decreased Progesterone Receptor Action. Journal of oncology. 2010;2010:139087. doi: 10.1155/2010/139087. PubMed PMID: 19884980; PMCID: 2768008.

138.   Fanning J. Long-term survival of intermediate risk endometrial cancer (stage IG3, IC, II) treated with full lymphadenectomy and brachytherapy without teletherapy. Gynecologic oncology. 2001;82(2):371-4. Epub 2001/09/05. doi: 10.1006/gyno.2001.6276. PubMed PMID: 11531297.

139.   Kim HI, Schultz CR, Buras AL, Friedman E, Fedorko A, Seamon L, Chandramouli GVR, Maxwell GL, Bachmann AS, Risinger JI. Ornithine decarboxylase as a therapeutic target for endometrial cancer. PloS one. 2017;12(12):e0189044. Epub 2017/12/15. doi: 10.1371/journal.pone.0189044. PubMed PMID: 29240775; PMCID: PMC5730160.

140.   Uegaki K, Kanamori Y, Kigawa J, Kawaguchi W, Kaneko R, Naniwa J, Takahashi M, Shimada M, Oishi T, Itamochi H, Terakawa N. PTEN-positive and phosphorylated-Akt-negative expression is a predictor of survival for patients with advanced endometrial carcinoma. Oncology reports. 2005;14(2):389-92. Epub 2005/07/14. PubMed PMID: 16012720.

141.   Risinger JI, Hayes K, Maxwell GL, Carney ME, Dodge RK, Barrett JC, Berchuck A. PTEN mutation in endometrial cancers is associated with favorable clinical and pathologic characteristics. Clinical cancer research : an official journal of the American Association for Cancer Research. 1998;4(12):3005-10. Epub 1998/12/29. PubMed PMID: 9865913.

142.   Allard JE, Risinger JI, Morrison C, Young G, Rose GS, Fowler J, Berchuck A, Maxwell GL. Overexpression of folate binding protein is associated with shortened progression-free survival in uterine adenocarcinomas. Gynecologic oncology. 2007;107(1):52-7. Epub 2007/06/22. doi: 10.1016/j.ygyno.2007.05.018. PubMed PMID: 17582475.

143.   Dainty LA, Risinger JI, Morrison C, Chandramouli GV, Bidus MA, Zahn C, Rose GS, Fowler J, Berchuck A, Maxwell GL. Overexpression of folate binding protein and

mesothelin are associated with uterine serous carcinoma. Gynecologic oncology. 2007;105(3):563-70. Epub 2007/04/03. doi: 10.1016/j.ygyno.2006.10.063. PubMed PMID: 17400285.

144.   Integrated Genomic Characterization of Endometrial Carcinoma. Nature. 2013;497(7447):67-73. PubMed PMID: 23636398.

145.   Kandoth C, Schultz N, Cherniack AD, Akbani R, Liu Y, Shen H, Robertson AG, Pashtan I, Shen R, Benz CC, Yau C, Laird PW, Ding L, Zhang W, Mills GB, Kucherlapati R, Mardis ER, Levine DA. Integrated genomic characterization of endometrial carcinoma. Nature. 2013;497(7447):67-73. Epub 2013/05/03. doi: 10.1038/nature12113. PubMed PMID: 23636398; PMCID: PMC3704730.

146.   Siegel RL, Miller KD, Jemal A. Cancer statistics, 2016. CA: a cancer journal for clinicians. 2016;66(1):7-30. Epub 2016/01/09. doi: 10.3322/caac.21332. PubMed PMID: 26742998.

147.   Morice P, Leary A, Creutzberg C, Abu-Rustum N, Darai E. Endometrial cancer. Lancet (London, England). 2016;387(10023):1094-108. Epub 2015/09/12. doi: 10.1016/s0140-6736(15)00130-0. PubMed PMID: 26354523.

148.   Burke WM, Orr J, Leitao M, Salom E, Gehrig P, Olawaiye AB, Brewer M, Boruta D, Villella J, Herzog T, Abu Shahin F. Endometrial cancer: a review and current management strategies: part I. Gynecologic oncology. 2014;134(2):385-92. Epub 2014/06/07. doi: 10.1016/j.ygyno.2014.05.018. PubMed PMID: 24905773.

149.   Burke WM, Orr J, Leitao M, Salom E, Gehrig P, Olawaiye AB, Brewer M, Boruta D, Herzog TJ, Shahin FA. Endometrial cancer: a review and current management strategies: part II. Gynecologic oncology. 2014;134(2):393-402. Epub 2014/06/15. doi: 10.1016/j.ygyno.2014.06.003. PubMed PMID: 24929052.

150.   Siegel RL, Miller KD, Jemal A. Cancer statistics, 2015. CA: a cancer journal for clinicians. 2015;65(1):5-29. Epub 2015/01/07. doi: 10.3322/caac.21254. PubMed PMID: 25559415.

151.   Vollmer G. Endometrial cancer: experimental models useful for studies on molecular aspects of endometrial cancer and carcinogenesis. Endocrine-related cancer. 2003;10(1):23-42. Epub 2003/03/26. PubMed PMID: 12653669.

152.	Cabrera S, Llaurado M, Castellvi J, Fernandez Y, Alameda F, Colas E, Ruiz A, Doll A, Schwartz S, Jr., Carreras R, Xercavins J, Abal M, Gil-Moreno A, Reventos J. Generation and characterization of orthotopic murine models for endometrial cancer. Clinical & experimental metastasis. 2012;29(3):217-27. Epub 2011/12/27. doi: 10.1007/s10585-011-9444-2. PubMed PMID: 22198674.

153.	Haldorsen IS, Popa M, Fonnes T, Brekke N, Kopperud R, Visser NC, Rygh CB, Pavlin T, Salvesen HB, McCormack E, Krakstad C. Multimodal Imaging of Orthotopic Mouse Model of Endometrial Carcinoma. PloS one. 2015;10(8):e0135220. Epub 2015/08/08. doi: 10.1371/journal.pone.0135220. PubMed PMID: 26252891; PMCID: PMC4529312.

154.	Doll A, Gonzalez M, Abal M, Llaurado M, Rigau M, Colas E, Monge M, Xercavins J, Capella G, Diaz B, Gil-Moreno A, Alameda F, Reventos J. An orthotopic endometrial cancer mouse model demonstrates a role for RUNX1 in distant metastasis. International journal of cancer Journal international du cancer. 2009;125(2):257-63. Epub 2009/04/23. doi: 10.1002/ijc.24330. PubMed PMID: 19384951.

155.	Depreeuw J, Hermans E, Schrauwen S, Annibali D, Coenegrachts L, Thomas D, Luyckx M, Gutierrez-Roelens I, Debruyne D, Konings K, Moerman P, Vergote I, Lambrechts D, Amant F. Characterization of patient-derived tumor xenograft models of endometrial cancer for preclinical evaluation of targeted therapies. Gynecologic oncology. 2015;139(1):118-26. Epub 2015/08/02. doi: 10.1016/j.ygyno.2015.07.104. PubMed PMID: 26232337.

156.	Kim TH, Franco HL, Jung SY, Qin J, Broaddus RR, Lydon JP, Jeong JW. The synergistic effect of Mig-6 and Pten ablation on endometrial cancer development and progression. Oncogene. 2010;29(26):3770-80. doi: 10.1038/onc.2010.126. PubMed PMID: 20418913; PMCID: 4013686.

157.	Lu TL, Chang JL, Liang CC, You LR, Chen CM. Tumor spectrum, tumor latency and tumor incidence of the Pten-deficient mice. PloS one. 2007;2(11):e1237. Epub 2007/11/29. doi: 10.1371/journal.pone.0001237. PubMed PMID: 18043744; PMCID: PMC2077932.

158.	Contreras CM, Akbay EA, Gallardo TD, Haynie JM, Sharma S, Tagao O, Bardeesy N, Takahashi M, Settleman J, Wong KK, Castrillon DH. Lkb1 inactivation is sufficient to drive endometrial cancers that are aggressive yet highly responsive to mTOR inhibitor monotherapy. Disease models & mechanisms. 2010;3(3-4):181-93. Epub 2010/02/10. doi: 10.1242/dmm.004440. PubMed PMID: 20142330; PMCID: PMC2869492.

159. Cheng H, Liu P, Zhang F, Xu E, Symonds L, Ohlson CE, Bronson RT, Maira SM, Di Tomaso E, Li J, Myers AP, Cantley LC, Mills GB, Zhao JJ. A genetic mouse model of invasive endometrial cancer driven by concurrent loss of Pten and Lkb1 Is highly responsive to mTOR inhibition. Cancer research. 2014;74(1):15-23. Epub 2013/12/11. doi: 10.1158/0008-5472.can-13-0544. PubMed PMID: 24322983; PMCID: PMC3982380.

160. Steck PA, Pershouse MA, Jasser SA, Yung WK, Lin H, Ligon AH, Langford LA, Baumgard ML, Hattier T, Davis T, Frye C, Hu R, Swedlund B, Teng DH, Tavtigian SV. Identification of a candidate tumour suppressor gene, MMAC1, at chromosome 10q23.3 that is mutated in multiple advanced cancers. Nature genetics. 1997;15(4):356-62. Epub 1997/04/01. doi: 10.1038/ng0497-356. PubMed PMID: 9090379.

161. Li DM, Sun H. TEP1, encoded by a candidate tumor suppressor locus, is a novel protein tyrosine phosphatase regulated by transforming growth factor beta. Cancer research. 1997;57(11):2124-9. Epub 1997/06/01. PubMed PMID: 9187108.

162. Maxwell GL, Risinger JI, Gumbs C, Shaw H, Bentley RC, Barrett JC, Berchuck A, Futreal PA. Mutation of the PTEN tumor suppressor gene in endometrial hyperplasias. Cancer research. 1998;58(12):2500-3. Epub 1998/07/04. PubMed PMID: 9635567.

163. Di Cristofano A, Ellenson LH. Endometrial carcinoma. Annual review of pathology. 2007;2:57-85. Epub 2007/11/28. doi: 10.1146/annurev.pathol.2.010506.091905. PubMed PMID: 18039093.

164. Miyasaka A, Oda K, Ikeda Y, Sone K, Fukuda T, Inaba K, Makii C, Enomoto A, Hosoya N, Tanikawa M, Uehara Y, Arimoto T, Kuramoto H, Wada-Hiraike O, Miyagawa K, Yano T, Kawana K, Osuga Y, Fujii T. PI3K/mTOR pathway inhibition overcomes radioresistance via suppression of the HIF1-alpha/VEGF pathway in endometrial cancer. Gynecologic oncology. 2015;138(1):174-80. Epub 2015/04/29. doi: 10.1016/j.ygyno.2015.04.015. PubMed PMID: 25913131.

165. Shorthouse AJ, Smyth JF, Steel GG, Ellison M, Mills J, Peckham MJ. The human tumour xenograft--a valid model in experimental chemotherapy? The British journal of surgery. 1980;67(10):715-22. Epub 1980/10/01. PubMed PMID: 6253000.

166. Tentler JJ, Tan AC, Weekes CD, Jimeno A, Leong S, Pitts TM, Arcaroli JJ, Messersmith WA, Eckhardt SG. Patient-derived tumour xenografts as models for oncology drug development. Nature reviews Clinical oncology. 2012;9(6):338-50. Epub 2012/04/18. doi: 10.1038/nrclinonc.2012.61. PubMed PMID: 22508028; PMCID: PMC3928688.

167.   Hidalgo M, Amant F, Biankin AV, Budinska E, Byrne AT, Caldas C, Clarke RB, de Jong S, Jonkers J, Maelandsmo GM, Roman-Roman S, Seoane J, Trusolino L, Villanueva A. Patient-derived xenograft models: an emerging platform for translational cancer research. Cancer discovery. 2014;4(9):998-1013. Epub 2014/09/04. doi: 10.1158/2159-8290.cd-14-0001. PubMed PMID: 25185190; PMCID: PMC4167608.

168.   Tan MH, Chu TM. Characterization of the tumorigenic and metastatic properties of a human pancreatic tumor cell line (AsPC-1) implanted orthotopically into nude mice. Tumour biology : the journal of the International Society for Oncodevelopmental Biology and Medicine. 1985;6(1):89-98. Epub 1985/01/01. PubMed PMID: 4023565.

169.   Merenda C, Sordat B, Mach JP, Carrel S. Human endometrial carcinomas serially transplanted in nude mice and established in continuous cell lines. International journal of cancer Journal international du cancer. 1975;16(4):559-70. Epub 1975/10/15. PubMed PMID: 1176207.

170.   Rygaard J, Povlsen CO. Heterotransplantation of a human malignant tumour to "Nude" mice. Acta pathologica et microbiologica Scandinavica. 1969;77(4):758-60. Epub 1969/01/01. PubMed PMID: 5383844.

171.   Palm JE, Teller MN, Merker PC, Woolley GW. Host conditioning in experimental chemotherapy. Annals of the New York Academy of Sciences. 1958;76(3):812-20. Epub 1958/12/05. PubMed PMID: 13627908.

172.   Unno K, Ono M, Winder AD, Maniar KP, Paintal AS, Yu Y, Wei JJ, Lurain JR, Kim JJ. Establishment of human patient-derived endometrial cancer xenografts in NOD scid gamma mice for the study of invasion and metastasis. PloS one. 2014;9(12):e116064. Epub 2014/12/30. doi: 10.1371/journal.pone.0116064. PubMed PMID: 25542024; PMCID: PMC4277433.

173.   Rubesa-Mihaljevic R, Babarovic E, Vrdoljak-Mozetic D, Stemberger-Papic S, Klaric M, Krasevic M, Jonjic N. The Immunohistochemical Pattern of Epithelial-Mesenchymal Transition Markers In Endometrial Carcinoma. Applied immunohistochemistry & molecular morphology : AIMM. 2019. Epub 2019/03/05. doi: 10.1097/pai.0000000000000754. PubMed PMID: 30829665.

174.   Zehir A, Benayed R, Shah RH, Syed A, Middha S, Kim HR, Srinivasan P, Gao J, Chakravarty D, Devlin SM, Hellmann MD, Barron DA, Schram AM, Hameed M, Dogan S, Ross DS, Hechtman JF, DeLair DF, Yao J, Mandelker DL, Cheng DT, Chandramohan R, Mohanty AS, Ptashkin RN, Jayakumaran G, Prasad M, Syed MH, Rema AB, Liu ZY, Nafa K, Borsu L, Sadowska J, Casanova J, Bacares R, Kiecka IJ,

Razumova A, Son JB, Stewart L, Baldi T, Mullaney KA, Al-Ahmadie H, Vakiani E, Abeshouse AA, Penson AV, Jonsson P, Camacho N, Chang MT, Won HH, Gross BE, Kundra R, Heins ZJ, Chen HW, Phillips S, Zhang H, Wang J, Ochoa A, Wills J, Eubank M, Thomas SB, Gardos SM, Reales DN, Galle J, Durany R, Cambria R, Abida W, Cercek A, Feldman DR, Gounder MM, Hakimi AA, Harding JJ, Iyer G, Janjigian YY, Jordan EJ, Kelly CM, Lowery MA, Morris LGT, Omuro AM, Raj N, Razavi P, Shoushtari AN, Shukla N, Soumerai TE, Varghese AM, Yaeger R, Coleman J, Bochner B, Riely GJ, Saltz LB, Scher HI, Sabbatini PJ, Robson ME, Klimstra DS, Taylor BS, Baselga J, Schultz N, Hyman DM, Arcila ME, Solit DB, Ladanyi M, Berger MF. Mutational landscape of metastatic cancer revealed from prospective clinical sequencing of 10,000 patients. Nature medicine. 2017;23(6):703-13. Epub 2017/05/10. doi: 10.1038/nm.4333. PubMed PMID: 28481359; PMCID: PMC5461196.

175.   Iijima M, Banno K, Okawa R, Yanokura M, Iida M, Takeda T, Kunitomi-Irie H, Adachi M, Nakamura K, Umene K, Nogami Y, Masuda K, Tominaga E, Aoki D. Genome-wide analysis of gynecologic cancer: The Cancer Genome Atlas in ovarian and endometrial cancer. Oncology letters. 2017;13(3):1063-70. Epub 2017/04/30. doi: 10.3892/ol.2017.5582. PubMed PMID: 28454214; PMCID: PMC5403284.

176.   Kamal AM, Bulmer JN, DeCruze SB, Stringfellow HF, Martin-Hirsch P, Hapangama DK. Androgen receptors are acquired by healthy postmenopausal endometrial epithelium and their subsequent loss in endometrial cancer is associated with poor survival. British journal of cancer. 2016;114(6):688-96. Epub 2016/03/02. doi: 10.1038/bjc.2016.16. PubMed PMID: 26930451; PMCID: PMC4800292.

177.   Vihko R, Alanko A, Isomaa V, Kauppila A. The predictive value of steroid hormone receptor analysis in breast, endometrial and ovarian cancer. Medical oncology and tumor pharmacotherapy. 1986;3(3-4):197-210. Epub 1986/01/01. PubMed PMID: 3543533.

178.   Tomica D, Ramic S, Danolic D, Susnjar L, Peric-Balja M, Puljiz M. Impact of oestrogen and progesterone receptor expression in the cancer cells and myometrium on survival of patients with endometrial cancer. Journal of obstetrics and gynaecology : the journal of the Institute of Obstetrics and Gynaecology. 2017:1-7. Epub 2017/08/03. doi: 10.1080/01443615.2017.1328591. PubMed PMID: 28764605.

179.   Burghardt RC, Mitchell PA, Kurten R. Gap junction modulation in rat uterus. II. Effects of antiestrogens on myometrial and serosal cells. Biology of reproduction. 1984;30(1):249-55. Epub 1984/02/01. PubMed PMID: 6421335.

180.   Zeng R, Li X, Gorodeski GI. Estrogen abrogates transcervical tight junctional resistance by acceleration of occludin modulation. The Journal of clinical endocrinology

and metabolism. 2004;89(10):5145-55. Epub 2004/10/09. doi: 10.1210/jc.2004-0823. PubMed PMID: 15472219.

181. Gorodeski GI. Estrogen modulation of epithelial permeability in cervical-vaginal cells of premenopausal and postmenopausal women. Menopause (New York, NY). 2007;14(6):1012-9. Epub 2007/06/19. doi: 10.1097/gme.0b013e3180587eb5. PubMed PMID: 17572644; PMCID: PMC2366810.

182. Herve MA, Meduri G, Petit FG, Domet TS, Lazennec G, Mourah S, Perrot-Applanat M. Regulation of the vascular endothelial growth factor (VEGF) receptor Flk-1/KDR by estradiol through VEGF in uterus. The Journal of endocrinology. 2006;188(1):91-9. Epub 2006/01/06. doi: 10.1677/joe.1.06184. PubMed PMID: 16394178.

183. Liu J, Liu Y, Wang W, Wang C, Che Y. Expression of immune checkpoint molecules in endometrial carcinoma. Experimental and therapeutic medicine. 2015;10(5):1947-52. Epub 2015/12/08. doi: 10.3892/etm.2015.2714. PubMed PMID: 26640578; PMCID: PMC4665362.

184. Jones NL, Xiu J, Reddy SK, Burke WM, Tergas AI, Wright JD, Hou JY. Identification of potential therapeutic targets by molecular profiling of 628 cases of uterine serous carcinoma. Gynecologic oncology. 2015;138(3):620-6. Epub 2015/07/01. doi: 10.1016/j.ygyno.2015.06.034. PubMed PMID: 26123645.

185. Mouse Alloantigens. Available from: www.biolegend.com/media_assets/support.../BioLegend_Mouse_Alloantigens.pdf.

186. Greenaway J, Moorehead R, Shaw P, Petrik J. Epithelial-stromal interaction increases cell proliferation, survival and tumorigenicity in a mouse model of human epithelial ovarian cancer. Gynecologic oncology. 2008;108(2):385-94. Epub 2007/11/27. doi: 10.1016/j.ygyno.2007.10.035. PubMed PMID: 18036641.

187. Ko M, An J, Bandukwala HS, Chavez L, Aijo T, Pastor WA, Segal MF, Li H, Koh KP, Lahdesmaki H, Hogan PG, Aravind L, Rao A. Modulation of TET2 expression and 5-methylcytosine oxidation by the CXXC domain protein IDAX. Nature. 2013;497(7447):122-6. doi: 10.1038/nature12052. PubMed PMID: 23563267; PMCID: 3643997.

188. Xu C, Bian C, Lam R, Dong A, Min J. The structural basis for selective binding of non-methylated CpG islands by the CFP1 CXXC domain. Nature communications. 2011;2:227. doi: 10.1038/ncomms1237. PubMed PMID: 21407193; PMCID: 3072069.

189.   Kim HY, Yoon JY, Yun JH, Cho KW, Lee SH, Rhee YM, Jung HS, Lim HJ, Lee H, Choi J, Heo JN, Lee W, No KT, Min D, Choi KY. CXXC5 is a negative-feedback regulator of the Wnt/beta-catenin pathway involved in osteoblast differentiation. Cell death and differentiation. 2015;22(6):912-20. doi: 10.1038/cdd.2014.238. PubMed PMID: 25633194; PMCID: 4423189.

190.   Andersson T, Sodersten E, Duckworth JK, Cascante A, Fritz N, Sacchetti P, Cervenka I, Bryja V, Hermanson O. CXXC5 is a novel BMP4-regulated modulator of Wnt signaling in neural stem cells. The Journal of biological chemistry. 2009;284(6):3672-81. doi: 10.1074/jbc.M808119200. PubMed PMID: 19001364.

191.   Zhang M, Wang R, Wang Y, Diao F, Lu F, Gao D, Chen D, Zhai Z, Shu H. The CXXC finger 5 protein is required for DNA damage-induced p53 activation. Science in China Series C, Life sciences / Chinese Academy of Sciences. 2009;52(6):528-38. doi: 10.1007/s11427-009-0083-7. PubMed PMID: 19557330.

192.   Liu N, Wang M, Deng W, Schmidt CS, Qin W, Leonhardt H, Spada F. Intrinsic and extrinsic connections of Tet3 dioxygenase with CXXC zinc finger modules. PloS one. 2013;8(5):e62755. Epub 2013/05/22. doi: 10.1371/journal.pone.0062755. PubMed PMID: 23690950; PMCID: PMC3653909.

193.   Pendino F, Nguyen E, Jonassen I, Dysvik B, Azouz A, Lanotte M, Segal-Bendirdjian E, Lillehaug JR. Functional involvement of RINF, retinoid-inducible nuclear factor (CXXC5), in normal and tumoral human myelopoiesis. Blood. 2009;113(14):3172-81. doi: 10.1182/blood-2008-07-170035. PubMed PMID: 19182210.

194.   Bruserud O, Reikvam H, Fredly H, Skavland J, Hagen KM, van Hoang TT, Brenner AK, Kadi A, Astori A, Gjertsen BT, Pendino F. Expression of the potential therapeutic target CXXC5 in primary acute myeloid leukemia cells - high expression is associated with adverse prognosis as well as altered intracellular signaling and transcriptional regulation. Oncotarget. 2015;6(5):2794-811. Epub 2015/01/22. doi: 10.18632/oncotarget.3056. PubMed PMID: 25605239; PMCID: PMC4413618.

195.   Kuhnl A, Valk PJ, Sanders MA, Ivey A, Hills RK, Mills KI, Gale RE, Kaiser MF, Dillon R, Joannides M, Gilkes A, Haferlach T, Schnittger S, Duprez E, Linch DC, Delwel R, Lowenberg B, Baldus CD, Solomon E, Burnett AK, Grimwade D. Downregulation of the Wnt inhibitor CXXC5 predicts a better prognosis in acute myeloid leukemia. Blood. 2015;125(19):2985-94. Epub 2015/03/26. doi: 10.1182/blood-2014-12-613703. PubMed PMID: 25805812; PMCID: PMC4463809.

196.   Lee SH, Kim MY, Kim HY, Lee YM, Kim H, Nam KA, Roh MR, Min do S, Chung KY, Choi KY. The Dishevelled-binding protein CXXC5 negatively regulates cutaneous wound healing. The Journal of experimental medicine. 2015;212(7):1061-80. Epub 2015/06/10. doi: 10.1084/jem.20141601. PubMed PMID: 26056233; PMCID: PMC4493411.

197.   Kim HY, Choi S, Yoon JH, Lim HJ, Lee H, Choi J, Ro EJ, Heo JN, Lee W, No KT, Choi KY. Small molecule inhibitors of the Dishevelled-CXXC5 interaction are new drug candidates for bone anabolic osteoporosis therapy. EMBO molecular medicine. 2016;8(4):375-87. Epub 2016/03/05. doi: 10.15252/emmm.201505714. PubMed PMID: 26941261; PMCID: PMC4818757.

198.   Yasar P, Ayaz G, Muyan M. Estradiol-Estrogen Receptor alpha Mediates the Expression of the CXXC5 Gene through the Estrogen Response Element-Dependent Signaling Pathway. Scientific reports. 2016;6:37808. Epub 2016/11/26. doi: 10.1038/srep37808. PubMed PMID: 27886276; PMCID: PMC5122896.

199.   Burney RO, Talbi S, Hamilton AE, Vo KC, Nyegaard M, Nezhat CR, Lessey BA, Giudice LC. Gene expression analysis of endometrium reveals progesterone resistance and candidate susceptibility genes in women with endometriosis. Endocrinology. 2007;148(8):3814-26. Epub 2007/05/19. doi: 10.1210/en.2006-1692. PubMed PMID: 17510236.

200.   Risinger JI, Allard J, Chandran U, Day R, Chandramouli GV, Miller C, Zahn C, Oliver J, Litzi T, Marcus C, Dubil E, Byrd K, Cassablanca Y, Becich M, Berchuck A, Darcy KM, Hamilton CA, Conrads TP, Maxwell GL. Gene expression analysis of early stage endometrial cancers reveals unique transcripts associated with grade and histology but not depth of invasion. Frontiers in oncology. 2013;3:139. Epub 2013/06/21. doi: 10.3389/fonc.2013.00139. PubMed PMID: 23785665; PMCID: 3683664.

201.   Maxwell GL, Allard J, Gadisetti CV, Litzi T, Casablanca Y, Chandran U, Darcy KM, Levine DA, Berchuck A, Hamilton CA, Conrads TP, Risinger JI. Transcript expression in endometrial cancers from Black and White patients. Gynecol Oncol. 2013;130(1):169-73. Epub 2013/04/23. doi: 10.1016/j.ygyno.2013.04.017. PubMed PMID: 23603370.

202.   Zhang C, Yin C, Wang L, Zhang S, Qian Y, Ma J, Zhang Z, Xu Y, Liu S. HSPC111 governs breast cancer growth by regulating ribosomal biogenesis. Molecular cancer research : MCR. 2014;12(4):583-94. Epub 2014/01/16. doi: 10.1158/1541-7786.Mcr-13-0168. PubMed PMID: 24425784.

203.   Kundel DW, Stromquist E, Greene AL, Zhdankin O, Regal RR, Rose-Hellekant TA. Molecular characterizations of Nop16 in murine mammary tumors with varying levels of c-Myc. Transgenic research. 2012;21(2):393-406. Epub 2011/08/25. doi: 10.1007/s11248-011-9529-3. PubMed PMID: 21863248; PMCID: PMC4043839.

204.   Fader AN, Santin AD, Gehrig PA. Early stage uterine serous carcinoma: management updates and genomic advances. Gynecologic oncology. 2013;129(1):244-50. doi: 10.1016/j.ygyno.2013.01.004. PubMed PMID: 23321062.

205.   Kim MS, Yoon SK, Bollig F, Kitagaki J, Hur W, Whye NJ, Wu YP, Rivera MN, Park JY, Kim HS, Malik K, Bell DW, Englert C, Perantoni AO, Lee SB. A novel Wilms tumor 1 (WT1) target gene negatively regulates the WNT signaling pathway. The Journal of biological chemistry. 2010;285(19):14585-93. doi: 10.1074/jbc.M109.094334. PubMed PMID: 20220130; PMCID: 2863207.

206.   Sal V, Demirkiran F, Erenel H, Tokgozoglu N, Kahramanoglu I, Bese T, Turan H, Sofiyeva N, Calay Z, Arvas M, Guralp O. Expression of PTEN and beta-Catenin and Their Relationship With Clinicopathological and Prognostic Factors in Endometrioid Type Endometrial Cancer. International journal of gynecological cancer : official journal of the International Gynecological Cancer Society. 2016;26(3):512-20. Epub 2016/02/20. doi: 10.1097/igc.0000000000000626. PubMed PMID: 26894937.

207.   Fukuchi T, Sakamoto M, Tsuda H, Maruyama K, Nozawa S, Hirohashi S. Beta-catenin mutation in carcinoma of the uterine endometrium. Cancer research. 1998;58(16):3526-8. Epub 1998/08/29. PubMed PMID: 9721853.

208.   Ma S, Choi J, Jin X, Kim HY, Yun JH, Lee W, Choi KY, No KT. Discovery of a small-molecule inhibitor of Dvl-CXXC5 interaction by computational approaches. Journal of computer-aided molecular design. 2018;32(5):643-55. Epub 2018/04/09. doi: 10.1007/s10822-018-0118-x. PubMed PMID: 29627878.

209.   Day RS, McDade KK, Chandran UR, Lisovich A, Conrads TP, Hood BL, Kolli VS, Kirchner D, Litzi T, Maxwell GL. Identifier mapping performance for integrating transcriptomics and proteomics experimental results. BMC bioinformatics. 2011;12:213. Epub 2011/05/31. doi: 10.1186/1471-2105-12-213. PubMed PMID: 21619611; PMCID: PMC3124437.

210.   Allard JE, Chandramouli GV, Stagliano K, Hood BL, Litzi T, Shoji Y, Boyd J, Berchuck A, Conrads TP, Maxwell GL, Risinger JI. Analysis of PSPHL as a Candidate Gene Influencing the Racial Disparity in Endometrial Cancer. Frontiers in oncology.

2012;2:65. Epub 2012/07/12. doi: 10.3389/fonc.2012.00065. PubMed PMID: 22783543; PMCID: 3389395.

211.   Risinger JI, Maxwell GL, Chandramouli GV, Aprelikova O, Litzi T, Umar A, Berchuck A, Barrett JC. Gene expression profiling of microsatellite unstable and microsatellite stable endometrial cancers indicates distinct pathways of aberrant signaling. Cancer research. 2005;65(12):5031-7. Epub 2005/06/17. doi: 10.1158/0008-5472.CAN-04-0850. PubMed PMID: 15958545.

212.   Kyo S, Nakamura M, Kiyono T, Maida Y, Kanaya T, Tanaka M, Yatabe N, Inoue M. Successful Immortalization of Endometrial Glandular Cells with Normal Structural and Functional Characteristics. The American journal of pathology. 2003;163(6):2259-69. doi: 10.1016/s0002-9440(10)63583-3.

213.   Comprehensive molecular characterization of human colon and rectal cancer. Nature. 2012;487(7407):330-7. Epub 2012/07/20. doi: 10.1038/nature11252. PubMed PMID: 22810696; PMCID: PMC3401966.

214.   Johnson GE. Mammalian cell HPRT gene mutation assay: test methods. Methods in molecular biology (Clifton, NJ). 2012;817:55-67. Epub 2011/12/08. doi: 10.1007/978-1-61779-421-6_4. PubMed PMID: 22147568.

215.   Puck TT, Marcus PI. A RAPID METHOD FOR VIABLE CELL TITRATION AND CLONE PRODUCTION WITH HELA CELLS IN TISSUE CULTURE: THE USE OF X-IRRADIATED CELLS TO SUPPLY CONDITIONING FACTORS. Proceedings of the National Academy of Sciences of the United States of America. 1955;41(7):432-7. Epub 1955/07/15. PubMed PMID: 16589695; PMCID: PMC528114.

216.   Scherer WF, Syverton JT, Gey GO. Studies on the propagation in vitro of poliomyelitis viruses. IV. Viral multiplication in a stable strain of human malignant epithelial cells (strain HeLa) derived from an epidermoid carcinoma of the cervix. The Journal of experimental medicine. 1953;97(5):695-710. Epub 1953/05/01. PubMed PMID: 13052828; PMCID: PMC2136303.

217.   C BJ. HeLa (for Henrietta Lacks). Science. 1974;184(4143):1268. Epub 1974/06/21. doi: 10.1126/science.184.4143.1268. PubMed PMID: 17784222.

218.   Agarwal S, Rimm DL. Making every cell like HeLa a giant step for cell culture. The American journal of pathology. 2012;180(2):443-5. doi: 10.1016/j.ajpath.2011.12.001. PubMed PMID: 22192626.

219. Jones HW, Jr. Record of the first physician to see Henrietta Lacks at the Johns Hopkins Hospital: history of the beginning of the HeLa cell line. American journal of obstetrics and gynecology. 1997;176(6):S227-8. Epub 1997/06/01. PubMed PMID: 9215212.

220. Kuramoto H, Hamano M. Cytogenetic studies of human endometrial carcinomas by means of tissue culture. Acta cytologica. 1977;21(4):559-65. Epub 1977/07/01. PubMed PMID: 269609.

221. Kuramoto H, Tamura S, Notake Y. Establishment of a cell line of human endometrial adenocarcinoma in vitro. American journal of obstetrics and gynecology. 1972;114(8):1012-9. Epub 1972/12/15. PubMed PMID: 4673779.

222. Kuramoto H. Studies of the growth and cytogenetic properties of human endometrial adenocarcinoma in culture and its development into an established line. Acta obstetrica et gynaecologica Japonica. 1972;19(1):47-58. Epub 1972/01/01. PubMed PMID: 4678779.

223. Abaan OD, Polley EC, Davis SR, Zhu YJ, Bilke S, Walker RL, Pineda M, Gindin Y, Jiang Y, Reinhold WC, Holbeck SL, Simon RM, Doroshow JH, Pommier Y, Meltzer PS. The exomes of the NCI-60 panel: a genomic resource for cancer biology and systems pharmacology. Cancer research. 2013;73(14):4372-82. Epub 2013/07/17. doi: 10.1158/0008-5472.can-12-3342. PubMed PMID: 23856246; PMCID: PMC4893961.

224. Daya-Grosjean L, Azzarone B, Maunoury R, Zaech P, Elia G, Zaniratti S, Benedetto A. SV40 immortalization of adult human mesenchymal cells from neuroretina. Biological, functional and molecular characterization. International journal of cancer Journal international du cancer. 1984;33(3):319-29. Epub 1984/03/15. PubMed PMID: 6321361.

225. Forest C, Czerucka D, Negrel R, Ailhaud G. Establishment of a human cell line after transformation by a plasmid containing the early region of the SV40 genome. Cell biology international reports. 1983;7(1):73-81. Epub 1983/01/01. PubMed PMID: 6299591.

226. Lubbe L, Rudolph M, Scherneck S, Zimmermann W, Geissler E. Immortalization of human Lesch-Nyhan-fibroblasts following infection with Simian virus 40. Archiv fur Geschwulstforschung. 1983;53(2):105-13. Epub 1983/01/01. PubMed PMID: 6305304.

227.   Miller G. Immortalization of human lymphocytes by Epstein-Barr virus. The Yale journal of biology and medicine. 1982;55(3-4):305-10. Epub 1982/05/01. PubMed PMID: 6295007; PMCID: PMC2596471.

228.   Petit CA, Gardes M, Feunteun J. Immortalization of rodent embryo fibroblasts by SV40 is maintained by the A gene. Virology. 1983;127(1):74-82. Epub 1983/05/01. PubMed PMID: 6305018.

229.   Yefenof E, Azar Y, Eidelsztein P, Ben-Sasson SZ. Immortalization of antigen specific, helper T cell lines by transformation with the radiation leukemia virus (RadLV). Journal of immunology (Baltimore, Md : 1950). 1982;128(2):625-8. Epub 1982/02/01. PubMed PMID: 6172500.

230.   Rhim JS. Generation of immortal human prostate cell lines for the study of prostate cancer. Methods in molecular medicine. 2003;81:69-77. Epub 2003/05/03. doi: 10.1385/1-59259-372-0:69. PubMed PMID: 12725115.

231.   Yasunaga Y, Nakamura K, Ewing CM, Isaacs WB, Hukku B, Rhim JS. A novel human cell culture model for the study of familial prostate cancer. Cancer research. 2001;61(16):5969-73. Epub 2001/08/17. PubMed PMID: 11507036.

232.   Freshney R. Culture of Animal Cells: A Manual of Basic Technique. New York: Alan R. Liss, Inc; 1987.

233.   Matsumoto S, Mashiba H, Okamoto K, Ekimoto H. [Evaluation of antitumor activity of etoposide administered orally for 21 consecutive days against human uterine cancer subcutaneous and/or orthotopic xenografts in nude mice]. Gan to kagaku ryoho Cancer & chemotherapy. 1999;26(9):1313-20. Epub 1999/09/09. PubMed PMID: 10478185.